Artificial Cells

Based on

Biodegradable Polymersomes

Committee

Chairman:	Prof. Dr. T. Reith	Universiteit Twente
Promotor:	Prof. Dr. J. Feijen	Universiteit Twente
Members:	Prof. Dr. M. Wessling	Universiteit Twente
	Prof. Dr. J. Greve	Universiteit Twente
	Prof. Dr. W. E. Hennink	Universiteit Utrecht
	Prof. Dr. J. F. J. Engbersen	Universiteit Twente
	Prof. Dr. H. J. Busscher	Rijksuniversiteit Groningen
	Prof. Dr. E. J. R. Sudhölter	Universiteit Wageningen
	Dr. G. H. M. Engbers	Universiteit Twente

Twente University **Press**

ARTIFICIAL CELLS BASED ON BIODEGRADABLE POLYMERSOMES

PROEFSCHRIFT

ter verkrijging van

de graad van doctor aan de Universiteit Twente,

op gezag van de rector magnificus,

prof.dr. F.A. van Vught,

volgens besluit van het College voor Promoties

in het openbaar te verdedigen

op woensdag 10 september 2003 om 15.00 uur

door

Fenghua Meng

geboren op 7 april 1973

te Jilin, P. R. China

Dit proefschrift is goedgekeurd door:

Promotor: Prof. dr. J. Feijen

Assistent-promotor: Dr. G. H. M. Engbers

Contents:

1   General introduction

Artificial cells refer to water-insoluble man-made particles that can perform specific bio-functions in the body without being rejected by the defense system. Besides as a model for natural cells, artificial cells are intended to be used for pharmaceutical applications and in biotechnology, for instance, treating enzyme defects in inborn errors of metabolism[1], gene therapy[2], targeted drug delivery systems[3,4], diagnostics like medical imaging[5-7], or as blood cell substitutes[8,9].

A principal application of artificial cells is the administration to the blood circulation after which they find their destination and locally perform their function. Artificial cells may consist of a cell body that contains the biofunctional material (e.g. drugs, proteins, DNA), and possesses a bioinert surface to prevent recognition of the cells by the defense system. This bioinert surface can be provided with a homing device that renders the artificial cell biospecific (see Figure 1). Preferably the whole cell is biodegradable with a tunable degradation time that depends on the desired duration of the biofunction. The components may vary according to the intended application.
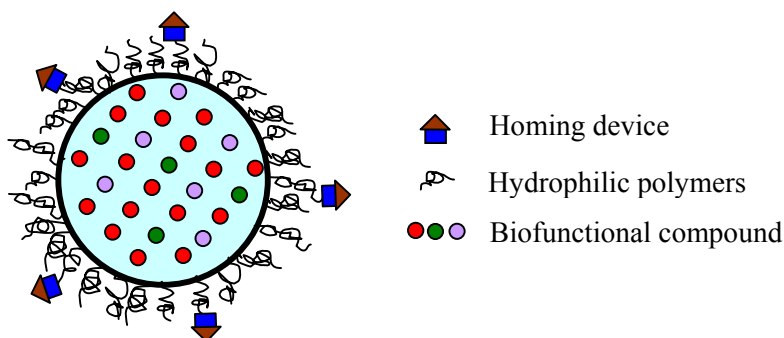
Figure 1. Schematic presentation of an artificial cell with encapsulated biofunctional compound and a homing device on a bioinert surface.

Liposome formulations[3,10] and nano-particle formulations[4,11] have received much attention in targeted drug delivery systems. Artificial cells developed by Chang contain isolated contents of red blood cells within semi-permeable capsules and have been evaluated as artificial red blood cells[8,12]. However, the major problems related to the applications of artificial cells are the lack of material biocompatibility, specificity, stability or, once they have performed their function, biodegradability.

Polymersomes, i.e., polymer vesicles, are similar to liposomes but based on amphiphilic block-copolymers instead of lipids, are of particular interest as a basis for artificial cells because of the relatively large compartment for efficient encapsulation, tunable membrane properties,

stability and large diversity of copolymers that can be applied. However, biodegradable biocompatible polymersomes have not been developed yet.
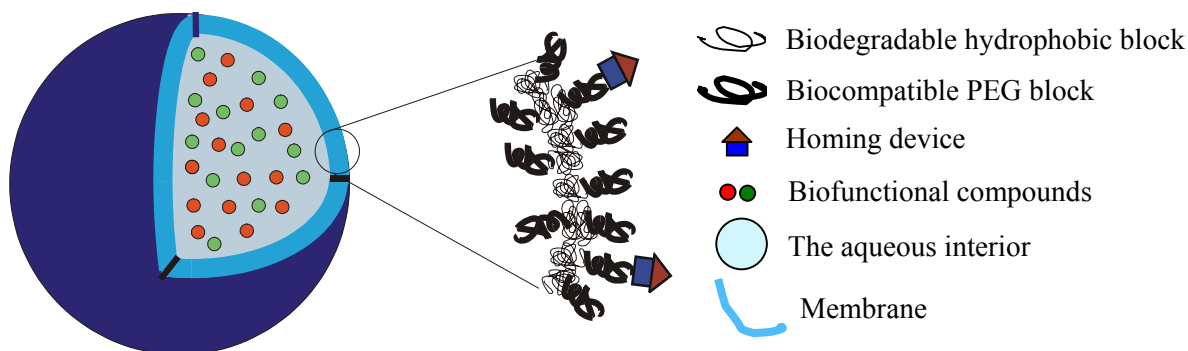

Figure 2. Schematic representation of an artificial cells based on biodegradable, biocompatible polymersomes with a magnified wall structure.

AIM OF THIS RESEARCH

The aim of the research that is described in this thesis is to develop biodegradable, biocompatible polymersomes that can serve as a basis for artificial cells. These artificial cells should be able to be delivered to the circulation, interact with specific sites where they perform their function, and biodegrade afterwards.

STRUCTURE OF THIS THESIS

Chapter 2 is a review of artificial cells, with an emphasis on artificial cell bodies, bio-functionality, bio-inert cell surfaces and homing devices that can render the artificial cell site specific. Although 'artificial cells' is a relative new topic, chapter 2 also contains a comprehensive historical overview of artificial cells.

The immobilization or grafting of polyethylene glycol (PEG) onto a surface, also called surface pegylation, is a frequently used method to make a surface bio-inert. The effect of surface pegylation largely depends on the surface density of the immobilized PEG chains. Chapter 3 describes the application of the pegylation strategy on carboxylated polystyrene (PS) particles that serve as a model for an artificial cell body. The PS particles are pegylated via carbodiimide chemistry and the optimal conditions for obtaining high surface concentrations of immobilized PEG are established.

In chapter 4, the results of the in vitro evaluation of these pegylated PS particles are described. Protein adsorption from human plasma dilutions, complement activation and the interaction of the particles with cultured human umbilical vein endothelial cells were studied.

The formation of biodegradable polymersomes as artificial cell bodies is the subject of Chapter 5 and 6. These polymersomes are based on amphiphilic PEG-polyester or PEG-polycarbonate

block-copolymers. By combining biodegradable, hydrophobic blocks with biocompatible hydrophilic blocks and a molecular weight that is such that the hydrophilic blocks can be excreted by the body, fully biodegradable polymersomes with an inert surface can be obtained, which can serve as the cell body of artificial cells. In chapter 5 the formation of polymersomes in chloroform/water systems is described, whereas chapter 6 deals with the formation of polymersomes in mixtures of an organic solvent and an aqueous phase. For both systems, the influence of the preparation parameters on the polymersome yield, size and size distribution was studied systematically, and mechanisms for polymersome formation are proposed.

To complete the polymersomes as artificial cells, biofunctionality and a homing device should be added. Chapter 7 describes the encapsulation and release properties of a model hydrophilic biofunctional compound, a fluorescent probe carboxyfluorescein. Furthermore, the immobilization of antibodies on the polymersome surface is described and the chapter ends with the evaluation of the targeting properties of these antibody-modified polymersomes with imaging surface plasmon resonance analyses.

REFERENCES

(1)   Bruni, S.; Chang, T. M. S. *Artif. Organs* **1995,** *19*, 449.

(2)   Chang, T. M. S. *Artif. Organs* **1998,** *22*, 958.

(3)   de Menezes, D. E. L.; Pilarski, L. M.; Allen, T. M. *Cancer Res.* **1998,** *58*, 3320.

(4)   Nakanishi, T.; Fukushima, S.; Okamoto, K.; Suzuki, M.; Matsumura, Y.; Yokoyama, M.; Okano, T.; Sakurai, Y.; Kataoka, K. *J. Control. Release* **2001,** *74*, 295.

(5)   Trubetskoy, V. S. *Adv. Drug Deliv. Rev.* **1999,** *37*, 81.

(6)   Davis, S. S.; Frier, M.; Illum, L. In *Polymeric Nanoparticles and Microspheres (chapter 6)*; Guiot, P., Couvreur, P., Eds.; CRC Press, Inc.: Boca Raton, FL, **1986**, p 175.

(7)   Delgado, A.; Soriano, I.; Sanchez, E.; Oliva, M.; Evora, C. *Eur. J. Pharm. Biopharm.* **2000,** *50*, 227.

(8)   Chang, T. M. S. *Science* **1964,** *146*, 524.

(9)   Chang, T. M. S. In *Bioartificial Organs II: Technology, Medicine, and Materials*; New York Acad Sciences: New York, **1999**; Vol. 875, p 71.

(10) Barratt, G. *Cell. Mol. Life Sci.* **2003,** *60*, 21.

(11) Gref, R.; Minamitake, Y.; Peracchia, M. T.; Trubetskoy, V.; Torchilin, V.; Langer, R. *Science* **1994,** *263*, 1600.

(12) Chang, T. M. S. *Biomater. Artif. Cells Artif. Organs* **1988,** *16*, 1.

2   Artificial cells: concept and development

1. INTRODUCTION

A cell is the fundamental unit of all living matter. A single cell is an entity, isolated from other cells by a cell membrane and contains a variety of sub-cellular structures and chemical material, which make it possible for the cell to function. Two fundamental types of cells are eucaryotes, which are cells that contain a nucleus like most animal and plant cells, and procaryotes (bacteria), which are cells having no nucleus. Figure 1 shows a schematic structure of an animal cell. Key structures of eucaryotes are the nucleus or nuclear region, where the information that is needed for cell reproduction is stored, and the cytoplasm, where the "machinery" for cell growth and function is present. Living cells are a complex chemical system and have distinct characteristics: self-feeding or nutrition, self-replication or growth, differentiation, chemical signaling, and evolution. Cells can vary enormously in appearance and function. For instance, red blood cells in mammals have no nucleus so they cannot reproduce themselves. Therefore, the structure of the cell depends on its function.
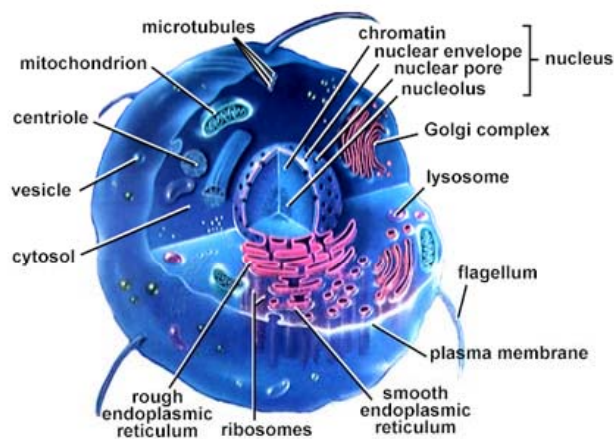
Figure 1. Schematic structure of an animal cell[1].

The organization of cells as well as physico-chemical principles such as self-assembly suggest synthetic routes for artificial cells, which are able to perform functions that are not possible for natural cells. Artificial cells refer to water-insoluble man-made particles that can perform specific biofunctions in the body without being rejected by the defense system. Besides as a model for real biological cells, artificial cells are intended to be used in pharmaceutical applications and biotechnology, for instance, in treating enzyme defects in inborn errors of metabolism[2], in gene therapy[3], in targeted drug delivery systems[4,5], as blood cell substitutes[6,7] and diagnostics like in medical imaging[8-10].

(A) (B) (C)

Homing devices

Hydrophilic polymers

Biofunctional materials

Hollow cell body

Solid cell body

Figure 2. Schematic presentation of possible forms of artificial cells with bioactive materials and a homing device on a bioinert surface. Bioactive materials can be encapsulated inside a hollow cell body (A), entrapped in a solid cell body (B), or immobilized on the surface of the cell body (C).
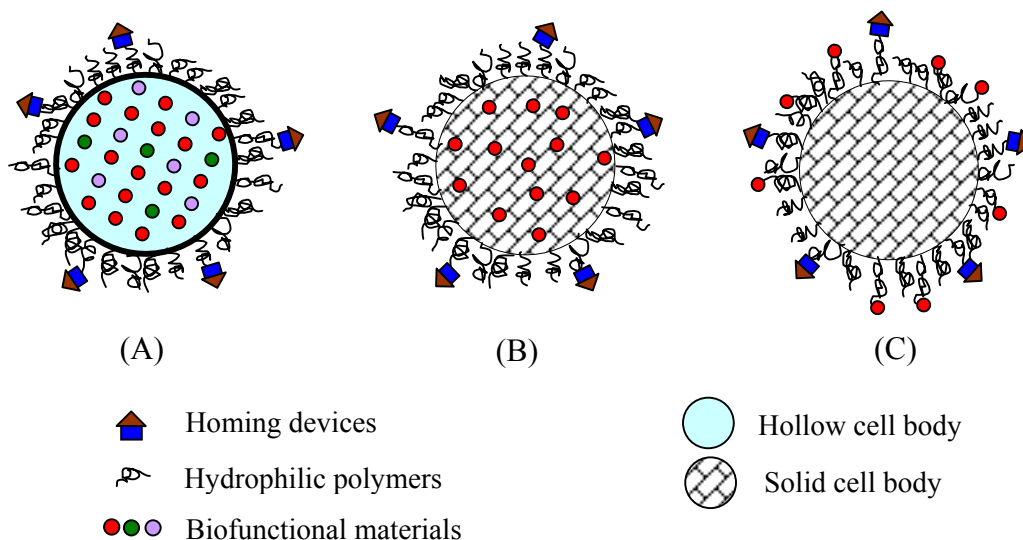
A principal application method of artificial cells is the administration to the blood circulation after which they find their destination and locally perform their function. Artificial cells, therefore, shall contain the following basic components: biofunctional compounds (e.g. drugs, proteins, DNA), a cell body that possesses a bioinert surface to prevent recognition of the artificial cells by the defense system, and a homing device to afford specificity (Figure 2). Preferably the whole system is biodegradable with a tunable degradation time that depends on the desired duration of the biofunction. The components may vary according to the intended application. For instance, if used as artificial red cells, the cells do not need homing devices. In the following sections the characteristics and the development of artificial cells will be reviewed.

2. CHARACTERISTICS OF ARTIFICIAL CELLS

The basic characteristics of artificial cells, namely the cell body (material and structure), its biofunctionality, the bioinert surface with its homing device are discussed in this section.

2.1. Artificial cell body

To be able to include a large amount of biofunctional material and/or to prevent degradation, solubility or stability problems of the biofunctional material, the architecture of an artificial cell body can be nano- or micro-particles including micelles, capsules, liposomes and polymersomes. In this section, different forms of the artificial cell body will be addressed.

For applications in the circulation, the size of artificial cell is of crucial importance[10-12]. Particles should be smaller than 1-2 μm to prevent obstruction of the capillaries. A size smaller than 200 nm is preferred to reach diseased sites[12,13]. On the other hand, non-biodegradable polymers remain in the body after the cells have performed their function, thus a specific treatment may be required to remove these cells. Therefore, biodegradable polymers such as polylactides (PLA), poly(lactic-co-glycolic acid) (PLGA) and poly(ε-caprolactone) (PCL),

which do not show major adverse reactions (depending on the application)[14,15], should preferably be used as the cell body material.

2.1.1. Solid nano- or micro-particles

Artificial cells with nano- or microparticles as cell body are mostly used in drug delivery system (DDS) with immobilized or encapsulated drugs (illustration see Figure 2 B and C). Many materials have been used as carriers for controlled drug delivery system[16-22]: proteins (collagen, gelatin, and albumin), polysaccharides (starch, alginate, dextran), and synthetic polymers (PLA, PLGA, PCL, polyanhydrides, poly(vinyl pyrrolidone), polyphosphazene, poly(vinyl alcohol), poly(hydroxyethyl methacrylate) and silicones).

For the delivery of protein drugs, hydrophilic carriers (e.g. polymer gels) are preferred because of their biosafety and high inertness towards proteins. In order to make them water-insoluble thus applicable for drug reservoirs, water-soluble natural polymers[16,17] such as specific collagen fractions, gelatin, albumin and starch have to be modified through derivatization or cross-linking. Polysaccharides and synthetic polyions are used as polyanion-polycation complexes[18].

Solid nano- or micro-particles have been prepared mainly by two methods[19-21]: dispersion of polymers and polymerization of monomers. The former includes emulsion evaporation, solvent displacement, salting out, and emulsification diffusion. The latter method generally consists of first introducing the monomer in a phase that is a non-solvent for the polymer. The polymerization then occurs in two steps: a nucleation phase followed by a growth phase. Bioactive materials such as bioactive peptides, proteins, and synthetic drugs (doxorubicin, savoxepine and cefadroxil etc.) can be immobilized onto or encapsulated by the particles.

2.1.2. Micelles

Block-copolymers with an amphiphilic character can assemble in an aqueous medium into micelles with a mesoscopic size range. These micelles have a fairly narrow size distribution and are characterized by a unique core–shell architecture, where hydrophobic blocks are segregated from the aqueous exterior, forming an inner core that is surrounded by a shell of hydrophilic blocks. Poly(ethylene glycol) (PEG) is frequently used as the hydrophilic block of the copolymer in order to prevent aggregation and the uptake of the micelles by the mononuclear phagocytic system (MPS). Micelles made from block-copolymers[5,8,23] can be used as a cell body for artificial cells mainly for drug delivery systems or diagnostic purposes.

As an example, a block-copolymer of PEG (Mn 5000) and poly(α,β-aspartic acid) (PAsp) (ca. 30 amino acid units) which contains conjugated doxorubicin (DXR) via a reaction between carboxyl groups of the PAsp segment and the glycosidic primary amino group of DXR, formed micelles (41.9 nm) in an aqueous medium[5,23]. Free DXR was then incorporated in the micelles through association with the conjugated DXR, and the loaded micelles showed antitumor activity by gradually release of DXR from the inner core within 8–24 h[5,23].

2.1.3. Capsules

Capsules, having relatively large cavities enclosed by membranes, are very suitable for the incorporation of a large volume of biofunctional materials. Depending on the preparation method, either hydrophilic or hydrophobic substances can be encapsulated (see Figure 2 A). Liposomes and polymersomes are also capsules, but distinguishable by the highly organized

membrane structures: head-tail structured lipids in liposome membranes and layered polymer stacks in polymersome membranes. Therefore, they will be discussed separately.

Semipermeable microcapsules are the first reported artificial cells[6,24]. These artificial cells may contain absorbents to remove toxins[25], hemoglobin to transport oxygen[24,26], enzymes to convert or remove metabolites and substrates[27], and cells or genetically engineered microorganisms[3] to carry out specific functions. Membrane materials[7,28] can be cellulose nitrate and acetate, cross-linked protein, cross-linked hemoglobin, alginate-polylysine and synthetic polymers including biodegradable polymers (e.g. PLA). The properties and functions of these artificial cells can be varied either by changing the type of the biofunctional material, or by changing the permeability, composition and configuration of the membrane by using different types of materials[7]. Depending on the nature of the bioactive material and the polymer membrane material, the method for the preparation of semipermeable microcapsules can vary. Three basic approaches were described by Chang in 1957[24]: the spray-dry method, the interfacial precipitation method, and the drop method. These form the basis of many of the present encapsulation approaches.

Nanocapsules that consist of an oil-based interior surrounded by a polymeric membrane can be prepared by two commonly used methods, i.e., the interfacial deposition of polymers[29] and the emulsification-diffusion method[19,30,31].

In the interfacial deposition method[29], a lipophilic drug, oil, polymer and optionally phospholipids are dissolved in a water miscible semi-polar solvent such as acetone. This solution is then added under stirring to an aqueous phase that may contain a surfactant. Nanocapsules are formed instantaneously by fast diffusion of the water miscible solvent into the aqueous phase, which provokes interfacial turbulence that results in spontaneous emulsification of the oily solution and the formation of a polymer film around the oily nano-droplets that contain the drug.

In the emulsification-diffusion method[19,30,31], a lipophilic drug, a polymer and an oil are dissolved in a partially water miscible solvent (e.g. ethyl acetate, benzyl alcohol or propylene carbonate), which is saturated with water. The aqueous phase that contains a stabilizer is saturated with the same solvent. The addition of the organic solution to the aqueous phase under stirring results in spontaneous emulsification of the partially water miscible solution. The addition of extra water to the system causes the partially water miscible solvent to diffuse into the aqueous phase, leading to the formation of the nanocapsules with the lipophilic drug encapsulated in the oil core. Hydrophobic drugs such as Taxol, progesterone, vitamin K, indomethacin, and chlorambucil can be encapsulated with high efficiencies[29,30].

2.1.4. Liposomes

Liposomes, i.e., vesicles composed of one or more lipid bilayers that surround an aqueous compartment, are among the most interesting supramolecular structures for biological, biomedical and biotechnological research and applications. The main characteristic of liposomes is that the lipid bilayers resemble the living cell membranes. Therefore, they are a useful model system for basic biological studies, such as studying intercellular transport phenomena and understanding how biological membranes recognize and respond to extracellular signals[32,33]. Moreover, liposomes can interact with natural cells by adsorption, fusion, endocytosis or lipid exchange, and thus they can be used to introduce foreign materials

like DNA or drugs in the cells[32,33]. Furthermore, liposomes provide relatively large compartments for storage of hydrophilic drugs and for enzymatic reactions.

Although the most popular uses of liposomes are currently in the cosmetic field, there is no doubt that, prospectively, the most important use of liposomes is in pharmacology and medicine, such as in topical and systemic drug delivery systems and diagnostics. In systemic applications, the main goals are to protect drugs loaded into the liposomes from being diluted or degraded in the blood, to reduce the toxic side effects by targeting highly toxic drugs to specific diseased cells or organs, and to obtain a prolonged release of their content, thus preventing peaks in the drug concentration. In ultrasound diagnostics, the concept of exploiting micro-bubbles, which are very effective scatterers of ultrasound, to perform refined ultrasound diagnostics with gas bubbles as echo contrast enhancers has drawn increasing attention. The general idea of this technique is to inject a micro-bubble suspension into a vein and to study the blood flow by detecting the bubbles' sound echo reaction to an applied acoustical field[34,35]. This leads to ultrasound images of higher contrast and quality as compared to conventional diagnostic techniques using only the ultrasound backscatter from the tissue itself. Inherently echogenic liposomes with antibodies specific for different components of atherosclerotic plaques and thrombi were prepared. Antifibrinogen immobilized liposomes attached to thrombi and fibrous portions of the atheroma and anti-ICAM-1 immobilized liposomes attached to the early atheroma. In addition, they were still acoustically reflective and provided enhanced ultrasonic images of the targeted structures[36]. There are a large number of reviews[37-39] and textbooks[32,33] dealing with the preparation and application of liposomes. Unfortunately, liposomes suffer from limited stability[32,33,40].

2.1.5. Polymersomes

Polymersomes refer to synthetic supra-structures that are similar to liposomes but are based on amphiphilic block-copolymers instead of lipids. Polymersomes have fluid-filled cores with walls that consist of amphiphilic membrane that separate the core from the outside medium.

Compared to liposomes, polymersomes have many distinct properties. The membrane thickness of polymersomes, which can be controlled by the molecular weight of the hydrophobic block of the copolymer[41], determines polymersome properties such as elasticity, permeability and mechanical stability[40]. Due to the higher molecular weight of the polymer as compared to lipids, the membrane of polymersomes is generally thicker, stronger and tougher than that of liposomes. Their toughness makes these polymersomes resistant to local perturbations[42]. Due to the fact that polymersome membranes are thicker and tougher, polymersomes are inherently more stable than conventional liposomes. For instance, the maximal areal strain of poly(ethylene oxide)-b-poly(butadiene) (PEO-PBD) based polymersomes varied from 20% to 40%, as compared to typically <5% for liposomes[41].

Formation of polymersomes by self-assembly of block-copolymers is driven by phase separation of the two blocks, resulting in a structure held together by non-covalent forces. Examples of polymersome-forming polymers and the relative measure of the membrane thickness of the corresponding polymersomes formed in different media are illustrated as gray bars in Figure 3[43]. Generally, the addition of a block selective solvent to a block-copolymer solution in a good solvent for both blocks leads to polymersome formation. In the following section different methods for the preparation of polymersomes will be discussed.
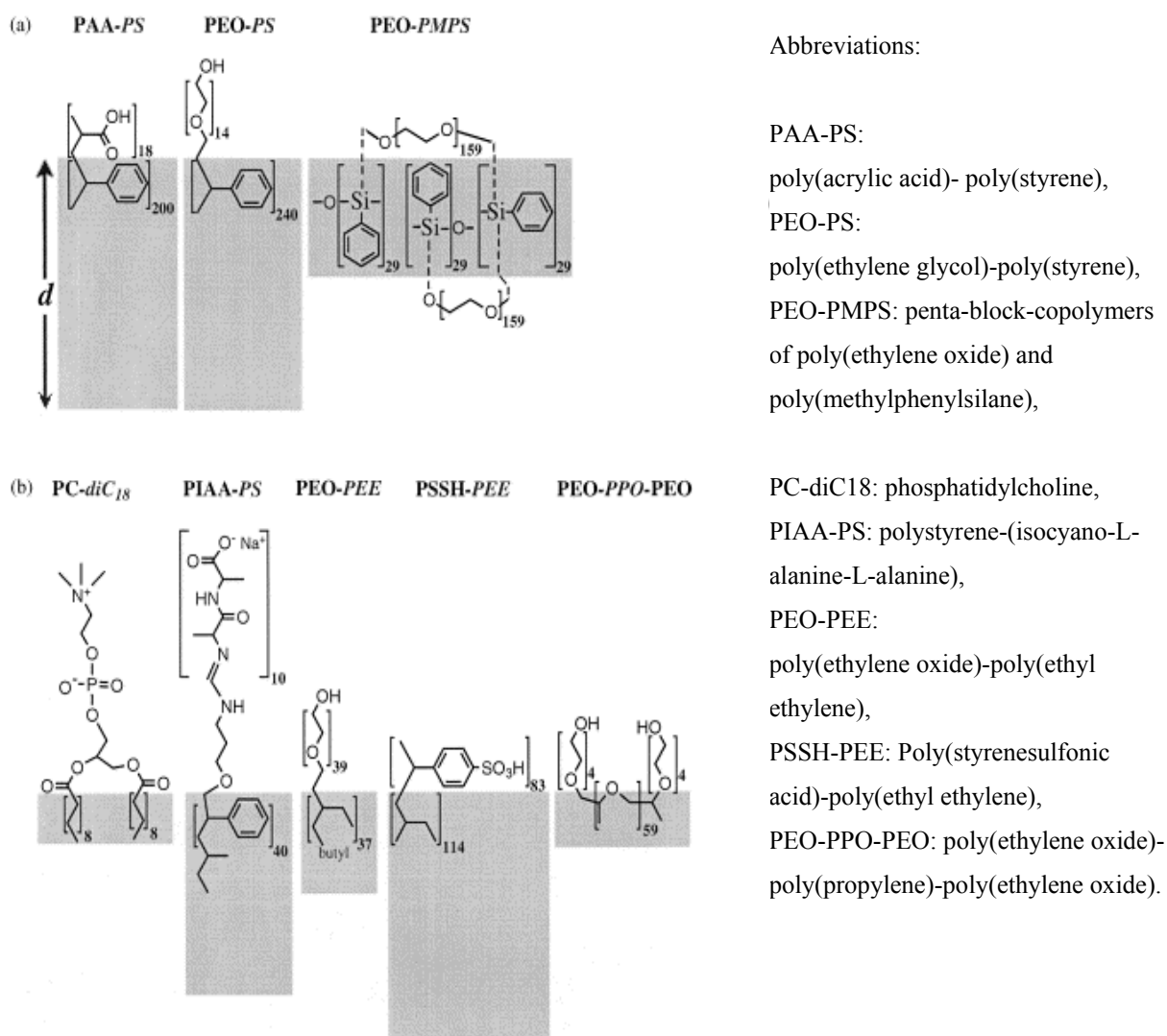
Abbreviations:

PAA-PS:

poly(acrylic acid)- poly(styrene),

PEO-PS:

poly(ethylene glycol)-poly(styrene),

PEO-PMPS: penta-block-copolymers

of poly(ethylene oxide) and

poly(methylphenylsilane),

PC-diC18: phosphatidylcholine,

PIAA-PS: polystyrene-(isocyano-L-

alanine-L-alanine),

PEO-PEE:

poly(ethylene oxide)-poly(ethyl

ethylene),

PSSH-PEE: Poly(styrenesulfonic

acid)-poly(ethyl ethylene),

PEO-PPO-PEO: poly(ethylene oxide)-

poly(propylene)-poly(ethylene oxide).

Figure 3. Polymersome-forming polymers and the relative measure of the membrane thickness of the corresponding polymersomes, d, as illustrated by gray bars[43]. (a) Polymers that form vesicles in solvent–water mixtures; and (b) natural lipids (for lipid membrane d is 3–4 nm) and polymers that form vesicles in an aqueous medium. The figure is reprinted from ref [43] with permission from Elsevier. The abbreviations are listed in the right side.

Polymersome formation in organic solvent mixtures. A few examples are available on the preparation of polymersomes in a mixture of organic solvents. For instance, polymersomes of poly(isoprene)-*b*-poly(2-cinnamoylethyl methacrylate) (PI_{88}-$PCEMA_{230}$) were obtained upon the addition of hexane, a selective precipitant of the PCEMA block, to a copolymer solution in THF[44]. The structure of un-crosslinked polymersomes and of polymersomes that were crosslinked by UV light was confirmed by TEM analysis after staining of the polymersomes with OsO_4.

Polymersome formation in water-solvent mixtures. Sub-micron diameter vesicle-like structures can be formed from many synthetic polymers using mixtures of water and organic solvents[45-49]. Solvents such as *N,N*-dimethylformamide (DMF) or tetrahydrofuran (THF) were used to facilitate polymersome formation. The diblock-copolymers poly(ethylene glycol)-poly(styrene)[47], e.g., EO_{15}-PS_{240}, formed polymersomes when water was slowly added to a

solution of the polymer in DMF. The polymersomes appeared to be stable after dialysis against water for several days. The formed spherical and tubular vesicles had a wall thickness of 20–25 nm as revealed by TEM. This thickness is much less than the extended length of PS_{240} (ca. 60 nm) and suggests relatively coiled, possibly entangled PS chains. For copolymers with the same PS length and PEO block lengths of 45 or 80 EO units, hardly or no polymersomes formed. Copolymers in which PEO was replaced by poly(acrylic acid) (PAA) and having longer PS chains (390-500 PS units) also formed polymersomes[50]. The thickness of these polymersome membranes ranged from 20–40 nm. It appeared that during polymersome formation the organic solvent that was trapped in the hydrophobic wall lowered the glass transition temperature of PS, thus enabling the rearrangement of polymer lamellae that closed upon itself to form sub-micron diameter spherical vesicles.

A penta- block-copolymer of poly(ethylene oxide) and poly(methylphenylsilane) (PMPS-PEO)$_2$-PMPS, (Mn of 27000, hydrophilic block of ca. 50 wt.% , polydispersity (Mw/Mn) of 1.6) was also reported to form polymersomes when water was added dropwise to a solution of the polymer in THF[48]. The hydrophobic PMPS segments formed an 8–12 nm thick hydrophobic wall as revealed by TEM. This suggests that for this particular system a low polydispersity of the copolymer is not a prerequisite for polymersome formation.

Polymersome formation in water. Polymersomes can also be formed directly in an aqueous medium[40,51-57], which is very favorable for the preparation of artificial cells. One of the earliest examples is based on a chiral construct poly(styrene)$_{40}$-poly(isocyano-L-alanine-L-alanine)$_n$. For the three amphiphiles that were studied (n = 10, 20 and 30), only the one with n = 10 resulted in polymersomes. Small collapsed polymersomes with diameters ranging from tens of nanometers to several hundred nanometers, and a bilayer thickness of 16 nm were observed by TEM[51]. Polymersomes coexisted with bilayer filaments and super-helical rods.

Polymersomes from poly(ethylene oxide)-b-poly(ethyl ethylene) (PEO-PEE) and its cross-linkable analogue, poly(ethylene oxide)-b-poly(butadiene) (PEO-PBD)[43,58,59] were also studied. These polymersomes were readily prepared by well-known liposome preparation methods, e.g., by sonication of an aqueous copolymer dispersion or hydration of a polymer film[40]. Also the membrane of these polymersomes was relatively thick and the membrane thickness increased more or less linearly with the square root of the molecular weight of the hydrophobic block[41]. In order to determine the membrane bending and area expansion moduli of the polymersomes using a micropipette manipulation technique, giant polymersomes (> 5 μm) are required, which were produced by an electroformation method[52,60]. In this method, the bottom layer of a closed chamber is coated with a conductive layer, e.g., indium tin oxide, to which the electrodes are connected. A solution of a lipid or block-polymer in an organic solvent is deposited on this conductive layer. Then the aqueous phase is injected into the chamber and an alternating electric field is applied, leading to giant liposome or polymersome formation[52,60]. Both the membrane bending and area expansion moduli of the electroformed polymersomes were similar to those of lipid membranes, but the giant polymersomes proved to be almost an order of magnitude tougher and able to sustain a far greater pressure before rupture. The polymersome membrane was also at least 10 times less permeable for water than common phospholipid bilayers[52].

Recently, peptosomes, polymersomes formed from a block-copolymer of a synthetic polymer and a polypeptide, e.g., poly(butadiene)-b-poly(L-glutamate), were obtained by directly mixing the copolymers in an aqueous phase[56,57]. These peptosomes showed an interesting pH sensitive helix-coil transition.

Besides polymersome formation that is driven by phase separation as described above, polymersome formation can also be induced by highly specific recognition, e.g., hydrogen bonding between complementary random copolymers featuring diamidopyridine and thymine functionalities, respectively[61,62].

Polymersomes are interesting for many potential applications. Previous studies have shown that plasma proteins had no immediate effect on the stability of PEO-PEE or PEO-PBD based polymersomes and that these polymersomes did not adhere to macrophages. These properties make these polymersomes attractive for mimicking red blood cells[40,59].

Prerequisites for polymersome formation. Apparently, not all block-copolymers can form polymersomes and certain prerequisites for the block-copolymer composition seem to exist. For the formation of polymersomes in water, block-copolymers should have a hydrophilic block volume fraction, f, of 20–40%[43], which is the same for natural lipids. At f = 45–55%, cylindrical micelles tend to form[42,63], and at f = 55–70%, spherical micelles are predominantly formed[63].

Block-copolymers PEO-PBD or PEO-PEE, of which the hydrophobic blocks have a low Tg (PEE has a Tg of −30 °C in PEO-PEE[64]), can directly form polymersomes in water. In contrast, copolymers with hydrophobic blocks with a high Tg cannot form polymersomes directly in a pure water medium[56], and an organic solvent has to be used to lower the Tg to provide enough chain mobility. In this case, not only the copolymer composition (MW of total copolymer, hydrophobic block (HB) and hydrophilic block (HL) or the MW ratio) but also the concentration of the polymer solution and the water percentage in the final mixture are important factors[46,65]. Shen at al showed that for PS-PAA copolymers a long HB and a high water percentage in the mixture favored the formation of polymersomes, while a short HB and a low water percentage favored the formation of open bilayer structures[46]. Copolymers used in that study all had an f value of 13-17 %[46]. Unlike for the formation of polymersomes in water, polymersome formation in water-organic solvent mixtures is possible when the f value is in the range of 3–60%[46,49,66]. The length of HB and HL both influence polymersome formation but in the opposite way: an increase in the total copolymer or HB length and a decrease in the PAA block length favor the formation of polymersomes.

2.2. Biofunctionality

Over the past decades important advances have been made in the field of biomaterials, of which many were related to rendering man-made materials "biofunctional". For an artificial cell, biofunction means that the biofunctional material that is included in the cell can locally alter physiological events or a physical parameter, such as preventing tumor cells to grow by delivering anticancer drugs, treating enzyme defects in inborn problems of metabolism by delivering encapsulated enzymes or modulating the expression of a gene by delivering oligonucleotides, transporting O_2/CO_2 or changing the electron density thus enhancing the contrast of certain organs. An artificial cell body can be provided with biofunctionality by

encapsulation or immobilization of many different kinds of biofunctional materials such as drugs, enzymes, peptides, antibodies, or DNA(see figure 2).

Immobilization of biofunctional materials onto the cell body surface can be done via covalent binding[67] (Figure 2C). For instance, antibody fragment Fab' and thiolated enzyme β-glucuronidase were covalently immobilized onto the surface of liposomes made of N-(4-p-maleimidophenyl)butyryl]phosphatidylethanolamine, resulting in liposomes with a high surface density of immobilized enzyme. These liposomes were able to completely convert the prodrug daunorubicin-glucuronide into active cytostatic compound which acts against ovarian carcinoma. Improved antitumor activity in cultured ovarian cancer cells was observed with increasing enzyme density on the liposome surface[68].

Antisense oligonucleotides (ODNs) with base sequences complementary to specific RNA can also be applied as biofunctional material. After binding to intracellular mRNA, ODNs can selectively modulate the expression of a gene. However, these molecules are poorly stable in biological fluids and are characterized by a low intracellular penetration. The surface of poly(alkylcyanoacrylate) nano-particles were provided with ODNs by adsorption, covalent binding or ionic complexation[20]. The loaded ODNs were able to improve the treatment of RAS cells that express the point mutated Ha-ras genes, which are directly involved in cell proliferation and tumorigenicity[69]. They markedly inhibited Ha-ras- dependent tumor growth in a nude mice model after subcutaneous injection[20,69].

Encapsulation of bioactive materials in nano-particles, vesicles or capsules (Figure 2 A and B), as compared to the surface immobilization method, has the advantage that a large amount of biofunctional material can be trapped. Both hydrophilic and hydrophobic materials can be encapsulated into vesicles with the hydrophilic ones entrapped in the aqueous interior and the hydrophobic ones in the membranes. The encapsulation procedures are usually mild and simple, and can be combined with the formation of the particles.

Also complete biological cells can provide artificial cell biofunctionality. Encapsulation of (genetically engineered) cells by a semipermeable membrane may prevent adverse immune response in non-autologous cell therapy[3]. Techniques like ionic gelation, interfacial precipitation, and complex coacervation have been developed to encapsulate various primary cells or cell lines for different tissue engineering or therapeutic applications[70,71]. Cell encapsulation has provided a range of promising therapeutic treatments for diabetes, hemophilia, cancer and renal failure[72]. The ideal approach would be to encapsulate cells and implant these into the body for long-term functioning. For example, microencapsulated islets have been implanted to maintain normal glucose levels in diabetic animals and in human[7,73,74]. Implanted microencapsulated hepatocytes can lower the elevated bilirubin level in Gunn rats with an inborn error of bilirubin metabolism[2].

2.3. Bioinert surfaces

The main problem that is encountered with the application of artificial cells in the circulation is the rapid clearance by the MPS[11,75] including the adhesion to or phagocytosis by the endothelial lining of the vascular system[76,77]. The exact mechanisms by which foreign particles are detected in vivo and removed from the blood by phagocytic cells are currently not fully resolved. It is generally assumed that the removal of particles proceeds via the binding of proteins, especially opsonins that can interact with appropriate receptors on the phagocytes

including IgG and complement components C3, C3b, to the particle surface (opsonization) and subsequent adhesion to the phagocytic cells followed by internalization of the particles[11]. The process of opsonization is strongly influenced by the surface characteristics of the particles such as charge[78-80] and hydrophobicity[81,82]. In order to prevent rapid clearance and thus to provide a prolonged circulation time, artificial cells should have favorable surface properties that upon introduction of the cells in the circulation induces as little protein (especially opsonins) adsorption and complement activation as possible.

Protein adsorption and complement activation can be reduced by grafting the cell surface[83-87] with hydrophilic, nonionic polymers, such as natural materials, e.g., proteins, polysaccharides and synthetic polymers, e.g., poly(hydroxyethyl methacrylate) and PEG. PEG surface grafting is the most promising and effective method because PEG can provide "stealth" properties by preventing interactions with blood proteins including opsonins[86,87]. The protein resistant character is generally ascribed to a combination of the low interfacial energy of PEG with water[88], its steric stabilization effect[89-91] and high mobility and flexibility[92].

The dysopsonic effect of a PEG coating is not substrate dependent as revealed by the studies of protein adsorption onto pegylated surfaces of polystyrene particles[93,94], PLGA or PLA particles[87,95], and has been applied for different devices like nano- and microspheres[94-96], including liposomes[11,75] and nanocapsules[97].

The dysopsonic capacity of a pegylated surface is determined by the molecular weight, surface concentration and conformation of PEG molecules. For linear PEG, a high density, preferably in the "brush" regime is demanded to completely prevent protein adsorption[89,90,98]. In the "brush" regime, the distance between two PEG chains is far smaller than the Flory radius of the PEG molecule[99]. The longer the PEG chains, the lower the required density is. For a star shaped PEG, an intermediate-grafting density was needed to avoid protein adsorption[98]. A theoretical study based on surface force measurement showed that the irreversible protein adsorption (primary adsorption, short range) depends on the grafting density of the PEG brush, and that the reversible adsorption (secondary adsorption, long range) relies on both the grafting density and the length of the PEG brush[100]. Therefore, it can be concluded that the surface concentration and the molecular weight (Mn) of the grafted PEG are not independent criteria for the prevention of protein adsorption. A PEG Mn higher than 2150[101] or 3400[102] has shown to result in minimal protein adsorption, but also self assembled monolayers (SAM) of thiolated oligo (ethylene oxide) (OEG, 2-6 units) on gold revealed a high resistance against protein adsorption. The latter was ascribed to highly dense OEG units in a helical molecular conformation, which can bind interfacial water more tightly than the all trans conformation thus proteins could not displace the bound water[103,104]. Force-distance measurements using AFM[105] showed that for these SAMs a unique long range repulsive force is responsible for the protein resistance, which is different from steric repulsion for the long chain PEG systems. Interestingly, it was also found that for these SAMs, OEG-OH adsorbed less protein than OEG-OCH$_3$ [104], implying that the end group of the OEG plays a role in protein adsorption. The influence of the end group of long chain PEG on protein adsorption has not been investigated.

Pegylated surfaces have many biomedical applications also because PEG is biocompatible and, for a Mn less than 50,000 g/mol, can be removed from the body by urinary excretion[106].

Pegylated surfaces can be obtained by adsorption of PEG-containing block-copolymers like PEO/PPO[22,107] or PDLLA/PEO[108], by surface grafting[98,109], by deposition of PEG-like coatings using a radio-frequency glow discharge technique[110,111], or by self-assembly of PEG containing surfactants into monolayers[104]. The last two methods are very substrate dependent and thus not straightforward for obtaining a pegylated artificial cell surface. Physical adsorption of PEG-containing copolymers has the disadvantage of possible desorption of the copolymer from the cell surface during contact with blood. Surface pegylated particles can also be obtained by emulsion polymerization of PEG-containing comonomers[112-114], and the formation of nano-particles[96,115,116] or micelles[117] from PEG-containing block-copolymers. Nevertheless, these methods have limitations with respect to the molecular weight of the PEG that can be used, and the particle size, and PEG density that can be obtained. Covalent grafting of PEG via functional groups present on the surface[118,119] is well controllable in terms of PEG length, density and orientation, but it requires surface functionality.

Despite that many studies have shown that PEG surfaces can reduce protein adsorption, there are still no general prerequisites for a PEG surface to prevent protein adsorption. In addition, from lab to lab different single protein solutions[103,104,107,109] or very dilute plasma or serum[93,120] were used to study protein adsorption. This is very different from the in vivo situation and makes it difficult to draw a conclusion by the comparison of these results.

2.4. Site specific targeting

An artificial cell with a bioinert surface can circulate in the body for a long time. A homing device on the artificial cell surface can give the cell specificity by guiding the cell to the site where it is intended to perform its function. Since most of the research on particle targeting is related to drug targeting, in the following part, drug targeting will be reviewed.

The principal schemes of drug targeting[121] include direct administration of a drug to the pathological zone, passive accumulation of drug through leaky vasculature (tumors, inflammation), physical targeting based on abnormal pH value and/or temperature in the pathological zone, magnetic targeting, and targeting using specific ligands that have an increased affinity for the area of interest. The last approach is the most challenging and provides many opportunities.

For every organ or tissue certain binding sites (antigens) can be found that are specific for that organ or tissue of interest. For successful targeting, a compound can be used, which is capable of specifically interacting with the target component (for example, a monoclonal antibody against the target antigen). Based on this principle, targeted delivery of pharmaceuticals to a variety of tissues and organs[122,123] has been performed.

Pharmaceutical carriers such as microcapsules, microparticles, liposomes, and micelles have been successfully used for targeted drug delivery[124-127], making use of proteins including antibodies (AB) and AB fragments, lipoproteins, lectins, hormones, mono-, oligo- and polysaccharides as targeting moieties. Providing a particle surface with a monoclonal antibodies is one of the most effective ways of targeting antigen expressing cells[125,128] and specific uptake of the particles by the target cells has been observed[129]. This approach is generally applied to improve the therapeutic efficacy of anticancer drugs[4,125] to reduce side effects of drugs and to design advanced diagnostic systems[130]. Of particular interest is the attachment of the antibodies through the distal end of PEG chains[125,131]. This is due to the fact

that by using PEG as a spacer the binding of antibody to the target cell won't be sterically hindered, and nonspecific binding is reduced[132]. In vitro experiments have shown that the specific binding of these immunoliposomes to target cells increased with the Ab density on the liposome surface[125,133].

Antibody-PEG conjugates that were stable in vivo have been obtained by coupling Ab to a PEG terminus through thioether[125], amide[131], hydrazone[4] linkages, or through a cleavable disulfide bond between the polymer chain and the Ab[133]. Since conventional immobilization of antibodies to particles generally produces a random orientation of the antibodies, which results in a very low binding efficiency, strategies for site-directed immobilization of antibodies have also been developed. Antibodies can be attached through the saccharide moieties in their Fc part[134], or through the free sulfhydryl group in the hinge region of Fab' fragments[135]. Immobilization of IgG via the Fc carbohydrate moieties has already been shown to produce higher binding efficiencies of antibody to the antigen[136] as compared to the random immobilization method via succinimide coupling to the amino groups of the protein.

3. DEVELOPMENT OF ARTIFICIAL CELLS

Artificial cells have found a variety of pharmaceutical and biomedical applications. Below a few examples of artificial cell systems will be addressed and the above-mentioned characteristics of the artificial cells (cell body, biofunctionality, inert surface and homing device) will be discussed in detail.

3.1. Artificial red blood cells

Although targeting is not introduced, artificial red blood cells can be categorized as artificial cells. The encapsulation of the content of red blood cells, including hemoglobin and enzymes, by an artificial membrane started in 1957[24]. Different materials including crosslinked protein, bilayer lipid complexed to protein or polymer have been used as membrane material[6,137]. Red blood cell enzymes like carbonic anhydrase[6] and catalase[27] retained their activities in these microcapsules. Encapsulated catalase was used successfully as an antioxidant against the toxic effects of hydrogen peroxide in experimental animals[27]. The major problem was the uptake by the MPS. Despite considerable effort[6,137], the circulation time was still not long enough for practical applications.

The next major step in the encapsulation of hemoglobin was the preparation of smaller lipid membrane based artificial red blood cells (0.2 μm)[138], which stayed in the circulation much longer. Modification of surface properties including surface charge and the use of sialic acid analogues further prolonged the circulation time. Recent studies have shown that the half-time was increased to more than 48 hours[139]. In a rat model it was shown that 25% of the red blood cells could be replaced with these artificial red blood cells. There were no adverse changes in the histology of brain, heart, kidneys and lungs of animals after red blood cell replacement.

Biodegradable polymer membranes of polylactide and polyglycolide were also used to prepare hemoglobin containing nanocapsules (80 to 200 nm)[140,141]. The polymer membranes are stronger and more porous than lipid membranes. The content of hemoglobin (11 gm/dL) could

be higher than that of hemoglobin lipid vesicles and resembled that of red blood cells (15 gm/dL). Superoxide dismutase and catalase could also be included with the hemoglobin[26]. Biodegradable polymeric membranes were permeable to glucose and other molecules and allowed the preparation of hemoglobin nanocapsules containing the methemoglobin reductase system. External glucose could diffuse into the nanocapsules and small molecular weight products of the reaction could diffuse out and therefore did not accumulate in the nanocapsules thus inhibiting the enzymatic reaction. In vitro studies[26,142] showed promising results for the conversion of methemoglobin into hemoglobin. One third of the red blood cells of rats could be replaced by these artificial red blood cells. Nonetheless, a further increase of the circulating time of these hemoglobin nanocapsules is still required.

3.2. Liposome formulation in drug delivery system

Liposome technology in pharmaceutical applications mainly focuses on the treatment of cancer[4,68,143] including leukaemia or solid tumors[143]. A doxorubicin-containing formulation based on 'stealth[TM]' liposomes, Doxil[TM] (Alza Corp. Mountain View, CA, USA), is commercially available. The anti-tumor drug doxorubicin (adriamycin) is active against a wide variety of tumors, but has dose-limiting cardiotoxicity. Encapsulation within liposomes or particles decreases side effects by reducing the amount of drug that reaches the myocardium. The ability to selectively target a liposome anticancer drug formulation via specific ligands against antigens expressed on malignant cells improves the therapeutic effectiveness of the liposome preparations as well as further reduces adverse side effects.

Sterically stabilized liposomes (SLs) were prepared from a mixture of pegylated and non-pegylated lipid via a hydration-extrusion method. An anticancer drug doxorubicin (DXR), which is useful in the treatment of hematological malignancies such as B-cell lymphomas, was then loaded by remote loading using an ammonium sulfate gradient. The final formulation was obtained by immobilizing murine monoclonal anti-CD19 using a hydrazide coupling method via the reaction of oxidized Ab with hydrazine end groups of PEG on the liposome surface[4]. This liposome formulation was tested on malignant B cells that express CD19 surface antigens. In comparison with non-targeted SLs, the targeted liposomes showed a 3-fold higher association with the B cells and selectively bound to B cells in a mixed culture of B and T cells. This formulation displayed a higher cytotoxicity to B cells than DXR that was entrapped in SLs. Therapeutic experiments in immunodeficient mice showed significantly increased effectiveness of this formulation as compared to control formulations of free DXR, DXR encapsulated in non-targeted SLs, or DXR in SLs with immobilized isotype-matched nonspecific Ab. Single doses (3 mg/kg) of this formulation administered i.v. resulted in a significantly improved therapeutic effect, including some long-term survivors[4].

3.3. Polymersomes

Polymersomes are relatively new, but some effort has been made to prepare artificial cell-like structures with encapsulated enzymes[49,144] and DNA[145]. Nardin et al.[146] prepared polymersomes of poly(2-methyl-oxazoline)-*b*-poly(dimethylsiloxane)-*b*-poly(2-methyl-oxazoline) (PMOXA-PDMS-PMOXA). DNA-containing polymersomes were also prepared[145]. To demonstrate that DNA translocation across a completely synthetic block-copolymer membrane was possible, a phage transfection strategy was used as a DNA transfer model system. For this purpose, the bacterial channel forming protein LamB was reconstituted

in polymersomes during the polymersome formation. The membrane protein LamB is a specific transporter for maltodextrins but also serves as a receptor for λ phage to trigger the ejection of λ phage DNA (Figure 4). The functionality of the LamB protein was fully preserved despite the artificial surrounding[145]. This could lead to a polymeric DNA vehicle that could be useful in gene therapy.
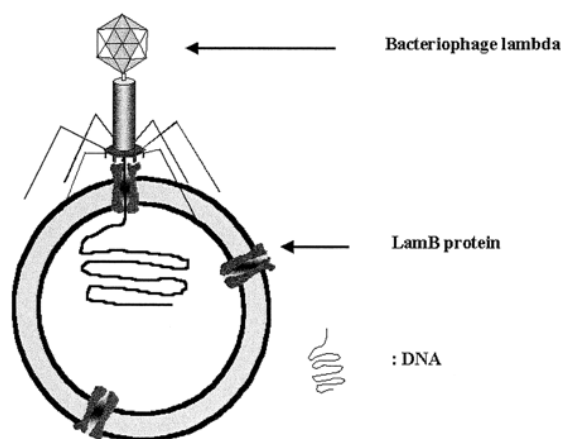

Figure 4. *Schematic representation of a DNA-loaded PMOXA-PDMS-PMOXA polymersome. λ phage binds a LamB protein, and the DNA is transferred across the block-copolymers membrane[145]. (The figure is reprinted from ref [145] with permission from National Academy of Sciences, U.S.A.).*

4. CONCLUSIONS AND PERSPECTIVES

Artificial cells are very promising for biomedical applications, e.g., as carriers for drug delivery, nano-reactors, and blood cell substitutes. However, they generally are plagued by the lack of material biocompatibility, specificity or tunable stability. Polymersomes are of particular interest because of the large compartment for efficient encapsulation, tunable membrane properties, stability and large diversity of copolymers that can be applied. However, biodegradable, biocompatible polymersomes as a basis for artificial cells have not been developed yet.

It is the aim of the research described in this thesis to develop biodegradable, biocompatible polymersomes as a basis for artificial cells that can freely circulate in the body and perform their specific function.

REFERENCES

(1)   http://www.emc.maricopa.edu/faculty/farabee/BIOBK/BioBookCELL2.html .
(2)   Bruni, S.; Chang, T. M. S. *Artif. Organs* **1995,** *19*, 449.
(3)   Chang, T. M. S. *Artif. Organs* **1998,** *22*, 958.
(4)   de Menezes, D. E. L.; Pilarski, L. M.; Allen, T. M. *Cancer Res.* **1998,** *58*, 3320.

(5)   Nakanishi, T.; Fukushima, S.; Okamoto, K.; Suzuki, M.; Matsumura, Y.; Yokoyama, M.; Okano, T.; Sakurai, Y.; Kataoka, K. *J. Control. Release* **2001,** *74*, 295.

(6)   Chang, T. M. S. *Science* **1964,** *146*, 524.

(7)   Chang, T. M. S. In *Bioartificial Organs II: Technology, Medicine, and Materials*; New York Acad Sciences: New York, **1999**; Vol. 875, p 71.

(8)   Trubetskoy, V. S. *Adv. Drug Deliv. Rev.* **1999,** *37*, 81.

(9)   Davis, S. S.; Frier, M.; Illum, L. In *Polymeric Nanoparticles and Microspheres (chapter 6)*; Guiot, P., Couvreur, P., Eds.; CRC Press, Inc.: Boca Raton, FL, **1986**, p 175.

(10) Delgado, A.; Soriano, I.; Sanchez, E.; Oliva, M.; Evora, C. *Eur. J. Pharm. Biopharm.* **2000,** *50*, 227.

(11) Patel, H. M. *Crit. Rev. Ther. Drug Carr. Syst.* **1992,** *9*, 39.

(12) Storm, G.; Belliot, S. O.; Daemen, T.; Lasic, D. D. *Adv. Drug Deliv. Rev.* **1995,** *17*, 31.

(13) Ishida, O.; Maruyama, K.; Sasaki, K.; Iwatsuru, M. *Int. J. Pharm.* **1999,** *190*, 49.

(14) Kelly, R. J. *Rev. Surg.* **1970,** *2*, 142.

(15) Schindler, A.; Jeffcoat, R.; Kimmel, G. L.; Pitt, C. G.; Wall, M. E.; Zweidinger, R. *Contemp. Top. Polym. Sci.* **1977,** *2*, 251.

(16) Fujioka, K.; Maeda, M.; Hojo, T.; Sano, A. *Adv. Drug Deliv. Rev.* **1998,** *31*, 247.

(17) Tabata, Y.; Ikada, Y. *Adv. Drug Deliv. Rev.* **1998,** *31*, 287.

(18) Dumitriu, S.; Chornet, E. *Adv. Drug Deliv. Rev.* **1998,** *31*, 223.

(19) Quintanar-Guerrero, D.; Allemann, E.; Fessi, H.; Doelker, E. *Drug Dev. Ind. Pharm.* **1998,** *24*, 1113.

(20) Lambert, G.; Fattal, E.; Couvreur, P. *Adv. Drug Deliv. Rev.* **2001,** *47*, 99.

(21) Soppimath, K. S.; Aminabhavi, T. M.; Kulkarni, A. R.; Rudzinski, W. E. *J. Control. Release* **2001,** *70*, 1.

(22) Davis, S. S.; Illum, L.; Moghimi, S. M.; Davies, M. C.; Porter, C. J. H.; Muir, I. S.; Brindley, A.; Christy, N. M.; Norman, M. E.; Williams, P.; Dunn, S. E. *J. Control. Release* **1993,** *24*, 157.

(23) Kataoka, K.; Harada, A.; Nagasaki, Y. *Adv. Drug Deliv. Rev.* **2001,** *47*, 113.

(24) Chang, T. M. S. *Biomater. Artif. Cells Artif. Organs* **1988,** *16*, 1.

(25) Chang, T. M. S. **1989,** *17*, 611.

(26) Chang, T. M. S.; Yu, W. P., U.S.A. Patent, No. 5670173, **1996**.

(27) Chang, T. M. S.; Poznansky, M. J. *Nature* **1968,** *218*, 242.

(28) Chang, T. M. S. *Eur. J. Pharm. Biopharm.* **1998,** *45*, 3.

(29) Fessi, H.; Puisieux, F.; Devissaguet, J. P.; Ammoury, N.; Benita, S. *Int. J. Pharm.* **1989,** *55*, R1.

(30) Quintanar-Guerrero, D.; Allemann, E.; Doelker, E.; Fessi, H. *Pharm. Res.* **1998,** *15*, 1056.

(31) Leroux, J. C.; Allemann, E.; Doelker, E.; Gurny, R. *Eur. J. Pharm. Biopharm.* **1995,** *41*, 14.

(32) Lasic, D. D. Liposomes: from physics to applications. Amsterdam: Elsevier, **1993**.

(33) Gregoriadis, G. Liposome technology. Boca Raton: CRC Press, Inc., **1984**.

(34) Hilgenfeldt, S.; Lohse, D.; Zomack, M. *Eur. Phys. J. B* **1998,** *4*, 247.

(35) Hilgenfeldt, S.; Lohse, D. *Ultrasonics* **2000,** *38*, 99.

(36) Demos, S. M.; Alkan-Onyuksel, H.; Kane, B. J.; Ramani, K.; Nagaraj, A.; Greene, R.; Klegerman, M.; McPherson, D. D. *J. Am. Coll. Cardiol.* **1999,** *33*, 867.

(37) Lasic, D. D. *Angew. Chem. Int. Edit. Engl.* **1994,** *33*, 1685.

(38) Annesini, M. C. *Chem. Biochem. Eng. Q.* **1998,** *12*, 1.

(39) Woodle, M. C. *Adv. Drug Deliv. Rev.* **1998,** *32*, 139.

(40) Lee, J. C. M.; Bermudez, H.; Discher, B. M.; Sheehan, M. A.; Won, Y. Y.; Bates, F. S.; Discher, D. E. *Biotechnol. Bioeng.* **2001,** *73*, 135.

(41) Bermudez, H.; Brannan, A. K.; Hammer, D. A.; Bates, F. S.; Discher, D. E. *Macromolecules* **2002,** *35*, 8203.

(42) Won, Y. Y.; Davis, H. T.; Bates, F. S. *Science* **1999,** *283*, 960.

(43) Discher, B. M.; Hammer, D. A.; Bates, F. S.; Discher, D. E. *Curr. Opin. Colloid Interface Sci.* **2000,** *5*, 125.

(44) Ding, J. F.; Liu, G. J. *Macromolecules* **1997,** *30*, 655.

(45) Zhang, L. F.; Eisenberg, A. *Science* **1995,** *268*, 1728.

(46) Shen, H. W.; Eisenberg, A. *Macromolecules* **2000,** *33*, 2561.

(47) Yu, K.; Eisenberg, A. *Macromolecules* **1998,** *31*, 3509.

(48) Holder, S. J.; Hiorns, R. C.; Sommerdijk, N. A. J. M.; Williams, S. J.; Jones, R. G.; Nolte, R. J. M. *Chem. Commun.* **1998**, 1445.

(49) Nardin, C.; Hirt, T.; Leukel, J.; Meier, W. *Langmuir* **2000,** *16*, 1035.

(50) Yu, Y. S.; Zhang, L. F.; Eisenberg, A. *Macromolecules* **1998,** *31*, 1144.

(51) Cornelissen, J. J. L. M.; Fischer, M.; Sommerdijk, N. A. J. M.; Nolte, R. J. M. *Science* **1998,** *280*, 1427.

(52) Discher, B. M.; Won, Y. Y.; Ege, D. S.; Lee, J. C. M.; Bates, F. S.; Discher, D. E.; Hammer, D. A. *Science* **1999,** *284*, 1143.

(53) Li, Z. C.; Jin, W.; Liu, F. M. *React. Funct. Polym.* **1999,** *42*, 21.

(54) Schillen, K.; Bryskhe, K.; Mel'nikova, Y. S. *Macromolecules* **1999,** *32*, 6885.

(55) Dimova, R.; Seifert, U.; Pouligny, B.; Forster, S.; Dobereiner, H. G. *Eur. Phys. J. E* **2002,** *7*, 241.

(56) Kukula, H.; Schlaad, H.; Antonietti, M.; Forster, S. *J. Am. Chem. Soc.* **2002,** *124*, 1658.

(57) Checot, F.; Lecommandoux, S.; Gnanou, Y.; Klok, H. A. *Angew. Chem.-Int. Edit.* **2002,** *41*, 1339.

(58) Discher, D. E.; Eisenberg, A. *Science* **2002,** *297*, 967.

(59) Hammer, D. A.; Discher, D. E. *Ann. Rev. Mater. Res.* **2001,** *31*, 387.

(60) Angelova, M.; Soleau, S.; Meleard, P.; Faucon, J.; Bothorel, P. **1992,** *89*, 127.

(61) Thibault, R. J.; Galow, T. H.; Turnberg, E. J.; Gray, M.; Hotchkiss, P. J.; Rotello, V. M. *J. Am. Chem. Soc.* **2002,** *124*, 15249.

(62) Drechsler, U.; Thibault, R. J.; Rotello, V. M. *Macromolecules* **2002,** *35*, 9621.

(63) Won, Y. Y.; Brannan, A. K.; Davis, H. T.; Bates, F. S. *J. Phys. Chem. B* **2002,** *106*, 3354.

(64) Hillmyer, M. A.; Bates, F. S. *Macromolecules* **1996,** *29*, 6994.

(65) Cameron, N. S.; Corbierre, M. K.; Eisenberg, A. *Can. J. Chem.-Rev. Can. Chim.* **1999,** *77*, 1311.

(66) Yu, K.; Bartels, C.; Eisenberg, A. *Macromolecules* **1998,** *31*, 9399.

(67) Inaki, Y. In *Functional monomers and polymers: procedures, synthesis, applications*; Takemoto, K., Inaki, Y., Ottenbrite, R. M., Eds.; Marcel Dekker: NewYork, **1987**, p 461.

(68) Vingerhoeds, M. H.; Haisma, H. J.; Belliot, S. O.; Smit, R. H. P.; Crommelin, D. J. A.; Storm, G. *Pharm. Res.* **1996,** *13*, 604.

(69) Schwab, G.; Chavany, C.; Duroux, I.; Goubin, G.; Lebeau, J.; Helene, C.; Saisonbehmoaras, T. *Proc. Natl. Acad. Sci. U. S. A.* **1994,** *91*, 10460.

(70) Gaumann, A.; Laudes, M.; Jacob, B.; Pommersheim, R.; Laue, C.; Vogt, W.; Schrezenmeir, J. *Biomaterials* **2000,** *21*, 1911.

(71) Chia, S. M.; Wan, A. C. A.; Quek, C. H.; Mao, H. Q.; Xu, X.; Shen, L.; Ng, M. L.; Leong, K. W.; Yu, H. *Biomaterials* **2002,** *23*, 849.

(72) Orive, G.; Hernandez, R. M.; Gascon, A. R.; Calafiore, R.; Chang, T. M. S.; De Vos, P.; Hortelano, G.; Hunkeler, D.; Lacik, I.; Shapiro, A. M. J.; Pedraz, J. L. *Nature Medicine* **2003,** *9*, 104.

(73) Lanza, R. P.; Cooper, D. K. C. *Mol. Med. Today* **1998,** *4*, 39.

(74) Sun, A. M. In *Bioartificial Organs*; New York Acad Sciences: New York, **1997**; Vol. 831, p 271.

(75) Juliano, R. L. *Adv. Drug Deliv. Rev.* **1988,** *2*, 31.

(76) Vora, M.; Karasek, M. A. *J. Cell. Physiol.* **1994,** *159*, 450.

(77) Steffan, A. M.; Gendrault, J. L.; McCuskey, R. S.; McCuskey, P. A.; Kim, A. *Hepatology* **1986,** *6*, 830.

(78) van Wachem, P. B.; Hogt, A. H.; Beugeling, T.; Feijen, J.; Bantjes, A.; Detmers, J. P.; van Aken, W. G. *Biomaterials* **1987,** *8*, 323.

(79) Tabata, Y.; Ikada, Y. *Biomaterials* **1988,** *9*, 356.

(80) Roser, M.; Fischer, D.; Kissel, T. *Eur. J. Pharm. Biopharm.* **1998,** *46*, 255.

(81) Mosqueira, V. C. F.; Legrand, P.; Gulik, A.; Bourdon, O.; Gref, R.; Labarre, D.; Barratt, G. *Biomaterials* **2001,** *22*, 2967.

(82) van Wachem, P. B.; Beugeling, T.; Feijen, J.; Bantjes, A.; Detmers, J. P.; van Aken, W. G. *Biomaterials* **1985,** *6*, 403.

(83) Elbert, D. L.; Hubbell, J. A. *Annu. Rev. Mater. Sci.* **1996,** *26*, 365.

(84) Hoffman, A. S. *Macromol. Symp.* **1996,** *101*, 443.

(85) Amiji, M.; Park, K. *J. Biomater. Sci.-Polym. Ed.* **1993,** *4*, 217.

(86) Gref, R.; Minamitake, Y.; Peracchia, M. T.; Trubetskoy, V.; Torchilin, V.; Langer, R. *Science* **1994,** *263*, 1600.

(87) Stolnik, S.; Dunn, S. E.; Garnett, M. C.; Davies, M. C.; Coombes, A. G. A.; Taylor, D. C.; Irving, M. P.; Purkiss, S. C.; Tadros, T. F.; Davis, S. S.; Illum, L. *Pharm. Res.* **1994,** *11*, 1800.

(88) Coleman, D. L.; Gregonis, D. E.; Andrade, J. D. *Journal of Biomedical Materials Research* **1982,** *16*, 381.

(89) Jeon, S. I.; Lee, J. H.; Andrade, J. D.; Degennes, P. G. *J. Colloid Interface Sci.* **1991,** *142*, 149.

(90) Jeon, S. I.; Andrade, J. D. *J. Colloid Interface Sci.* **1991,** *142*, 159.

(91) Josmond, D. W.; Vincent, B.; Waite, F. A. *Colloid and Polymer Science* **1983,** *253*, 676.

(92) Merrill, E. W.; Salzman, E. W. *Am. Soc. Art. Int. Org. J.* **1983,** *6*, 60.

(93) Norman, M. E.; Williams, P.; Illum, L. *Biomaterials* **1993,** *14*, 193.

(94) Norman, M. E.; Williams, P.; Illum, L. *J. Biomed. Mater. Res.* **1993,** *27*, 861.

(95) Gref, R.; Luck, M.; Quellec, P.; Marchand, M.; Dellacherie, E.; Harnisch, S.; Blunk, T.; Muller, R. H. *Colloid Surf. B-Biointerfaces* **2000,** *18*, 301.

(96) Gref, R.; Miralles, G.; Dellacherie, E. *Polym. Int.* **1999,** *48*, 251.

(97) Mosqueira, V. C. F.; Legrand, P.; Morgat, J. L.; Vert, M.; Mysiakine, E.; Gref, R.; Devissaguet, J. P.; Barratt, G. *Pharm. Res.* **2001,** *18*, 1411.

(98) Sofia, S. J.; Premnath, V.; Merrill, E. W. *Macromolecules* **1998,** *31*, 5059.

(99) de Gennes, P. G. *Adv. Colloid Interface Sci.* **1987,** *27*, 189.

(100) Leckband, D.; Sheth, S.; Halperin, A. *J. Biomater. Sci.-Polym. Ed.* **1999,** *10*, 1125.

(101) Nagaoka, S.; Mori, Y.; K., Y.; Tanzawa, H.; Nishiumi, S. In *Polymers as Biomaterials*; Shalaby, S., Hoffman, S., Ratner, D., Horbett, T. A., Eds.; Plenum Press: New York, **1984**, p 361.

(102) Gombotz, W. R.; Guanghui, W.; Horbett, T. A.; Hoffman, A. S. *J. Biomed. Mater. Res.* **1991,** *25*, 1547.

(103) Harder, P.; Grunze, M.; Dahint, R.; Whitesides, G. M.; Laibinis, P. E. *J. Phys. Chem. B* **1998,** *102*, 426.

(104) Prime, K. L.; Whitesides, G. M. *J. Am. Chem. Soc.* **1993,** *115*, 10714.

(105) Feldman, K.; Hahner, G.; Spencer, N. D.; Harder, P.; Grunze, M. *J. Am. Chem. Soc.* **1999,** *121*, 10134.

(106) Yamaoka, T.; Tabata, Y.; Ikada, Y. *J. Pharm. Sci.* **1994,** *83*, 601.

(107) Norman, M. E.; Williams, P.; Illum, L. *Biomaterials* **1992,** *13*, 841.

(108) Stolnik, S.; Felumb, N. C.; Heald, C. R.; Garnett, M. C.; Illum, L.; Davis, S. S. *Colloid Surf. A-Physicochem. Eng. Asp.* **1997,** *122*, 151.

(109) Stenius, P.; Berg, J.; Claesson, P.; Golander, C. G.; Herder, C.; Kronberg, B. *Croat. Chem. Acta* **1990,** *63*, 501.

(110) Ratner, B. D. *J. Biomater. Sci. Polym. Ed.* **1992,** *4*, 3.

(111) Sheu, M. S.; Hoffman, A. S.; Ratner, B. D.; Feijen, J.; Harris, J. M. *J. Adhes. Sci. Technol.* **1993,** *7*, 1065.

(112) Harper, G. R.; Davies, M. C.; Davis, S. S.; Tadros, T. F.; Taylor, D. C.; Irving, M. P.; Waters, J. A. *Biomaterials* **1991,** *12*, 695.

(113) Brindley, A.; Davis, S. S.; Davies, M. C.; Watts, J. F. *J. Colloid Interface Sci.* **1995,** *171*, 150.

(114) Bromley, C. W. A. *Colloids Surf.* **1986,** *17*, 1.

(115) Quellec, P.; Gref, R.; Dellacherie, E.; Sommer, F.; Tran, M. D.; Alonso, M. J. *J. Biomed. Mater. Res.* **1999,** *47*, 388.

(116) Tobio, M.; Gref, R.; Sanchez, A.; Langer, R.; Alonso, M. J. *Pharm. Res.* **1998,** *15*, 270.

(117) Emoto, K.; Nagasaki, Y.; Kataoka, K. *Langmuir* **1999,** *15*, 5212.

(118) Van Delden, C. J.; Bezemer, J. M.; Engbers, G. H. M.; Feijen, J. *J. Biomater. Sci. Polym. Ed.* **1996,** *8*, 251.

(119) Han, D. K.; Park, K. D.; Ryu, G. H.; Kim, U. Y.; Min, B. G.; Kim, Y. H. *J. Biomed. Mater. Res.* **1996,** *30*, 23.

(120) Blunk, T.; Luck, M.; Calvor, A.; Hochstrasser, D. F.; Sanchez, J. C.; Muller, B. W.; Muller, R. H. *Eur. J. Pharm. Biopharm.* **1996,** *42*, 262.

(121) Torchilin, V. P. *Eur. J. Pharm. Sci.* **2000,** *11*, S81.

(122) Poste, G.; Kirsh, R. *Biotechnology* **1983,** *1*, 869.

(123) Gregoriadis, G. *Nature* **1977,** *165*, 407.

(124) Davis, S. S.; Illum, L.; Stolnik, S. *Curr. Opin. Colloid Interface Sci.* **1996,** *1*, 660.

(125) Allen, T. M.; Brandeis, E.; Hansen, C. B.; Kao, G. Y.; Zalipsky, S. *Biochim. Biophys. Acta-Biomembr.* **1995,** *1240*, 285.

(126) Bendas, G.; Krause, A.; Bakowsky, U.; Vogel, J.; Rothe, U. *Int. J. Pharm.* **1999,** *181*, 79.

(127) Mosqueira, V. C. F.; Legrand, P.; Gref, R.; Heurtault, B.; Appel, M.; Barratt, G. *J. Drug Target.* **1999,** *7*, 65.

(128) Hansen, C. B.; Kao, G. Y.; Moase, E. H.; Zalipsky, S.; Allen, T. M. *Biochim. Biophys. Acta-Biomembr.* **1995,** *1239*, 133.

(129) Zalipsky, S.; Hansen, C. B.; deMenezes, D. E. L.; Allen, T. M. *J. Control. Release* **1996,** *39*, 153.

(130) Basinska, T.; Slomkowski, S. *J. Biomater. Sci.-Polym. Ed.* **1991,** *3*, 115.

(131) Maruyama, K.; Takizawa, T.; Takahashi, N.; Tagawa, T.; Nagaike, K.; Iwatsuru, M. *Adv. Drug Deliv. Rev.* **1997,** *24*, 235.

(132) Emanuel, N.; Kedar, E.; Bolotin, E. M.; Smorodinsky, N. I.; Barenholz, Y. *Pharm. Res.* **1996,** *13*, 352.

(133) Mercadal, M.; Domingo, J. C.; Petriz, J.; Garcia, J.; de Madariaga, M. A. *Biochim. Biophys. Acta-Biomembr.* **2000,** *1509*, 299.

(134) Hoffman, W. L.; Oshannessy, D. J. *J. Immunol. Methods* **1988,** *112*, 113.

(135) Fischer, B.; Heyn, S. P.; Egger, M.; Gaub, H. E. *Langmuir* **1993,** *9*, 136.

(136) Shriver-Lake, L. C.; Donner, B.; Edelstein, R.; Breslin, K.; Bhatia, S. K.; Ligler, F. S. *Biosens. Bioelectron.* **1997,** *12*, 1101.

(137) Chang, T. M. S. *Artificial cells*; Charles C Thomas: Springfield, **1972**.

(138) Djordjevich, L.; Miller, I. F. *Exp. Hematol.* **1980,** *8*, 584.

(139) Phillips, W. T.; Klipper, R. W.; Awasthi, V. D.; Rudolph, A. S.; Cliff, R.; Kwasiborski, V.; Goins, B. A. *J. Pharmacol. Exp. Ther.* **1999,** *288*, 665.

(140) Yu, W. P.; Chang, T. M. S. *Artif. Cells Blood Substit. Immobil. Biotechnol.* **1996,** *24*, 169.

(141) Yu, W. P.; Chang, T. M. S. *Artif. Cells Blood Substit. Immobil. Biotechnol.* **1994,** *22*, 889.

(142) Chang, T. M. S.; Yu, W. P., Great Britan Patent, No. 92194265, **1992**.

(143) Barratt, G. *Cell. Mol. Life Sci.* **2003,** *60*, 21.

(144) Nardin, C.; Widmer, J.; Winterhalter, M.; Meier, W. *Eur. Phys. J. E* **2001,** *4*, 403.

(145) Graff, A.; Sauer, M.; Van Gelder, P.; Meier, W. *Proc. Natl. Acad. Sci. U. S. A.* **2002,** *99*, 5064.

(146) Nardin, C.; Thoeni, S.; Widmer, J.; Winterhalter, M.; Meier, W. *Chem. Commun.* **2000**, 1433.

3

# Polyethylene glycol grafted polystyrene particles

ABSTRACT: Highly pegylated particles, which can serve as a model system for artificial cells, were prepared by covalently grafting amino polyethylene glycol (PEG, molecular weight 3400, 5000) onto carboxyl polystyrene particles (PS-COOH) using carbodiimide chemistry. PEG modified particles (PS-PEG) were characterized by determination of the PEG surface concentration, zeta-potential, size and morphology. Under optimized grafting conditions, a dense "brush-like" PEG layer was formed. A PEG surface concentration of approximately 60 $p$mol/cm^2 corresponding with an average distance between grafted PEG chains of ~17 Å can be realized. It was shown that by grafting PEG onto PS-COOH the adsorption of protein from human plasma in PBS (85 v.%) could be reduced up to 90 % as compared to PS-COOH.

INTRODUCTION

Tailoring the surface properties of polymeric nano-/microspheres and particles in order to prevent rapid clearance via opsonization and subsequent removal by the mononuclear phagocyte system (MPS) has received great interest, especially with respect to carriers for controlled drug delivery[1-4]. The removal of particles by the MPS begins with the adsorption of plasma proteins on the surface. It is known that protein adsorption can be reduced by grafting the particle surface with hydrophilic, nonionic polymer chains especially poly(ethylene glycol) (PEG), which can give "stealth" properties to the particles[4,5]. The protein resistant character of PEG is generally ascribed to a combination of the low interfacial energy of PEG with water[6] and its steric stabilization effect[7,8]. The PEG molecular weight and PEG surface concentration as well as molecular conformation are of importance for preparing non-fouling surfaces. Long PEG chains and high PEG surface concentrations are desirable for the resistance to protein adsorption[7,8]. Moreover, thiolated oligo (ethylene oxide) (2-6 units) self assembled onto gold surfaces into monolayers also reveals a high resistance against protein adsorption. This has been ascribed to a high surface density and a helical structure of ethylene oxide oligomers[9,10].
Pegylation of a surface can be achieved by adsorbing PEG-containing block copolymers like PEO/PPO[11,12] or PDLLA/PEO[13] on the surface, surface grafting using established strategies[14,15], depositing PEG-like coatings using a radio-frequency glow discharge technique[16,17], or forming self assembled monolayers[10]. However, to obtain pegylated microsphere surfaces, the last two methods are not straightforward, and physical adsorption of PEG-containing copolymers is plagued by the possible desorption of the copolymer from the particle surface during contact with blood. Covalent grafting of PEG via functional groups present on the surface[18,19] is well controllable in terms of PEG length, density and orientation.

Furthermore, surface pegylation of particles can be readily obtained via the following methods: the emulsion polymerization of PEG-containing comonomers[20-22], and the formation of nano-particles[23,24] or micelles[25] from PEG-containing block copolymers. Nevertheless, they have limitations with respect to molecular weight of the PEG used, particle size and PEG density obtained.

Despite that many studies have shown that PEG surfaces can reduce protein adsorption, there are still no general requirements for the PEG surfaces needed in preventing protein adsorption. This is partially because there is a lack of efficient strategies which only involve non-toxic, water soluble reagents and can yield PEG (with different molecular weights, MW) surfaces with a wide range of PEG surface concentrations (including the "brush" regime).
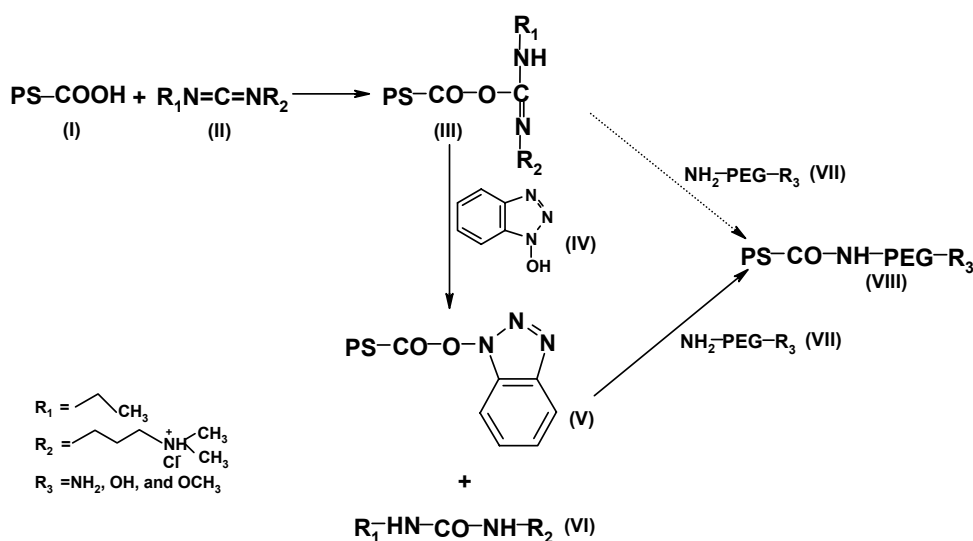
Scheme 1. *Modification of carboxyl polystyrene particles with PEG via carbodiimide chemistry. Carboxyl groups on PS-COOH (I) are activated by 1-dimethylaminopropyl-ethylcarbodiimide hydrochloride (EDC, II) into O-acylisourea groups (III), which are prone to hydrolysis and rearrangement. A trapping agent 1-hydroxybenzotriazole (HOBt, IV) is used to convert O-acylisoureas into HOBt activated esters (V) and dimethylaminopropylethyl urea (VI). The amine groups of PEG (VII) react with the HOBt activated esters leading to PEG modified particles (PS-PEG, VIII).*

The aim of this study is to prepare PEG surfaces with a wide range of surface concentrations by covalently attaching PEG onto carboxyl polystyrene particles and to get insight in the effect on protein adsorption. The results can be used to design artificial cells, which show minimal protein adsorption, thus prevent opsonization, resulting in long circulation times. This chapter reports the preparation and characterization of PEG modified carboxyl polystyrene particles (PS-PEG) obtained via the carbodiimide method (Scheme 1). Carboxyl polystyrene particles used in this study are commercially available and can be obtained with different surface concentrations of carboxyl groups and with a wide range in size and a narrow size distribution. Therefore these particles are ideal as a model system for artificial cells and can be used to study the effect of pegylation on the properties of the particles including protein adsorption. The carbodiimide method was chosen for surface grafting since it affords high efficiency in peptide synthesis[26,27] and the reagents used, 1-dimethylaminopropyl-ethylcarbodiimide

hydrochloride, N-hydroxysuccinimide or 1-hydroxybenzotriazole are water-soluble and nontoxic. PS-PEG was prepared by reacting carboxyl polystyrene particles (PS-COOH) with homo- and hetero- bifunctional PEG that contained an amino end group for immobilization and an amino, hydroxyl or methoxy end group that is exposed at the surface after immobilization. The PEG surface concentration, zeta potential, morphology, stability and protein adsorption of the particles were determined. Detailed study on the effect of PEG (MW, surface concentration and end group) on protein adsorption from human plasma is the subject of chapter 4.

MATERIALS AND METHODS

Materials

Ultra-clean carboxyl polystyrene particles (batch no. 1163: diameter= 1.45 μm; surface area per carboxyl group= 109 Å^2) and amidine PS particles (batch no. 10-273-60,1: diameter= 1.45 μm; surface area per amidine group= 83 Å^2) were purchased from Interfacial Dynamics Corporation (Portland, Oregon, USA). α,ω-Di-amino-poly(ethylene glycol), chromatographically pure, MW 3400 (diamino PEG 3400), α-amino, ω-methoxy-poly(ethylene glycol), chromatographically pure, MW 5000 (methoxy amino PEG 5000) and α-amino, ω-hydroxy-poly(ethylene glycol) MW 3400 (hydroxyl amino PEG 3400) were bought from Shearwater Polymers, Inc. (Huntsville, AL, USA). 1-Dimethylaminopropyl-ethylcarbodiimide hydrochloride (EDC), N-hydroxy-succinimide (NHS), 1-hydroxybenzotriazole (HOBt), 2-(N-morpholino)ethanesulfonic acid (MES) and N-tri(hydroxymethyl)methyl-2-aminoethanesulfonic acid (TES) were obtained from SIGMA Chemical Inc. (St. Louis, MO, USA). 2,4,6-Trinitrobenzene sulfonic acid (TNBS) solution (1 M) and barium hydroxide solution (0.05 M) were obtained from FLUKA Chemical (Buchs, Switzerland). Phosphate buffered saline (PBS) (pH 7.4) was purchased from NPBI (Emmer Compascuum, The Netherlands). Micro BCA protein assay kit was purchased from Pierce (Rockford, IL, USA). Polystyrene (Mw 50,000) was supplied by PolyScience, Inc. (Warrington, PA, USA). De-ionized water (DI water) was obtained from a Milli-Q water purification system (Millipore, Molsheim, France). All other chemicals were from Merck (Darmstadt, Germany) and used as received.

Conductometric titration of carboxyl groups on PS-COOH particles

The surface concentration of carboxyl groups on PS-COOH particle was determined by conductometric titration with a 0.005 M Ba(OH)$_2$ solution[28], which was prepared by a standardized method from a 0.05 M stock solution[29]. One drop (ca. 20 μL) of 0.04M HCl and 0.5 mL of PS-COOH suspension (3 wt.%) were added to 25 mL of DI water (final pH 4.5-5). The mixture was titrated with the 0.005M Ba(OH)$_2$ solution at a rate of 0.01 mL/min using a Titrino 702 SM pH-stat (Metrohm, Herisau, Switzerland). The conductivity of the mixture was continuously measured by a conductometer (Konduktometer CG 845, Schott Geräte GmbH, Mainz, Germany) and recorded. Blanks were obtained by titrating 25.5 mL of DI water in the same way without adding the particle suspension. All titrations were carried out at room temperature. The surface concentration of COOH groups was determined from the titration curves by calculating the Ba(OH)$_2$ consumption by the COOH groups comparing to the blank titration and the surface area.

Immobilization of PEGs containing at least one amine end group (amino PEG)

Immobilization of amino PEG onto PS-COOH using EDC in the presence of NHS or HOBt was carried out in an aqueous solution at 4ºC. Solutions of EDC, HOBt and NHS were freshly made. The effect of variables on the immobilization reaction was studied by varying the activation (reaction of EDC with COOH groups) time up to 2 h, activation pH in between 5.3 and 7.3, and the EDC/COOH molar ratio

from 0 to 8. Either NHS or HOBt activated esters were prepared from EDC activated carboxyl PS particles with NHS/EDC or HOBt/EDC ratios of 0.3 or 0.4. The coupling reactions of amino PEG were performed for different times up to 68 h in the pH range of 5.3 to 11.5 and at PEG concentrations up to 12 wt.%.

In a typical immobilization procedure, 4.04 mL of a PS-COOH particle suspension (3 wt.%, 0.1211g, 0.75 μmol COOH groups) suspended in DI water (3.2 mL) was pipetted into a tube. Stock solutions of 12 mM HOBt and 30 mM EDC in DI water were adjusted to pH 5.3 using 0.01M NaOH and 0.2 mL of each solution was added to the suspension. After 30 min a solution of diamino-PEG 3400 (0.42 g in 1.65 mL of DI water) was added. Then the pH of the mixture was adjusted to 8.6 using 0.5 M NaOH. After 44 h the reaction was terminated by adjusting the pH of the mixture to 12 using 1.0 M NaOH and kept for 5 min. This treatment results in hydrolysis of activated carboxyl groups and deprotonation of the amine groups of PEG. Subsequently, the suspension was centrifuged at 10000×g for 8 min at room temperature and the supernatant was discarded. PEG-modified particles were then washed once with 5 mL of HCl (0.01 M) followed by washing three times with 5 mL of PBS via redispersion and centrifugation. Finally the particles were re-suspended in PBS (1.61 wt.%) and stored at 4ºC until use. The efficiency of the removal of free PEG by the washing procedure was examined using a TNBS assay (see the following part).

Determination of PEG surface concentration

TNBS method: The surface concentration of diamino PEG was determined by measuring free amine groups using a TNBS assay. Borate buffer (1.2 mL, 0.1M, pH 9.0) and TNBS solution (300 μL, 6 mM) were added to 0.3 mL of a suspension of PS-PEG particles (1.61 wt.%) and stirred for 2 h at 37ºC. After centrifugation at 10000×g for 10 min the supernatant containing the un-reacted TNBS was collected. To 0.2 mL of the supernatant, 1.5 mL of borate buffer and an excess amount of 1,8-diamino-3,6-dioxaoctane (0.5 mL, 3 mM) were added. After reaction at 37ºC for 40 min and cooling to room temperature, the concentration of the TNBS derivative, thus the un-reacted TNBS, was determined by UV spectrophotometry (CARY 300 BIO UV visible spectrophotometer) at 421 nm using a calibration curve. The calibration curve was obtained similarly as in the above-mentioned procedure only by replacing the TNBS sample solutions with 0.2 mL of TNBS solutions with known concentrations (0.75, 0.30, 0.15 and 0.075 mM). For a blank, 1,8-diamino-3,6-dioxaoctane solution was substituted by DI water. By applying the absorbance at 421 nm in the calibration curve, the amount of un-reacted TNBS in the supernatant can be determined. By subtracting the amount of un-reacted TNBS from the total amount of TNBS added, the PEG surface concentration was derived from the TNBS consumption by the surface amine groups.

NMR measurement: The PEG surface concentration can be obtained by determining the weight percentage of PEG in PS-PEG by H[1] NMR spectroscopy. To a PS-PEG suspension in PBS (~0.4 mL, 1.61 wt.%), 1.5 mL of DI water were added. The sample was centrifuged and the supernatant was discarded. The pellet was dried in a vacuum oven for 24 h before dissolved in CDCl$_3$. Long delay (dl=15 sec) proton NMR (H[1]L NMR, 300 MHz) spectra were recorded on a Varian Inova Spectrometer with chemical shifts relative to the non-deuterated solvent peak (CHCl$_3$, δ 7.25). For the calibration curve, mixtures of monomethoxy polyethylene glycol (Mw 5000) and polystyrene (Mw 50000) with known weight percentage of PEG were dissolved in CDCl$_3$ and NMR spectra were recorded. The calibration curve was obtained by plotting the integral ratios of different polystyrene protons (at δ: 6.85-7.25 (3H, arom.), 6.28-6.85 (2H, arom.), 1.70-2.40 (1H, CH) and 1.20-1.70 (2H, CH$_2$)) to the PEG methylene protons (δ 3.63) against the PEG percentages in the PS/PEG mixtures. For PS-PEG samples, by measuring the integral ratios of different PS protons to PEG protons in the calibration curves, average PEG percentages can be derived. With the known surface area of the particles used, the surface concentration of PEG can be determined accordingly.

ξ-Potential measurement

Zeta potentials of the particles were measured with a Zetasizer 2000 instrument (Malvern Instruments Ltd, Malvern, UK) using the Laser Doppler Velocimetry (LDV) technique in which the velocity of particles in a fluid that results from an applied electric field, is measured. By applying the Smoluchowski equation[30] the ξ-potential can be determined. Measurements were carried out at 25ºC, a 1000Hz modulator frequency and a cell drive voltage of 120V. All samples were diluted with DI water (~pH 5.5) to obtain a proper particle concentration, and the conductivity was adjusted to 0.03 mS/cm by adding NaCl solution (10 mM). Data presented are the mean of measurements of three samples, which were each measured 4 times.

To study the influence of the pH on the zeta-potential of PS and PS-PEG particles, 0.01 M MES (pH 3, 4, 5 or 6) and TES buffer (pH 7, 8 or 9) were used to dilute the particles. Measurements were performed at a conductivity of ~1.00 mS/cm under otherwise the same conditions as described above.

Morphology

For SEM, a particle suspension (ca. 0.02 mL of 1.61 wt.%) was added to 1.5 mL of DI water. The mixture was centrifuged to remove the supernatant. The solid particles were then re-suspended in 0.1 mL of DI water and placed on a polished aluminum sample holder. The sample was dried in air for 24 h before visualization by SEM (HITACHI S800 Field emission scanning electron microscopy) at magnifications ranging from 2000× to 15000×. For the morphology of the particles in the wet state (in PBS), a drop of particle suspension was directly put in between two clean glass slides and observed by light microscopy (LM, magnification: 100×). The particle size was measured after calibration with standard polystyrene lattices. The results of the particle size analysis were based on ~30 particles per sample.

Protein adsorption

Freshly frozen, citrated human plasma was obtained from the Blood Transfusion Service Twente-Achterhoek (Enschede, The Netherlands). In a typical adsorption experiment, 0.4 mL of a PS-PEG suspension (1.61 wt.%) was incubated with the plasma in PBS with a final concentration of 85 v.% at 37ºC for 2 h. Subsequently, the plasma was removed and the particles were washed four times with PBS via centrifugation (10000 g for 8 min) and redispersion. Proteins were desorbed from the particle surface by adding 1.5 mL of sodium dodecyl sulfate (SDS, 6 wt.%) solution in DI water at 40ºC in a Bransonic® ultrasonic cleaner (70w, Branson Ultrasonics Corporation, Danbury, Connecticut, USA). After centrifugation the supernatant was collected and diluted to determine the protein concentration by a micro BCA assay according to the procedure recommended by the supplier.

RESULTS AND DISCUSSION

PS-COOH surfaces were used as a model system to study the effect of pegylation reaction conditions on the PEG surface concentrations. The PEG surface concentration, zeta potential, morphology and the stability of the PEG modified PS-COOH were investigated. These pegylated surfaces were used to study the effect of surface pegylation on protein adsorption from human plasma (85 v.%) in PBS.

Properties of carboxyl polystyrene particles (PS-COOH)

The surface properties of PS-COOH that was used in this study were determined. The mobility and ξ-potential in NaCl solution (pH 5.4, ~0.02 mM) were -5.543×10^{-8} m^2/sec/V and -69.5 ± 2.1 mV, respectively. The particles had smooth surfaces and a mean diameter of 1.56 μm as

measured by SEM and light microscopy. The surface concentration of COOH groups was determined via conductometric titration. An excess of hydrochloric acid was added to the particle suspension to ensure that all surface carboxylic acid groups were protonated. Titration with a $Ba(OH)_2$ solution resulted in the titration curve as shown in Figure 1, in which three stages are observed. The shape of the titration curve suggests a surface with weak acid groups. The first stage corresponds to the titration of strong acid (H_3O^+), the second stage to the titration of carboxylic acid groups and the third is due to the increase of the ion concentration resulting from the $Ba(OH)_2$ addition. A surface concentration of COOH groups of 153±6 *p*mol/cm^2 can thus be calculated.
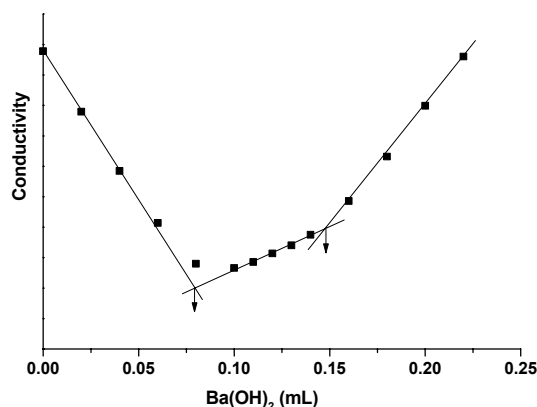

Figure 1. *Conductometric titration of carboxyl polystyrene particles. One drop of HCl solution (0.04 M) was added to a suspension of PS-COOH (0.5 mL, surface area of 610 cm^2) in 25 mL of DI water. Then the suspension was titrated with a 0.005M Ba(OH)$_2$ solution at a rate of 0.01 mL/min. The conductivity was recorded. Blanks were obtained by titrating 25.5 mL of DI water in the same way without adding the particle suspension.*

Effect of activation time on the coupling of diamino-PEG onto PS-COOH

The immobilization of PEG onto the PS-COOH was performed by activation of the free carboxyl groups and subsequent reaction with diamino PEG. Activation of the carboxyl groups was performed by reaction with EDC. The thus obtained O-acylisourea is prone to fast hydrolysis and was therefore converted into the corresponding HOBt esters. The hydrolysis of resulting HOBt esters is much slower and the nucleophilic reaction with diamino-PEG at a pH 8.5 is fast enough to compete with it. An activation time of 30 min afforded the highest PEG surface concentration, which was also indicated by zeta potential data (Figure 2).

Influence of Trapping agent and coupling time

A trapping agent (HOBt or NHS) in combination with carbodiimide has been used to suppress side reactions such as N-acyl urea formation[26,27]. HOBt or NHS reacts rapidly with the O-acylisourea to form activated esters, which also can rapidly acylate amine groups, and thus prevent the rearrangement into inactive N-acyl urea. Figure 3 shows the zeta potential and PEG surface concentration of PS-PEG as a function of coupling time for both trapping agents. The coupling reaction, as expected, was quite slow due to the heterogeneity of the system. The increase in PEG surface concentration with immobilization time leveled off after coupling for 44 h. Although the differences were small, the EDC/HOBt system seems to be somewhat more effective to obtain a high PEG surface concentration than the EDC/NHS system. This could be

due either to the higher yield or the higher stability of the HOBt ester towards hydrolysis. Moreover, a higher reactivity of the HOBt ester, due to the participation of the heterocyclic nitrogen in the formation of a H-bond with the nucleophilic amine in the transition state, and to the fact that the oxybenzotriazole anion is a better leaving group (HOBt is a relatively strong acid (pKa 4.0))[31] may contribute to a more efficient PEG coupling. Additionally, side reactions occurring between NHS and carbodiimide could diminish the coupling yield of this system[27].

The zeta-potential of the particles, which is the potential at the shear plane, gives an indication of the net charge on the surface of solid particles[30]. The change in zeta potential between surface modified and bare particles has been used to calculate the thickness of the layer of grafted or adsorbed polymers[32,33]. In this study, the covalent grafting of nonionic PEG molecules on the PS-COOH surface not only consumes surface carboxylic acid groups but also displaces the shear plane further from the PS particle surface. This will lead to an increase of the zeta-potential, which becomes less negative. The higher the PEG surface concentration, the less surface carboxyl groups are left and the further the shear plane is located away from the PS particle surface. Therefore, it is reasonable to correlate the zeta-potential and the PEG surface concentration, as is also demonstrated in Figure 2 and Figure 3.

Figure 4 displays a linear relationship with a correlation coefficient of 0.988 between the zeta-potential and the surface concentration of grafted diamino PEG 3400. The PEG surface concentration that was determined by the TNBS assay and H^1L NMR agreed reasonably ($\pm20\%$, see Table I). An increase of the PEG surface concentration leads to a less negative zeta-potential. This shows that the zeta-potential can be used to estimate the PEG surface concentration. Nevertheless, for a given particle-PEG system this relationship will depend on the nature (e.g. end group and length) of the PEG that is used as well as on the density of the surface charge of the starting particles and the immobilization chemistry.
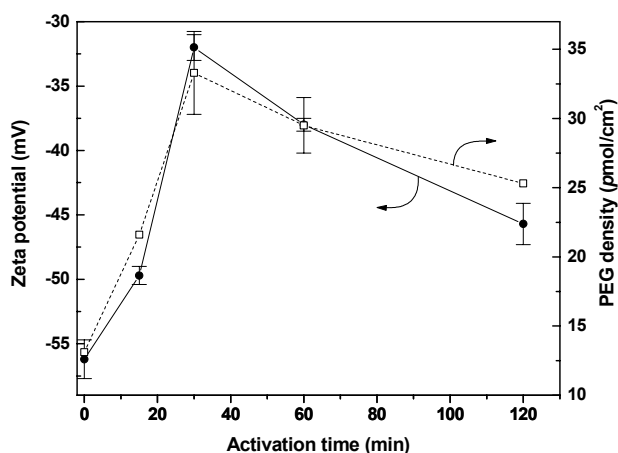

Figure 2. *Influence of the activation time of COOH groups on PS-COOH particles on the PEG surface concentration (□, right axis) and the zeta-potential (pH 5.5) of PS-PEG (●, left axis). Diamino PEG 3400 immobilization conditions: all reactions were conducted at 4°C under stirring. The activation step was conducted at pH 5.3 with a molar ratio EDC/HOBt/COOH of 8:3.2:1. The amino PEG coupling was performed at pH 8.5 for 68 h with a PEG concentration of 8 wt.%. Data points without error bar represent the average of two measurements. Data points with error bars represent the average of three measurements ±s.d.*

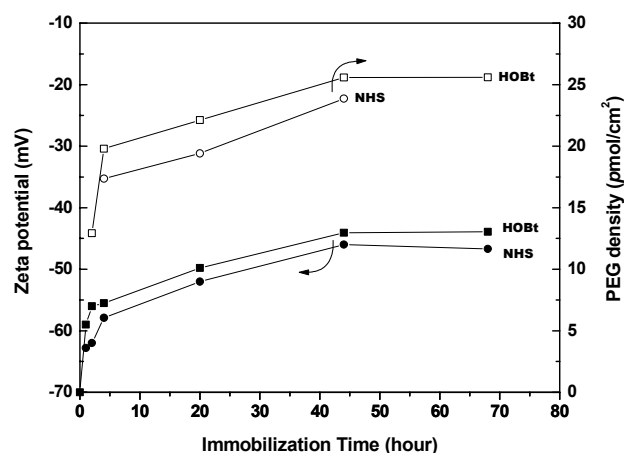***Figure 3.*** *Influence of immobilization time and type of trapping agent (HOBt or NHS) on the PEG surface concentration (○, □, right axis) and the zeta-potential (●, ■, left axis) of PS-PEG. Diamino PEG 3400 immobilization conditions: the activation step was conducted at pH 5.3 for 30 min with a molar ratio EDC/trapping agent/COOH of 2:0.6:1. The amino PEG coupling was performed at pH 8.5 with a PEG concentration of 8 wt.%. Other conditions are the same as mentioned for Figure 2.*
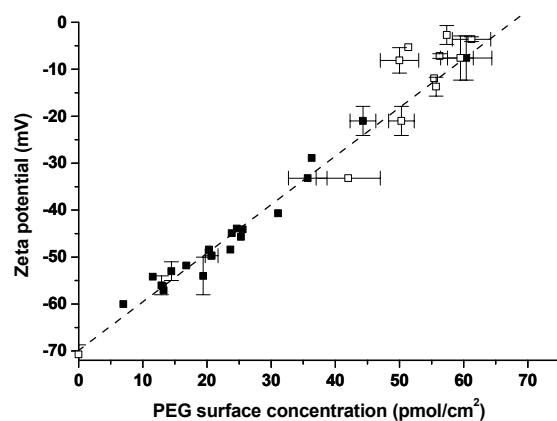

Figure 4. *Correlation between the zeta-potential and the surface concentration of grafted amino PEG (diamino PEG 3400). The surface concentration of PEG was determined with the TNBS assay (■) and/or H^1L NMR (□) measurements, and the dashed line is the linear fit of the TNBS results: $Y= -72.30+1.15X$, $R=0.988$.*

At a high surface concentration of diamino PEG3400, i.e., 60 pmol/cm^2, which corresponds with ca. 40% substitution of surface COOH groups, and a pH≤ 5.5, positive zeta potentials should be possible. However, no positive zeta potentials of the PS-PEG particles were observed in this study. This could be because the amine groups are not protruding out of the PEG layer thus do not contribute much to the positive zeta potential, and/or because the amine groups could not compensate the negative charge of the surface.

Effect of the pH

Generally, using carbodiimide chemistry, activation of carboxyl groups requires acidic to neutral media (pH 4-7)[27]. However, PS-COOH particles (pKa ~5.0) aggregate in acidic media (pH ≤ 5). Therefore, it is expected that there will be an optimal pH for the activation step including the activation of the COOH groups by EDC, subsequent conversion into a HOBt

activated ester, the hydrolysis and the O-N shift. Similarly, the optimal pH for PEG immobilization is a compromise between a relatively high pH to deprotonate amine groups (pKa of diamino PEG 3400 is 9.2[18]) and a low pH to prevent deactivation of activated esters. Therefore, pH ranges of 5.3-7.3 for the activation of carboxyl groups and 5.3-11.5 for the immobilization of diamino-PEG were used to investigate the effect of pH on the immobilization of PEG. Figure 5 shows the influence of the pH during activation and incubation on the zeta potential of the particles after PEG immobilization. For PS-COOH activation a low pH (~5.3), close to the pKa of surface COOH groups, is beneficial. For PEG immobilization a high pH (8.5-9.2), near the pKa of diamino PEG 3400, is favorable for obtaining a high surface concentration of PEG.
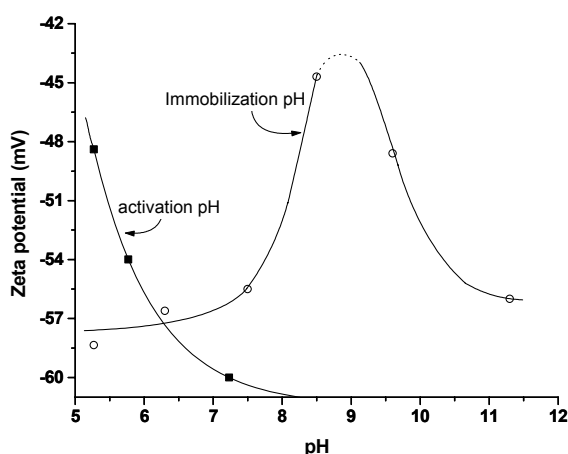

Figure 5. Effect of the pH in the activation and coupling reaction on the zeta-potential of the resulting PS-PEG. Diamino PEG 3400 immobilization conditions: (■) Influence of the pH in the activation reaction: the activation step was conducted at a molar ratio EDC/HOBt/COOH of 2:0.6:1 for 30 min; and amino PEG coupling at pH 8.5 for 68 h with a PEG concentration of 8 wt.%. (○) Influence of the pH in the PEG coupling reaction: the activation reaction was conducted at pH 5.3 for 30 min with a molar ratio EDC/HOBt/COOH of 8:3.2:1; and the amino PEG coupling was carried out with a PEG concentration of 4 wt.% for 68 h. Other conditions are the same as mentioned for Figure 2.

Effect of EDC/COOH molar ratio

A molar ratio of HOBt/EDC of 0.1-0.4 was the most effective for peptide synthesis in a N,N-dimethylformamide/water mixture, giving 100% yield[26]. Also an NHS/EDC ratio of 0.1-0.4 as used in the cross-linking of collagen[34] and gelatin[35] has been shown to give optimal results. Therefore, to study the influence of the EDC/COOH molar ratio on the surface concentration of PEG, the molar ratio of HOBt/EDC was kept constant at 0.4 and the ratio of EDC/COOH was varied from 0 to 8. The zeta-potentials of the obtained PS-PEG increased (became less negative) with increasing EDC/COOH molar ratio (Figure 6), indicating an increase of PEG surface concentration with increasing EDC concentration. However, at an EDC/COOH ratio >~6, there was no effect of further increase of the ratio on the zeta-potential, probably due to the high ratio of HOBt/COOH (> 2.4), which may cause competitive hydrolysis of HOBt activated esters in water-containing media, which is accelerated by the presence of excess acidic HOBt.[26] Thus it can be concluded that for a HOBt/EDC ratio of 0.4 EDC/COOH should be higher than 6. However, other HOBt/EDC ratio's could result in other optimal EDC/COOH
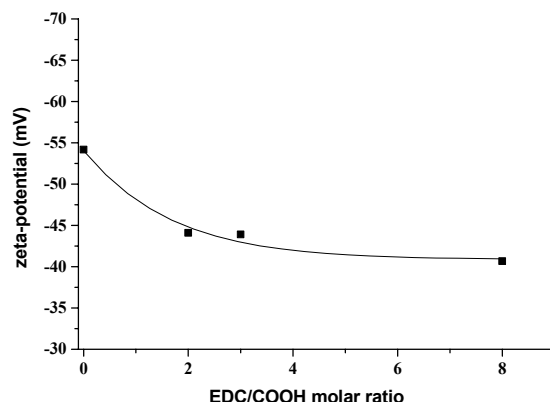
ratio's.

Figure 6. *Effect of the molar ratio of EDC and COOH used for PEG immobilization on the zeta-potential of PS-PEG at fixed molar ratio EDC/HOBt of 1:0.4. Diamino PEG 3400 immobilization conditions: the activation reaction was conducted at pH 5.3 for 30 min; and the amino PEG coupling reaction was at pH 8.5 for 68 h with a PEG concentration of 4 wt.%. Other conditions are the same as mentioned for Figure 2.*

Effect of the PEG concentration in feed

Figure 7 displays the effect of the concentration of diamino PEG 3400 used for the coupling reaction on the zeta potential of PS-PEG. In the range from 0 to 4 wt.%, a substantial increase of the zeta-potential (less negative) of PS-PEG was observed with increasing PEG concentration in the feed. At higher PEG concentrations (4-8 wt.%) only a small additional increase was found, which is due to the inherent chain repulsion that retards further increase of the PEG surface concentration. In further experiments a high PEG concentration (8 wt.%) was used for coupling of diamino PEG in order to obtain a high PEG surface concentration, and to minimize the possibility of grafting PEG with both end groups on the particle surface.
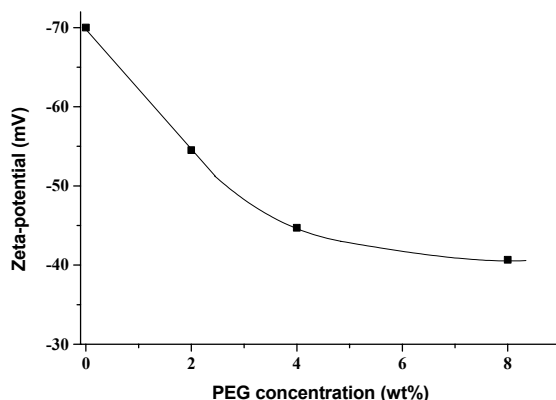

Figure 7. *Influence of the diamino PEG 3400 concentration in the feed on the zeta-potential of PS-PEG. PEG immobilization conditions: the activation reaction was conducted at pH 5.3 for 30 min with a molar ratio EDC/HOBt/COOH of 2:0.6:1; and the amino PEG coupling reaction was at pH 8.5 for 68 h. Other conditions are the same as mentioned for Figure 2.*

Estimation of the conformation of PEG on the particle surface

Knowledge about the conformation of PEG on the particle surface can help to predict the protein resistance of a particle surface. In order to do so, we calculated the average distance between graft sites and the thickness of the surface PEG layer. This calculation is based on the de Gennes theory[36] of grafted linear, flexible and neutral polymers in good solvents. The average distance between two graft sites, D, is given by the square root of the area, A, occupied by a single PEG molecule on the particle surface (as calculated from PEG surface concentration, d in pmol/cm^2),

$$D = \sqrt{\frac{4}{\pi} A} = \sqrt{\frac{1.21 \times 10^{28}}{A_0 \times d}} \quad (A_0, \text{ Avogadro constant, } 6.02 \times 10^{23}/\text{mol, and } D \text{ in Å}) \qquad (1)$$

The coil size (the Flory radius) R_F, of a polymer of N subunits of length a is

$$R_F = a \cdot N^{3/5}. \qquad (2)$$

When D is not smaller than R_F ($D \geq R_F$), the thickness of the PEG layer L equals R_F. The average shape of the polymer on the surface is a mushroom with a size of R_F. In this regime, the polymer is assumed to interact neither with the surface nor with its nearest neighbors.

When D is smaller than R_F ($D < R_F$), the polymers will interact laterally and will stretch farther out from the surface. Based on the scaling theory a dense polymer "brush" is formed on the surface if $D \ll R_F$. The overall thickness of the PEG polymer brush, L, is

$$L = a \cdot N(a/D)^{2/3}. \qquad (3)$$

In case of our model PEG with a Mw of 3400, N is 77, a is 3.5 Å [37], R_F is ~47.6 Å. For a PS-PEG with a PEG surface concentration of ~60 $p$mol/cm^2, D is ~16.6 Å. This distance is much smaller than R_F, indicating a large extent of PEG chain overlapping and a "brush-like" regime. The thickness of the PEG layer L would be 95.5 Å. It has been suggested that the minimal thickness of a nonionic hydrophilic layer to reduce van der Waals attraction and hydrophobic interaction and to prevent the adsorption of BSA and IgG is ~50 Å[15]. On the other hand, protein adsorption will also depend on the size of the proteins. However, a high density of long PEG molecules combined with an associated water layer is able to prevent even small proteins to approach, due to the flexibility of the PEG in aqueous environment. Therefore, the interaction between PS-PEG with a high surface concentration of PEG is minimized, and protein adsorption onto these particles is expected to be prevented to a large extent.

Microscopic Characterization and stability of PS-PEG particles

The morphology study showed that PS-PEG in both the wet and the dry state are spherical without significant deformation. As compared to unmodified PS-COOH, PS-PEG did not show significant differences in size in the dry state (SEM), but it displayed some swelling in the wet state (LM) due to the presence of the hydrophilic PEG on the surface.

The pegylation process resulted in a stable PEG layer as shown by negligible PEG leakage from the surface during storage in PBS at 4°C for a period of 3 months as checked by UV measurement of the supernatant and zeta-potential measurement of the particles. It was

observed that PS-PEG with a high PEG surface concentration ($>$ ~35 $p$mol/cm^2) did not aggregate in aqueous solutions at a pH between 2 and 12 and at high ionic strength (1.5 M NaCl). In contrast, PS-COOH flocculated at pH $\leq$ 5.0 and/or at [NaCl] $\geq$ 0.3 M. The stability of PS-PEG with a "brush-like" PEG layer in aqueous media with a high concentration of ions results from the highly hydrated PEG layer that does not allow to be compressed thus preventing aggregation. This effect is also known as the steric repulsion effect[8].

In the pH range of 3-9, the zeta potentials of PS-COOH and PS-PEG with a relatively low surface concentration of PEG (20 $p$mol/cm^2) decreased (became more negative) with increasing pH (Figure 8). This is due to the deprotonation of carboxylic acid groups on the particle surface with the increase of pH. PS-PEG with PEG surface concentration of ~20 $p$mol/cm^2 showed much less decrease as compared to PS-COOH. For these PS-PEG a relatively small shift of the shear plane from the PS surface and little consumption of surface COOH groups has occurred, so the dissociation of COOH groups of the PS-COOH (pKa ~5) could be still observed as indicated by the presence of a gentle inflexion at ~pH 6. In contrast, the zeta-potential of PS-PEG with a higher PEG surface concentration ($\geq$~35 $p$mol/cm^2) was relatively constant. Minor or no inflexion indicated negligible or no charged groups on the surface of PS-PEG, resulting from the shift of the shear plane to the position located in the PEG layer and/or the shielding of unreacted COOH by the coverage of PEG. Together with the observation of the stability of the particles, it is concluded that the PS-PEG was stabilized by steric repulsion of highly hydrated PEG chains and not by electrostatic repulsion.
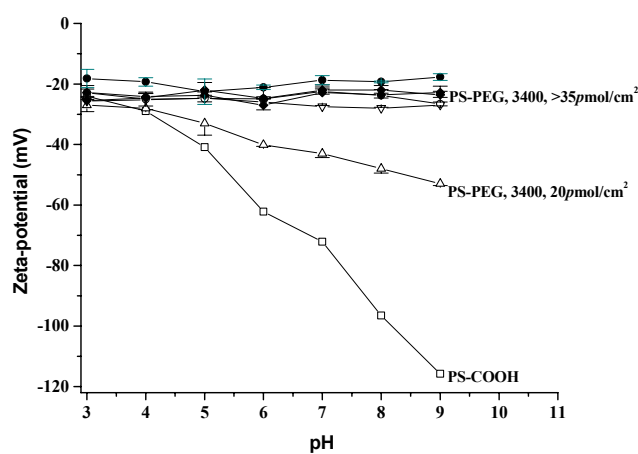

Figure 8. *Effect of the pH of the medium on the zeta-potential of PS-COOH (□) and PS-PEG. Δ: PS-PEG (diamino PEG 3400, 20.0 pmol/cm^2), ∇: PS-PEG (diamino PEG 3400, 42.0 pmol/cm^2), ○: PS-PEG (diamino PEG 3400, 59.3 pmol/cm^2), ◊: PS-PEG (molar ratio of amino hydroxyl PEG 3400 to diamino PEG 3400 in feed is 1, 62.3 pmol/cm^2), ●: PS-PEG (amino methoxy PEG 5000, 50.8 pmol/cm^2), ◆: PS-PEG (molar ratio of amino methoxy PEG 5000 to diamino PEG 3400 in feed is 1, 56.3 pmol/cm^2). PEG surface concentration was determined by H^{1}L NMR measurements.*

rotein adsorption from 85 v.% human plasma dilutions

The steric repulsion effect was also observed when the PS-PEG was incubated with plasma dilutions. Table 1 shows that with increasing surface concentration of PEG, the protein adsorption onto PS-PEG is dramatically reduced. With a surface concentration of PEG of ~60

$p$mol/cm^2, PS-PEG only adsorbed ~17 ng/cm^2 of protein, which is a ~91 % reduction in comparison with unmodified PS-COOH particles.

Table 1. Characteristics of PS-COOH and PS-PEG [a]

Sample ID	PEG content($p$mol/cm^2)		Zeta Potential	Protein adsorption	Reduction[b]
	TNBS	H^{1}L NMR	(mV)	(ng/cm^2)	(%)
PS-amidine	n.a.	n.a.	20.2±1.4	260.9±7.5	-
PS-COOH	n.a.	n.a.	-69.5±2.1	185.7±1.8	-
PS-PEG	35.3±2.4	42±5.1	-33.2±2.2	46.4±3.5	75.2±3.1
PS-PEG	44.3±2.1	50.2±2.1	-21.0±3.1	23.3±2.1	87.5±5.1
PS-PEG	60.4±4.2	59.3±2	-8.5±4.7	17±3.1	91.2±2.5

[a]PS-PEG (modified by diamino PEG 3400) was prepared by the carbodiimide method; Protein adsorption was measured by the micro BCA assay. N.a. not applicable. [b]Reduction with respect to PS-COOH.

In conclusion, particles with a "brush-like" covalently bound PEG layer could be prepared by optimized carbodiimide coupling chemistry. These surfaces are passive in protein containing media and can serve as a model for artificial cells with long circulation time.

REFERENCES

(1)   Allemann, E.; Leroux, J. C.; Gurny, R. *Adv. Drug Deliv. Rev.* **1998,** *34*, 171.
(2)   Davis, S. S.; Illum, L.; Stolnik, S. *Curr. Opin. Colloid Interface Sci.* **1996,** *1*, 660.
(3)   Leroux, J. C.; Allemann, E.; DeJaeghere, F.; Doelker, E.; Gurny, R. *J. Control. Release* **1996,** *39*, 339.
(4)   Stolnik, S.; Illum, L.; Davis, S. S. *Adv. Drug Deliv. Rev.* **1995,** *16*, 195.
(5)   Gref, R.; Minamitake, Y.; Peracchia, M. T.; Trubetskoy, V.; Torchilin, V.; Langer, R. *Science* **1994,** *263*, 1600.
(6)   Lee, J. H.; Kopeckova, P.; Zhang, J.; Kopecek, J.; Andrade, J. D. *Abstr. Pap. Am. Chem. Soc.* **1988,** *196*, 50.
(7)   Jeon, S. I.; Andrade, J. D. *J. Colloid Interface Sci.* **1991,** *142*, 159.
(8)   Jeon, S. I.; Lee, J. H.; Andrade, J. D.; Degennes, P. G. *J. Colloid Interface Sci.* **1991,** *142*, 149.
(9)   Harder, P.; Grunze, M.; Dahint, R.; Whitesides, G. M.; Laibinis, P. E. *J. Phys. Chem. B* **1998,** *102*, 426.
(10)   Prime, K. L.; Whitesides, G. M. *J. Am. Chem. Soc.* **1993,** *115*, 10714.
(11)   Davis, S. S.; Illum, L.; Moghimi, S. M.; Davies, M. C.; Porter, C. J. H.; Muir, I. S.; Brindley, A.; Christy, N. M.; Norman, M. E.; Williams, P.; Dunn, S. E. *J. Control. Release* **1993,** *24*, 157.
(12)   Norman, M. E.; Williams, P.; Illum, L. *Biomaterials* **1992,** *13*, 841.
(13)   Stolnik, S.; Felumb, N. C.; Heald, C. R.; Garnett, M. C.; Illum, L.; Davis, S. S. *Colloid Surf. A-Physicochem. Eng. Asp.* **1997,** *122*, 151.
(14)   Sofia, S. J.; Premnath, V.; Merrill, E. W. *Macromolecules* **1998,** *31*, 5059.
(15)   Stenius, P.; Berg, J.; Claesson, P.; Golander, C. G.; Herder, C.; Kronberg, B. *Croat. Chem. Acta* **1990,** *63*, 501.
(16)   Sheu, M. S.; Hoffman, A. S.; Ratner, B. D.; Feijen, J.; Harris, J. M. *J. Adhes. Sci. Technol.* **1993,** *7*, 1065.
(17)   Ratner, B. D. *J. Biomater. Sci. Polym. Ed.* **1992,** *4*, 3.
(18)   Van Delden, C. J.; Bezemer, J. M.; Engbers, G. H. M.; Feijen, J. *J. Biomater. Sci. Polym. Ed.* **1996,** *8*, 251.
(19)   Han, D. K.; Park, K. D.; Ryu, G. H.; Kim, U. Y.; Min, B. G.; Kim, Y. H. *J. Biomed. Mater. Res.* **1996,** *30*, 23.

(20) Harper, G. R.; Davies, M. C.; Davis, S. S.; Tadros, T. F.; Taylor, D. C.; Irving, M. P.; Waters, J. A. *Biomaterials* **1991,** *12*, 695.

(21) Brindley, A.; Davis, S. S.; Davies, M. C.; Watts, J. F. *J. Colloid Interface Sci.* **1995,** *171*, 150.

(22) Bromley, C. W. A. *Colloids Surf.* **1986,** *17*, 1.

(23) Quellec, P.; Gref, R.; Dellacherie, E.; Sommer, F.; Tran, M. D.; Alonso, M. J. *J. Biomed. Mater. Res.* **1999,** *47*, 388.

(24) Tobio, M.; Gref, R.; Sanchez, A.; Langer, R.; Alonso, M. J. *Pharm. Res.* **1998,** *15*, 270.

(25) Emoto, K.; Nagasaki, Y.; Kataoka, K. *Langmuir* **1999,** *15*, 5212.

(26) Nozaki, S. *Chem. Lett.* **1997,** *1*, 1.

(27) Rich, D. H.; Singh, J. In *The peptides: analysis, synthesis, biology*; Ed.Gross, E., Eds.; Academic Press: New York, **1979**; Vol. volume 1, p 241.

(28) Van der Hoff, J. W.; Van Den Hul, H. J.; Tausk, R. J. M.; Overbeek, J. T. G. In *Clean Surfaces: their preparation and characterization for interfacial studies*; Ed.Goldfinger, G., Eds.; Marcel Dekker Inc.: New York, **1970**, p 15.

(29) Vogel, A. I.; Mendham, J. *Vogel's Textbook of Quantitative Chemical Analysis*, 6th ed.; Prentice Hall: Harlow, **2000**.

(30) Hunter, R. J. *Zeta potential in colloid science: principles and applications*, 3rd ed.; Academic Press: London, **1988**.

(31) Zalipsky, S.; Gilon, C.; Zilkha, A. *Eur. Polym. J.* **1983,** *19*, 1177.

(32) Churaev, N. V.; Nikologorskaja, E. A. *Colloid Surface* **1991,** *59*, 71.

(33) Suzawa, T.; Shirahama, H. *Adv. Colloid Interface Sci.* **1991,** *35*, 139.

(34) Olde Damink, L. H. H.; Dijkstra, P. J.; vanLuyn, M. J. A.; vanWachem, P. B.; Nieuwenhuis, P.; Feijen, J. *Biomaterials* **1996,** *17*, 765.

(35) Kuijpers, A. J.; Engbers, G. H. M.; Krijgsveld, J.; Zaat, S. A. J.; Dankert, J.; Feijen, J. *J. Biomater. Sci.-Polym. Ed.* **2000,** *11*, 225.

(36) de Gennes, P. G. *Adv. Colloid Interface Sci.* **1987,** *27*, 189.

(37) Wagner, P. *FEBS Lett.* **1998,** *430*, 112.

4

Pegylated polystyrene particles as a model system for artificial cells

ABSTRACT: Pegylated polystyrene particles (PS-PEG) serving as a model system for artificial cells were prepared by modification of carboxyl polystyrene particles (PS-COOH) with homo- and hetero-bifunctional polyethylene glycols (PEG, Mw 1500, 3400, 5000) containing an amino end group for immobilization and an amino, hydroxyl or methoxy end group that is exposed at the surface after immobilization. Protein adsorption from human plasma dilutions (85 v.%) onto PS-PEG with a PEG surface concentration higher than 40 pmol/cm^2 was reduced up to 90-95 % as compared to PS-COOH, with a final protein surface concentration of ~20 ng/cm^2. From two dimensional gel electrophoresis analyses, it was found that about 30 % of total optical densities of the gel images of PS-PEG, thus 30 % of the total amount of adsorbed proteins onto PS-PEG are dysopsonins, *i.e.,* non-adhesive proteins like albumin and apolipoproteins. For PS-COOH, only <15 % of adsorbed proteins are dysopsonins. In addition, the generation of terminal complement compound (TCC) by PS-PEG is not significant at PEG surface concentrations lower than ~55 pmol/cm^2. The low protein adsorption, the relatively high percentage of adsorbed dysopsonins and the low level of complement activation may prevent the uptake of PS-PEG by the mononuclear phagocytic system (MPS) in vivo. Moreover, PS-PEG (PEG surface concentration >~35 pmol/cm^2) shows minimal interaction with cultured human umbilical vein endothelial cells (HUVEC), which mimics the endothelial lining of the blood vessel wall.

INTRODUCTION

The main problems that are encountered with the application of microparticles in the circulation are the rapid clearance by the cells of the mononuclear phagocytic system (MPS)[1,2] and the adhesion to the endothelial lining of the vascular system[3-5]. Phagocytosis of the particles proceeds via opsonization and adhesion followed by internalization[2].

When administered intravenously, a spectrum of blood proteins may adsorb onto the particle surface, of which some are opsonins, some are dysopsonins[2], and some have no influence on phagocytosis. Opsonins adapt the particles for their adhesion and internalization by the cells of the MPS. Particle surfaces associated with specific opsonins (e.g. IgG, C3, C3b) are internalized by specific interaction with receptors present on macrophages. For example, the specific interaction of the protruding Fc portion of IgG with the Fc-receptor on macrophages triggers phagocytosis. Furthermore, adsorbed complement activation related fragments C3b, iC3b are recognized by their receptors (CR1 and CR3, respectively) present on the membrane of macrophages. Adsorbed nonspecific opsonins like fibronectin, fibrinogen or vWF spread around the surface of the particles and expose the epitopes for adhesion after a change in conformation. Grafting of albumin onto surfaces improves their blood compatibility[6,7].

Albumin, Apo E, Apo B, HDL, and VLDL adsorbed onto poly(d,l-lactic acid) nanoparticles did not alter the uptake of the nanoparticles by human monocytes[8].

Endothelial cells (EC) possess the capacity to phagocytose foreign particles upon contact. After intravenous administration of particles they may adhere to the vascular endothelium and/or be phagocytosed by the endothelial cells[9]. Phagocytosis of the particles by endothelial cells is slower as compared to Kupffer cells of the liver. Only a few studies dealing with the interaction of microspheres with EC have been reported[3-5].

The interaction and/or uptake of particles by macrophages or by the endothelial lining is strongly influenced by the surface characteristics of the particles like charge[10-12] and hydrophobicity[13,14]. In order to prevent rapid clearance, micro-particles should have such surface properties that only low or no protein (especially opsonin) adsorption and complement activation is induced. This will lead to minimal interactions with phagocytic and endothelial cells and thus a prolonged circulation time.

The removal of particles by the MPS can be reduced by grafting the particle surface with hydrophilic, nonionic polymers for instance poly(ethylene glycol) (PEG). These polymers can give "stealth" properties to the particles by preventing the interaction with blood proteins including opsonins[15,16]. The protein resistant character of pegylated surfaces is generally ascribed to a combination of the low interfacial energy of PEG with water and its steric stabilization effect[17,18]. The dysopsonic effect of a PEG coating is neither substrate dependent as seen from protein adsorption studies with pegylated polystyrene particles[19,20], PLGA or PLA particles[16,21] and liposomes[1,2], nor is "device" dependent as evidenced by protein adsorption studies with liposomes[1,2], nanocapsules[22,23], or nano- and microspheres[15,19-21,24]. The dysopsonic capacity of a PEG coating is dependent on the molecular weight, surface concentration[17,18] and conformation of PEG molecules[25].

Despite the growing amount of theoretical and experimental work with PEG surfaces, the requisites to prevent protein adsorption during the presence of these surfaces in the circulation and/or the uptake of pegylated particles by the cells are still poorly defined. Moreover, from lab to lab different protein solutions were used to evaluate protein adsorption, many of which were single protein solutions[25-28] or strongly diluted plasma[19,29]. This is different from the in vivo situation, which makes it more difficult to draw a general conclusion from the comparison of these results.

In our research program towards the design of artificial cells, pegylated polystyrene particles (PS-PEG) were used as a model system for artificial cells. PS-PEG were prepared by covalent immobilization of amine functionalized PEG onto carboxyl polystyrene particles (PS-COOH) via the carbodiimide pathway[30]. The aim of the present study is to evaluate PS-PEG in vitro with respect to protein adsorption and complement activation using a relevant medium for extrapolation of the results to the in vivo situation. Instead of a single protein solution or strongly diluted plasma, 85 v.% human plasma or serum was applied to investigate protein adsorption and complement activation, respectively. The adhesion of the particles to cultured human umbilical vein endothelial cells (HUVEC) was explored in order to mimic the interaction with the endothelial lining of the blood vessel wall. The influence of surface concentration, end group and molecular weight of PEG was investigated. The results of this study can be used to define an optimal bio-inert pegylated surface.

MATERIALS AND METHODS

Materials

A bicinchoninic acid protein assay kit (micro BCA assay) together with bovine serum albumin (BSA) was supplied by Pierce (Rockford, IL, USA). An SC5b-9 (TCC) enzyme immunoassay kit was purchased from Quidel Corporation (Mountain View, CA, USA). Freshly frozen, citrated, human plasma was obtained from the Blood Transfusion Service Twente-Achterhoek (Enschede, The Netherlands). Lipopolysaccharide was obtained from SIGMA Chemical Inc. (St. Louis, MO, USA). Phosphate buffered saline (PBS, pH 7.4) was purchased from NPBI (Emmer Compascuum, The Netherlands). De-ionized water (DI water) was obtained from a Milli-Q water purification system (Millipore, Molsheim, France). Polyethylene films (Stamylan L2100TN100) were obtained from DSM Polyethylenes (Geleen, The Netherlands). All other chemicals (Merck, Darmstadt, Germany) were of analytical grade and used as received.

Preparation of pegylated polystyrene particles (PS-PEG)

PS-PEG was prepared by coupling amine functionalized PEG onto PS-COOH as reported elsewhere[30]. Briefly, 4.04 mL of a PS-COOH suspension (0.1211g, 0.75 μmol COOH groups) was allowed to react with 1-dimethylaminopropyl-ethylcarbodiimide hydrochloride (EDC, 6 μmol) and 1-hydroxybenzotriazole (HOBt, 2.4 μmol) at 4 ºC for 35 min. Subsequently an excess of a homo- and/or hetero- bifunctional PEG (Mw 1500, 3400, 5000) was added to the mixture. PEG contains an amino end group for immobilization and an amino, hydroxyl or methoxy end group that after immobilization is exposed at the surface. The coupling reaction was performed for 44 h and terminated by changing the pH to 10 with 1.0 M NaOH and leaving the reaction mixture for 5 min. Then the particles were washed once with an HCl solution (pH 2) and three times with PBS via centrifugation and redispersion. After the last washing step PS-PEG was re-suspended in PBS (1.61 wt.%) and stored at 4ºC. The particles are denoted by PS, a dash, the PEG end group (A for amine, H for hydroxyl and M for methoxy) and the molecular weight (Mn $\times 10^{-3}$) followed by a dash and the surface concentration of PEG ($p$mol/cm^2). For PS-PEG modified with mixed PEG's, the molar ratio of the two PEG's in feed is given in between (Table 1). As examples, the notation of methoxy PEG (Mw 5000) modified particles is PS-M5, and PS-PEG modified with hydroxyl PEG 3400 with a final PEG surface concentration of 64.5 $p$mol/cm^2 is denoted as PS-H3.4-64.5.

Protein adsorption and micro BCA assay

In a typical protein adsorption experiment, 0.3 mL of a PS-PEG suspension (1.61 wt.%) was incubated with human plasma with a final concentration of 15 or 85 v.% in PBS at 37ºC for 2 h under mild stirring. Thereafter, the particles were separated from the plasma using centrifugation (Biofuge 13, Heraeus Instruments GmbH, Hanau, Germany) at 10000 ×g for 8 min and washed four times with 1.5 mL of PBS. Proteins were desorbed from the particle surfaces by sonication at 40ºC for 30 min in the presence of 1.5 mL of sodium dodecyl sulfate (SDS, 6 wt.%) solution. After centrifugation at 10000 ×g for 8 min the supernatant was collected to perform a micro BCA assay according to the supplier's information.

Efficiency of protein desorption determined by XPS measurements

The efficiency of the protein desorption procedure using SDS was determined by comparing the nitrogen contents of the particles before and after SDS desorption. The nitrogen content was determined by X-ray photoelectron spectroscopy (XPS). To prepare samples for XPS measurements, particle suspensions were dropped on clean polyethylene films (using hexane to clean) and dried under vacuum at room temperature for 24 h. XPS measurements were performed on a Quantum 2000 spectrometer (Physical Electronics Inc. Eden Prairie, MN, USA) with a mono-chromatized Al Kα X-ray source at a power of 300 W. Survey scans (0-1400 eV) were recorded to qualitatively determine the elemental

composition of the sample surface. The element (C, O and N) core level peaks were acquired using a pass energy of 20 eV for detail scans. The surface charge was corrected by setting the main C1s C-C/C-H peak at 285 eV. Surface compositions were calculated by considering the integrated peak areas of the corresponding elements and their sensitivity factors[31]. The spectra were obtained using Multipak V6.1 software. The desorption efficiency was estimated according to the following equation:

$$Efficiency = \frac{N_1 - N_2}{N_1 - N_0} \times 100\%$$

Where N_0, N_1 and N_2 are the nitrogen content of the original particles, protein-adsorbed particles and SDS treated protein-adsorbed particles, respectively.

Identification of adsorbed proteins using two-dimensional gel electrophoresis (2-DE)

Particles (surface area ~0.25 m^2) were incubated in 5.0 mL of citrated human plasma (final concentration of 85 v.%) for 5 min at 37°C. The particles were separated from the protein solution by centrifugation and washed four times with 5 mL of DI water. The protein desorption, sample loading to the 2-DE and processing were the same as described previously[32]. During 2-DE, the proteins are separated according to their isoelectric point (pI) and molecular weight (MW). After 2-DE, the gels were silver stained and scanned (Model Power Look, Amersham Pharmacia Biotech, Germany). The gel images were then analyzed by employing the MELANIE 3 software (GeneBio, Geneva, Italy). The results can be used to calculate the amount of adsorbed proteins, which is given in arbitrary units (VOL). Protein spots were identified by matching the gels to the master map of human plasma[33]

Activation of the complement system

Blood (50 mL) was slowly drawn from three healthy volunteers into polypropylene tubes and allowed to clot for 75 min at room temperature. Subsequently, the samples were centrifuged at 2000 ×g for 20 min at 4°C, after which the serum was separated from the clot by decantation. The serum aliquots were quickly frozen in liquid nitrogen, and then stored in a freezer (-80° C) until use.

Prior to the complement activation assay, serum was thawed at 37°C, pooled and then stored on ice. Particle suspensions (0.05 mL of 1.61 wt.% in PBS) with a surface area of ~32.8 cm^2 were placed in polypropylene (PP) tubes and 0.5 mL of pooled serum was added. PP tubes without particles were used as control. Glass tubes without particles, and PP tubes with serum containing lipopolysaccharide (10 mg/mL)[34] were used as positive controls. After 2 h incubation at 37°C, the mixtures were subjected to centrifugation at 10000 ×g for 10 min and serum samples were taken from the supernatant. The TCC concentrations of serum samples were determined using an SC5b-9 kit according to the procedure recommended by the manufacturer.

Interaction of the particles with cultured HUVEC layers

HUVECs were isolated from one umbilical vein according to the method of Jaffe et al.[35] with a modification of using trypsin/EDTA (Gibco 35400-019) instead of collagenase. The endothelial cells from a single umbilical vein were cultured, under 5% CO$_2$/95% air at 37°C in a humidified incubator, on TCPS (Costar®, Corning, NY, USA) pre-coated with partially purified fibronectin (co-product from coagulation factor VIII production, Central Laboratory of the Blood Transfusion Service (CLB), Amsterdam, The Netherlands). HUVECs were identified by their characteristic polygonal shape and "cobble-stone" growth pattern. Passaging of cells was performed by detachment with trypsin/EDTA (Gibco 35400-019) and subsequent seeding on fibronectin-coated TCPS at a growth surface ratio of 1:4. Culture medium (CM) consisted of 50% M199 (with Hank's solution; Gibco 21151-030) and 50% RPMI 1640 (with 25mM HEPES; Gibco 42401-018) and contained 100U/ml penicillin-G, 100mg/ml streptomycin (Gibco 15140-114), and 2mM Glutamax-I (Gibco 35050-038). Prior to use in cell culture, CM was supplemented with filter-sterilized pooled human serum (20 v.%, CMS). Serum was acquired

by overnight incubation of whole blood (from 13 healthy donors) at room temperature. The serum was subsequently obtained by centrifugation, pooled and stored at -80°C.

In a typical interaction experiment, immediately after mixing of 0.01 mL of particle suspension (1.61 wt.%) and 0.24 mL of CMS, the mixture was incubated in endothelial cell-covered wells at 37°C for 5, 15, 45 and 140 min, respectively. Thereafter, the particle suspension was removed using a pipette. Subsequently 0.25 mL of PBS was added and quickly refreshed with 0.25 mL of PBS for five times. After removal of PBS, 0.25 mL of CMS was added into each well and the number of particles attached to a cell surface area of 0.04 mm^2 was determined by light microscopy.

RESULTS AND DISCUSSION

Efficiency of protein desorption with SDS

SDS has been applied for the desorption of proteins from particle surfaces in many studies[32,36,37]. In order to verify the efficiency of the SDS (6 wt.%) desorption procedure, the nitrogen contents of particles that had been incubated in 85 v.% plasma before and after SDS treatment were measured. The XPS technique has also been used to estimate the amount of protein adsorbed by determining the atomic composition of the surfaces by others[38]. The nitrogen content of PS-COOH, PS-M5-56.4 and PS-H3.4-81.0 was 0.79, 0.82 and 0.87 %, respectively. After incubating the particles in plasma dilution (85 v.%) and washing four times with PBS (the same procedure as used in protein adsorption experiments), nitrogen contents of 11.0, 1.6 and 2.4 % respectively were measured. After SDS treatment, these particles displayed nitrogen contents of 2.03, 0.81, and 1.10 %, respectively, indicating that most of the adsorbed proteins (~84 %) were removed from the particle surfaces. This result was confirmed by surface plasmon resonance measurements which showed that the efficiency of the SDS protein desorption procedure was ~90 %. In this experiment, the desorption process was studied in real time using an SPR sensor disk of which the surface was chemically similar to that of a PS-COOH particle (data not shown).

Protein adsorption from 85 v.% plasma

The effect of the surface concentration, molecular weight and the end group of PEG on the protein adsorption of PS-PEG from 85 v.% plasma was subsequently studied.

PEG surface concentration. Table 1 displays the surface compositions of PS-PEG particles and the surface concentration of proteins adsorbed onto the particles from 85 v.% plasma as determined by the micro BCA assay. As compared to the unmodified particles PS-COOH and PS-amidine, PS-PEG adsorbed lower amounts of proteins. The level of reduction depends on the surface concentration of PEG. For either PS-A3.4 or PS-A3.4H3.4 and PS-A3.4M5, protein adsorption was decreased by 75-95 % when the surface concentration of PEG was higher than ~35 *p*mol/cm^2, which corresponds to a "brush-like" PEG layer[30]. The XPS data as discussed in the previous part support these results. For these PS-PEG particles the steric repulsion provided by the PEG layer was sufficient to prevent aggregation of the particles in solutions with high ionic strength and in protein containing solutions. Protein adsorption from 85 v.% plasma on PS-PEG was reduced to a low level of ~ 30 ng/cm^2, equivalent to one-eighth of a monolayer of albumin. Figure 1 shows the reduction in protein adsorption as a function of the surface concentration of amino PEG 3400. A linear relationship (R = 0.966) was observed for PEG

surface concentrations below ~45 $p$mol/cm^2. Further increase in PEG surface concentration did not lead to a higher reduction in protein adsorption.

PEG molecular weight. The influence of PEG length on the reduction in protein adsorption can also be deducted from Figure 1. Longer PEG chains (Mw 3400) prevented protein adsorption from 85 v.% plasma to a higher extent than shorter PEG chains (Mw 1500).

PEG end group. When the reduction in protein adsorption of PS-PEG with similar PEG surface concentration and PEG molecular weight (Figure 1) is compared, no effect of PEG end group (NH$_2$ or OH) could be established. The OCH$_3$ end group could not be included in this comparison.

Table 1. Characteristics of the particles and results of protein adsorption from 85 v.% plasma dilutions

Particles [a]	Protein adsorption (ng/cm^2)	Reduction[b] (%)	Zeta potential (mV)
PS-amidine	260.9±7.5	-	20.2±1.4
PS-COOH	210±20	-	-69.7±2.1
PS-A3.4-14.8 [c]	138.1	25.6	-55.7±3.0
PS-A3.4-38.7 [c]	46.4	75.2	-33.2±2.2
PS-A3.4-47.3 [c]	23.3	87.5	-21.2±4.2
PS-A3.4-56.1 [c]	20.1	90.6	-8.6±1.9
PS-A3.4-59.7 [c]	17.0	91.2	-9±2.1
PS-H3.4-64.5	35.1	81.3	-24.7±2.2
PS-H3.4-71.4	34.8	81.3	-24.2±3.3
PS-H3.4-81.0	28.0	85	-26.1±1.8
PS-A3.4H3.4(1/3)-55.4	28.1	84.9	-
PS-A3.4H3.4(1/1)-68.1	26.9	83.3	-21.4±1.2
PS-A3.4H3.4(3/1)-52.4	24.4	86.9	-
PS-A3.4M5(3/1)-57.4	13.0	93.4	-
PS-A1.5M5(4/1)-91.2	37.1	80.7	-9.5±2.2
PS-M5-42.7	46.1	75.6	-25±1.2
PS-M5-46.2	26.8	83.4	-22.8±2.2
PS-M5-52.7	28.1	84.9	-25.5±2.8
PS-M5-56.4	21.2	88.6	-24.6±1.2
PS-A1.5-52.3	90.1	57.2	20.2±4.1
PS-A1.5-71.6	120.0	42.2	36.4±2.4
PS-A1.5-74.6	70.5	62.1	36.3±2.2

[a] PS-PEG are named by PS, a dash, PEG end group (A for amine, H for hydroxyl and M for methoxy) and molecular weight (Mn $\times 10^{-3}$) followed by one dash and the surface concentration of PEG ($p$mol/cm^2). For PS-PEG modified with mixed PEG's, the molar ratio of the two PEG's in feed is given in between. PEG surface concentration (average of at least two measurements) was determined by NMR; [b] Reduction in protein adsorption is based on the protein adsorption by PS-COOH; [c] average value of NMR and TNBS measurements.
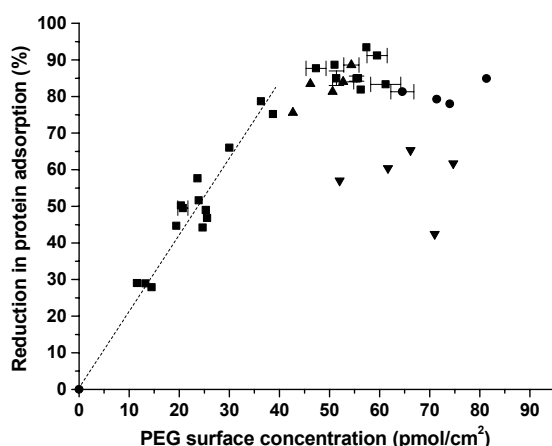
Figure 1. *The influence of PEG surface concentration, end groups and length of PS-PEG on the reduction in protein adsorption from human plasma dilutions (85 v.%) as compared to PS-COOH. Results of PEG-A3.4 (■), PEG-H3.4 (●), PEG-M5.0 (▲) and PEG-A1.5 (▼) were shown. The dotted line is the fit for PS-A3.4 data in the first part (Y=3.021X, R=0.966).*
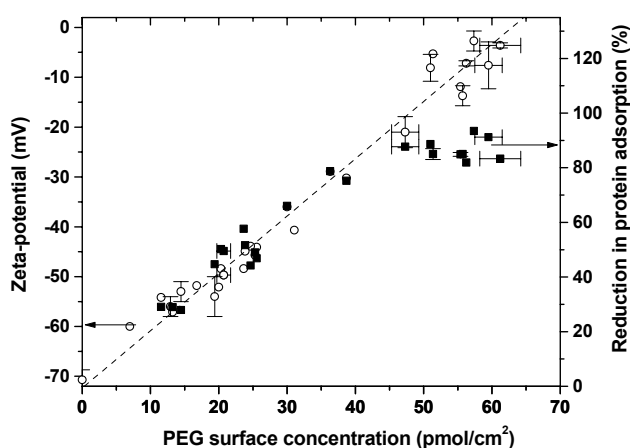

Figure 2. *Cross-correlation between zeta-potential, surface concentration of diamino PEG 3400 of PS-A3.4 and the reduction in protein adsorption from human plasma dilutions (85 v.%). ○ represents zeta potential data, ■ represents reduction in protein adsorption, and dashed line is the fit (Y= −72.30+1.15X, R=0.988) for the zeta potential against PEG surface concentration.*

The surface concentration of amino PEG 3400 and the zeta potential of the particles as determined in the previous chapter revealed a cross correlation with the reduction in protein adsorption (Figure 2). The zeta potential of PS-PEG, a parameter relatively easy to measure, can be used to estimate the surface concentration of PEG and to predict the amount of adsorbed protein from plasma[30] (up to ~45 $p$mol/cm^2). Nevertheless, this relationship will depend on the properties of the starting particles (type and density of surface functional groups or the nature of the particle matrix), immobilization chemistry and the PEG used (length, end groups).

Compared to the unmodified surface, the protein adsorption onto the PEG surface was maximally reduced by 90-95% (Figures 1 and 2), which means that PEG layers failed to completely prevent protein adsorption at the surface. The discrepancy between the PEG

surface concentration and protein adsorption at high PEG concentrations can be ascribed to the decreased chain flexibility[27] of the PEG molecules at PEG surface concentrations higher than ~45 $p$mol/cm^2 and/or to the inherent interaction of PEG itself or the end group with plasma proteins.

Identification of Adsorbed Proteins

Both the amount and type of the adsorbed proteins are of importance in predicting the clearance of micro-particles by the body. Therefore, besides the determination of the total amount of adsorbed protein, the adsorbed proteins were also identified using two dimensional electrophoresis (2-DE)[32,39-41]. Figure 3 demonstrates two representative 2-DE gel images of PS-A3.4M5(3/1)-57.4 (A) and PS-COOH (B). A comparison of the optical densities of protein spots of the images of PS-PEG and of PS-COOH revealed that the total amount of proteins adsorbed onto PS-A3.4M5(3/1)-57.4 was about five times less than that of PS-COOH. All the particles studied (Table 2) except PS-N1.5-71.6 showed a similar effect. This is in agreement with the results obtained from the micro BCA assay, which showed that the PEG coatings (Mw ≥ 3400) gave a reduction in protein adsorption of up to 95 %. The total amount of adsorbed protein determined by the micro BCA assay and 2-DE shows a linear relationship (Figure 4).
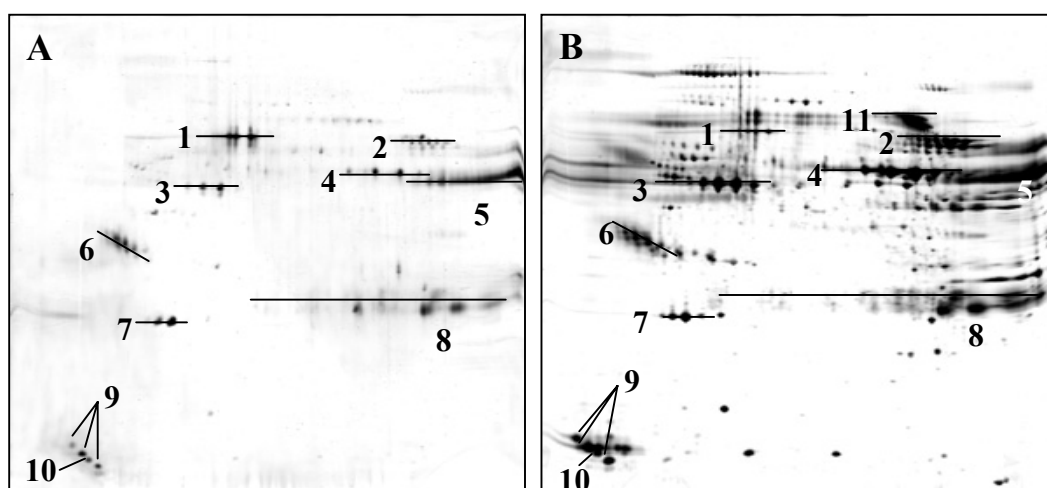

Figure 3. *Two dimensional electrophoresis gels of PS-A3.4M5(3/1)-57.4 (A) and PS-COOH (B). X-axis: pI ranging from 4 to 10 (left to right); y-axis: MW ranging from 250 to 6 kDa (top to bottom). (1) albumin, (2) fibrinogen α-chain, (3) fibrinogen γ-chain, (4) fibrinogen β-chain, (5) IgG γ-chain, (6) apoJ, (7) apo A-I, (8) Ig light-chains, (9) apo C-III, (10) apo C-II, (11) transferrin.*

Besides the total amount of proteins adsorbed, Table 2 displays the main (of which the amount of protein adsorbed was higher than 1.5% of total amount of proteins adsorbed) proteins that could be identified on the gel images: albumin, fibrinogen, IgG-γ chain, IgG light-chains, apolipoproteins apo-A-I, A-IV, E, J, C-II, and C-III. The PEG coating also altered the composition of the proteins adsorbed. As compared to PS-COOH, PEG modification drastically reduced fibrinogen adsorption. The adsorption of proteins like albumin, IgG-γ chain, IgG light-chains, apo A-I, apo A-IV, apo E, and apo J was relatively higher.
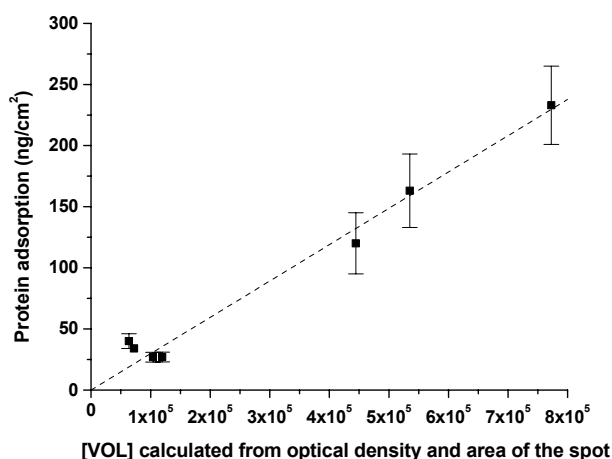
Figure 4. Correlation between the amounts of adsorbed protein as determined with the micro BCA assay (y-axis) and the two dimensional electrophoresis technique (x-axis).

Table 2. Main proteins adsorbed onto different particle surfaces as determined by 2-DE [a]

	PS-H3.4-71.4	PS-A3.4-56.1	PS-A3.4H3.4(1/1)-68.1	PS-A3.4M5(3/1)-57.4	PS-A1.5-71.6	PS-amidine	PS-COOH
Albumin	4.9	5.4	8.5	11.3	2.6	10.0	2.4
Fibrinogen	10.5	11.5	11.6	19.8	4.9	42.3	28.1
IgG-γ chain	13.8	22.9	13.4	19.0	3.5	1.7	8.9
Ig light-chains	3.8	11.9	13.9	9.3	6.1	4.0	7.3
Apo A-I	13.3	5.7	7.4	11.7	4.4	2.8	2.8
Apo A-IV	2.0	-	1.8	-	-	1.6	-
Apo J	9.9	14.8	15.0	6.6	22.6	-	3.0
Apo E	-	2.9	2.6	-	-	-	-
Apo C-III	17.4	6.8	9.7	6.1	10.2	7.7	4.2
Apo C-II	6.5	2.3	3.9	2.1	2.8	2.3	1.4
α1-Antitrypsin	-	-	-	-	3.1	3.9	-
Transferrin	-	-	-	-	-	-	5.2
Gel [VOL]	72240	119428	103954	63672	444588	772729	535195

[a]The values for each protein are given as the percentage of the overall detected protein amount given in VOL, which is an arbitrary unit given by the analysis software; and sample nomenclature is the same as in Table 1. Only proteins having percentages higher than 1.5 % are shown in the table.

Albumin and apolipoproteins can be considered as dysopsonins i.e. non-adhesive proteins[40]. The adsorption of these proteins onto particles could retard or inhibit the uptake of the particles by the MPS[9]. Alb, HDL, Apo B, Apo E and VLDL adsorbed onto poly(*d,l*-lactic acid)-PEG particles did not show an influence on the uptake by human monocytes[8]. Apo A-IV and A-I do not facilitate uptake or degradation of the whole particle, and they were each able to displace Apo E from liposomes and thereby reduce uptake by the cells[42]. A study including in vivo experiments[37] proposed that a "team work" of Apo A-I, Apo A-IV and Apo E causes lipid-drug conjugate particles to escape the hepatic uptake and to target the blood brain barrier. In

this study, dysopsonins accounted for ~30 % of overall protein adsorption on PS-PEG, whereas they amounted only <15 % on PS-COOH particles. In addition, the PEG coating significantly reduced the absolute amount of adsorption of the nonspecific opsonin fibrinogen and the specific opsonin IgG-γ chain. Therefore, the PEG layer does not only reduce the protein adsorption to a large extent but also alters the protein composition by adsorbing a relatively high amount of dysopsonins.

Activation of the Complement System

The in vivo use of drug carriers, like PDLLA and PLGA nano-spheres is particularly hampered by the activation of the complement system initiated by the attachment of C3b to the particle surface[41,43]. PEG coatings are reported to reduce the complement activation on nano-capsules[22,23] and particles[44,45]. To evaluate the extent of complement activation of the particles with and without a PEG coating, an ELISA SC5b-9 kit was used to determine the generation of TCC upon exposure of PS-PEG and PS-COOH to serum.
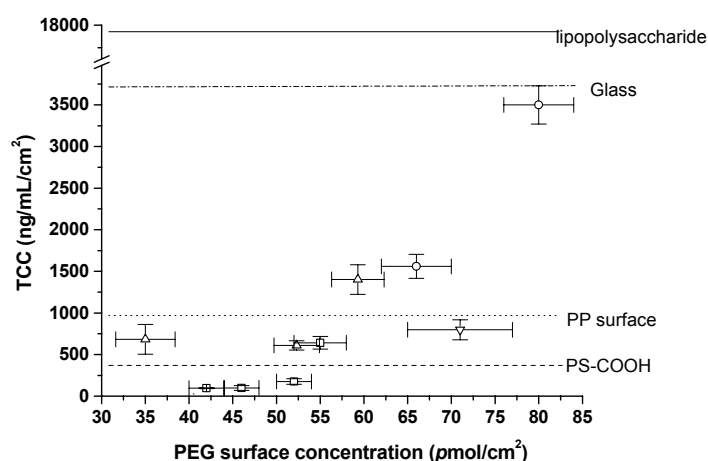

Figure 5. *Generation of TCC by PS-PEG with different surface concentrations, end groups and molecular weight of PEG. Results of PEG-M5.0 (□), PEG-H3.4 (○), PEG-A3.4 (△) and PEG-A1.5 (▽) are shown. The lines for PS-COOH (dash), PP tubes (dot), glass surfaces (dash dot) and lipopolysaccharide (solid) are drawn for comparison. TCC values of PS-PEG samples are corrected for the amount of TCC generated by the PP surface. For particles, the surface area is ~32.8 cm^2, and for glass or PP surfaces, the surface area is ~5 cm^2.*

Figure 5 shows the generation of TCC by PS-PEG with different PEG end groups, PEG chain lengths and PEG surface concentrations. The horizontal lines that correspond to the amount of TCC generated by PS-COOH, PP tube and positive controls (lipopolysaccharide containing serum and glass) are shown for comparison. Lipopolysaccharide containing serum and glass generated significant amounts of TCC (17300 and 3700 ng/mL/cm^2, respectively). The control PP surface, known as a non-activating surface, induced 960 ng/mL/cm^2 TCC. The general tendency is that TCC generation increased with increasing PEG surface concentration. This is in line with the finding that trichlorovinylsilane-treated glass modified with Pluronic F108 (EO$_{128}$-PO$_{54}$-EO$_{128}$) displayed a significant increase in complement activation, and that C3a production was linearly dependent on the surface concentration of Pluronic F108[34]. This PEG surface concentration dependency is probably due to an increased exposure of end groups to

serum proteins with increasing PEG surface concentration. Amino and hydroxyl groups are known to be able to react with a labile thioester group on the C3b molecules resulting in a covalent attachment, and thus activation of the complement system[46]. For methoxy end groups, surface hydrophobicity might play a role. Although PEG end group and length of PS-PEG are important parameters that influence protein adsorption as discussed in previous sections, no clear end group or chain length effect can be deduced from the complement activation data.

Except for PS-PEG with a relatively low surface concentration of methoxy PEG 5000 (< 52 pmol/cm^2), all other PS-PEG studied generated more TCC than PS-COOH (~ 330 ng/mL/cm^2). PS-PEG surfaces with lower amino PEG surface concentrations (< 56 pmol/cm^2) induced more complement activation than PS-COOH but less than PP surfaces. PS-PEG with hydroxyl groups or a high surface concentration of amino groups can provoke much more TCC generation than PP surfaces. At high concentrations of hydroxyl groups (e.g. 80 pmol/cm^2), PS-PEG induced similar amounts of TCC as a glass surface.

This study demonstrates that pegylated surfaces can activate the complement system. PEG surface concentration and PEG end groups are of crucial importance. A PEG surface concentration below ~55 pmol/cm^2 will give a satisfactory result with respect to complement activation. Therefore, for an artificial cell surface that has no/low protein adsorption and complement activation, the optimal PEG surface concentration is in between 40 and 55 pmol/cm^2, and the end group is preferably a methoxy or an amine group.

Interaction of the particles with HUVEC layers

Following intravenous administration, the injected particles might adhere to the vascular endothelium and be phagocytosed by the endothelial cells[9]. HUVEC's, cultured on TCPS plates, can be used to mimic the blood vessel wall. Therefore, a study of the interaction of particles with or without PEG coating with cultured HUVEC was performed to evaluate the adhesion of the particles onto an endothelial lining. Table 3 shows the number of particles with or without PEG coating that adhered to the HUVEC layers (per 0.04 mm^2) for different incubation times up to 140 min. In general, PS-PEG (Mw 3400, 5000) adhered much less to HUVEC layers than PS-COOH and PS-amidine.

The available data allow a general evaluation of the influence of the PEG molecular weight and the PEG end group on the interaction of pegylated surfaces with HUVEC. It appears that long PEG (Mw 5000) is much more effective in preventing the adhesion to the HUVEC layers than short PEG (Mw 1500). For instance, PEG 1500 modified particles adhered more than those modified with longer PEG e.g. 3400, and even more than PS-COOH. With respect to the PEG end group, NH$_2$ and OH end groups have the same effect on the adhesion to EC layers, and again the influence of OCH$_3$ is not clear, although PS-M5.0 adhered much less than other particles.

Most particles with mixed amino functionalized PEG layers showed a higher adhesion onto HUVEC layers than those with pure diamino PEG, which is in agreement with the finding that cell attachment, also mediated by adsorbed proteins, is promoted by multi chemical sites[36,47] which resembles the array of surface properties present in the natural ECM of the cells in vivo[48].

Table 3. Number of particles adhering to HUVEC layers cultured on TCPS at different times[a]

Sample ID	5 min	15 min	45 min	140 min	I/P ratio[b]
PS-COOH	-	75±15	240±50	1250±185	0.66
PS-amidine	-	2000±100	3600±300	4500±260	0.463
PS-H3.4-71.4	1±1	3±2	16±6	200±34	2.143
PS-A3.4-56.1	2±1	4±3	29±7	100±27	3.49
PS-M5-52.7	1±1	1±1	12±5	6±6	-
PS-A3.4H3.4(1/1)-68.1	2±2	3±2	22±10	480±27	3.09
PS-A3.4H3.4(1/3)-55.4	-	-	19±10	200±42	-
PS-A3.4H3.4(3/1)-52.4	-	-	8±6	400±50	-
PS-A3.4M5(3/1)-57.4	-	-	6±4	160±23	2.00
PS-A1.5-71.6	-	-	410±90	1800±170	3.10

[a] Nomenclature of PS-PEG is the same as in Table 1, and particle number used is equivalent to the number of particles needed to form a monolayer on the top of the HUVEC layers.
[b] I/P ratio is the ratio of cell-adhesion-inhibiting proteins to cell-adhesion-promoting proteins, and in this case is the ratio of the sum of Alb, IgG and At to Fb adsorbing on the particle surfaces.

The minimal interaction of PS-PEG (Mw 3400 and 5000) with HUVEC layers can be primarily attributed to the low protein adsorption and to the composition of the proteins adsorbed on these particles, as discussed in the previous parts. Low amounts of (partially) native proteins at the PS-PEG surfaces do not interact with ECs because the proteins on the particles are non-adhesive. Therefore, PS-PEG does not induce EC activation and subsequent adherence of particles. Meanwhile, the adsorption of proteins like Fn, Fb, Vn, vWF and collagen onto the surfaces promotes EC adhesion, whereas the adsorption of e.g. albumin, IgG, HDL, and α_1-antitrypsin onto the surfaces delays or inhibits cell adhesion[49]. Considering the composition of proteins adsorbed from 85 v.% plasma that was obtained from 2-DE analyses, we found that as compared to PS-COOH and PS-amidine, PS-PEG adsorbed a low amount of Fb and relatively high amount of albumin, IgG and α_1-antitrypsin, resulting in a high ratio of cell-adhesion-inhibiting proteins to cell-adhesion-promoting proteins (I/P ratio).

Figure 6 demonstrates the I/P ratio and the number of particles that adhered to HUVEC layers for different particles. The I/P ratios of PS-PEG are between 2.1 to 3.5, which is in contrast with the I/P values of 0.47 and 0.67 of PS-COOH and PS-amidine, respectively. A study on the effect of specific chemical functionalities on the growth of EC also showed that high ratios of albumin to adsorbed Fn on $-CO_2CH_3$ and -OH self-assembled monolayers resulted in poor EC growth on these substrates[36]. Fn, the most potent protein promoting EC adhesion, was not detected on the PEG surfaces. This might be due to the fact that Fn adsorption is relatively high at a low serum concentration (~0.1 %), but is significantly decreased or completely blocked by other proteins when the serum concentration was higher than 1 %[49].
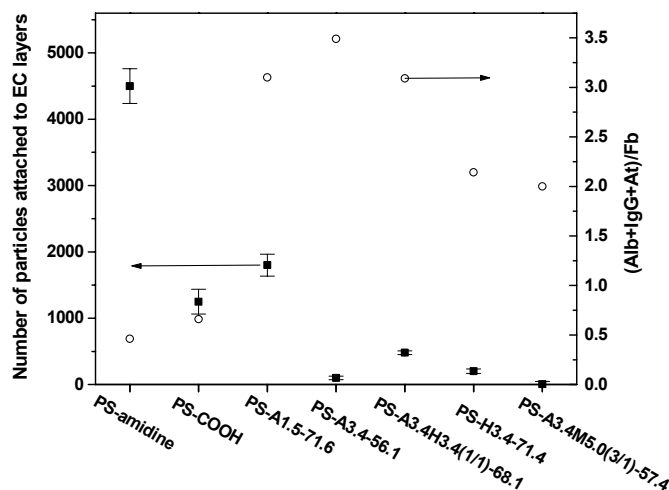
Figure 6. *Relation between the number of the particles adhering to cultured HUVEC layers (140 min) determined microscopically (■) and the ratio of the sum of Alb, IgG and At and Fb adsorbed on the particles determined by the 2-DE technique (○).*

CONCLUSIONS AND OUTLOOK

Particles with a high surface concentration of PEG showed very low protein adsorption and low adhesion onto HUVEC layers. PEG coatings reduce protein adsorption from 85 v.% plasma up to 90-95 % as compared with PS-COOH with ~30 % of the amount of adsorbed protein being non-adhesive. Instead of being non-immunogenic surfaces, PEG surfaces can actually activate the complement system as judged from the higher TCC generation by some particles than by polypropylene surfaces and from the increasing TCC generation with PEG surface concentration. Only at low PEG (Mw$\geq$ 3400) surface concentrations (< 55 pmol/cm^2) can PEG surfaces be considered as non-activating surfaces of the complement system. PS-COOH modified with PEG 3400 or 5000 with PEG surface concentrations of ~50 pmol/cm^2 showed a low adhesion onto HUVEC layers.

Aiming at developing artificial cells with a long circulation time and no uptake by the MPS, a preferable PEG modification in terms of surface concentration, end group and molecular weight of PEG can be deduced from a general consideration of the evaluations conducted. Long PEG (3400, 5000) is much more favorable than short PEG (1500). Although PEG 1500 modified particles did not generate significant amounts of TCC, they adsorbed much more proteins and adhered avidly onto HUVEC layers. In contrast, for PEG 3400 and 5000 modified particles, when the PEG surface concentration is higher than ~45 pmol/cm^2, protein adsorption and adhesion to HUVEC reached minimal values. Nevertheless, a surface with a PEG concentration higher than ~55 pmol/cm^2 could activate the complement system, especially when it contains hydroxyl end groups. Amine and hydroxyl end groups seem to have similar effects with respect to protein adsorption and adhesion to HUVEC, and the influence of methoxy groups is not clear from the present study. Therefore, an artificial cell surface should

preferably contain a PEG coating with PEG molecular weight $\geq$ 3400 g/mol, surface concentration ca. 45-55 pmol/cm^2 (for PEG 3400-5000), and methoxy end groups or methoxy groups mixed with amine groups. The latter can be used for further particle surface modification.

ACKNOWLEDGEMENT

REFERENCES

(1)   Juliano, R. L. *Adv. Drug Deliv. Rev.* **1988,** *2*, 31.

(2)   Patel, H. M. *Crit. Rev. Ther. Drug Carr. Syst.* **1992,** *9*, 39.

(3)   Vora, M.; Karasek, M. A. *J. Cell. Physiol.* **1994,** *159*, 450.

(4)   Steffan, A. M.; Gendrault, J. L.; McCuskey, R. S.; McCuskey, P. A.; Kim, A. *Hepatology* **1986,** *6*, 830.

(5)   Dan, C.; Wake, K. *Exp. Cell Res.* **1985,** *158*, 75.

(6)   Kamath, K. R.; Park, K. *J. Appl. Biomater.* **1994,** *5*, 163.

(7)   Amiji, M.; Park, K. *J. Biomater. Sci.-Polym. Ed.* **1993,** *4*, 217.

(8)   Leroux, J. C.; Dejaeghere, F.; Anner, B.; Doelker, E.; Gurny, R. *Life Sci.* **1995,** *57*, 695.

(9)   Moghimi, S. M.; Patel, H. M. *Adv. Drug Deliv. Rev.* **1998,** *32*, 45.

(10)   van Wachem, P. B.; Hogt, A. H.; Beugeling, T.; Feijen, J.; Bantjes, A.; Detmers, J. P.; van Aken, W. G. *Biomaterials* **1987,** *8*, 323.

(11)   Tabata, Y.; Ikada, Y. *Biomaterials* **1988,** *9*, 356.

(12)   Roser, M.; Fischer, D.; Kissel, T. *Eur. J. Pharm. Biopharm.* **1998,** *46*, 255.

(13)   Mosqueira, V. C. F.; Legrand, P.; Gulik, A.; Bourdon, O.; Gref, R.; Labarre, D.; Barratt, G. *Biomaterials* **2001,** *22*, 2967.

(14)   van Wachem, P. B.; Beugeling, T.; Feijen, J.; Bantjes, A.; Detmers, J. P.; van Aken, W. G. *Biomaterials* **1985,** *6*, 403.

(15)   Gref, R.; Minamitake, Y.; Peracchia, M. T.; Trubetskoy, V.; Torchilin, V.; Langer, R. *Science* **1994,** *263*, 1600.

(16)   Stolnik, S.; Dunn, S. E.; Garnett, M. C.; Davies, M. C.; Coombes, A. G. A.; Taylor, D. C.; Irving, M. P.; Purkiss, S. C.; Tadros, T. F.; Davis, S. S.; Illum, L. *Pharm. Res.* **1994,** *11*, 1800.

(17)   Jeon, S. I.; Lee, J. H.; Andrade, J. D.; Degennes, P. G. *J. Colloid Interface Sci.* **1991,** *142*, 149.

(18)   Jeon, S. I.; Andrade, J. D. *J. Colloid Interface Sci.* **1991,** *142*, 159.

(19)   Norman, M. E.; Williams, P.; Illum, L. *Biomaterials* **1993,** *14*, 193.

(20)   Norman, M. E.; Williams, P.; Illum, L. *J. Biomed. Mater. Res.* **1993,** *27*, 861.

(21)   Gref, R.; Luck, M.; Quellec, P.; Marchand, M.; Dellacherie, E.; Harnisch, S.; Blunk, T.; Muller, R. H. *Colloid Surf. B-Biointerfaces* **2000,** *18*, 301.

(22)   Mosqueira, V. C. F.; Legrand, P.; Gref, R.; Heurtault, B.; Appel, M.; Barratt, G. *J. Drug Target.* **1999,** *7*, 65.

(23)   Mosqueira, V. C. F.; Legrand, P.; Morgat, J. L.; Vert, M.; Mysiakine, E.; Gref, R.; Devissaguet, J. P.; Barratt, G. *Pharm. Res.* **2001,** *18*, 1411.

(24)   Gref, R.; Miralles, G.; Dellacherie, E. *Polym. Int.* **1999,** *48*, 251.

(25)   Harder, P.; Grunze, M.; Dahint, R.; Whitesides, G. M.; Laibinis, P. E. *J. Phys. Chem. B* **1998,** *102*, 426.

(26)   Norman, M. E.; Williams, P.; Illum, L. *Biomaterials* **1992,** *13*, 841.

(27)   Stenius, P.; Berg, J.; Claesson, P.; Golander, C. G.; Herder, C.; Kronberg, B. *Croat. Chem. Acta* **1990,** *63*, 501.

(28)   Prime, K. L.; Whitesides, G. M. *J. Am. Chem. Soc.* **1993,** *115*, 10714.

(29)   Blunk, T.; Luck, M.; Calvor, A.; Hochstrasser, D. F.; Sanchez, J. C.; Muller, B. W.; Muller, R. H. *Eur. J. Pharm. Biopharm.* **1996,** *42*, 262.

(30)   Chapter 3 of this thesis .

(31)   Briggs, D.; Seah, M. P. *Practical Surface Analysis: vol 1, Auger and X-ray Photoelectron Spectroscopy,* 2nd ed. ed.; Wiley: Chichester etc., **1990**.

(32)   Blunk, T.; Hochstrasser, D. F.; Sanchez, J. C.; Muller, B. W.; Muller, R. H. *Electrophoresis* **1993,** *14*, 1382.

(33)   Golaz, O.; Hughes, G. J.; Frutiger, S.; Paquet, N.; Bairoch, A.; Pasquali, C.; Sanchez, J. C.; Tissot, J. D.; Appel, R. D.; Walzer, C.; Balant, L.; Hochstrasser, D. F. *Electrophoresis* **1993,** *14*, 1223.

(34)   Kidane, A.; Park, K. *J. Biomed. Mater. Res.* **1999,** *48*, 640.

(35)   Jaffe, E. A.; Nachman, R. L.; Becker, C. G.; Minick, C. R. *J. Clin. Invest.* **1973,** *52*, 2745.

(36)   Tidwell, C. D.; Ertel, S. I.; Ratner, B. D.; Tarasevich, B. J.; Atre, S.; Allara, D. L. *Langmuir* **1997,** *13*, 3404.

(37)   Gessner, A.; Olbrich, C.; Schroder, W.; Kayser, O.; Muller, R. H. *Int. J. Pharm.* **2001,** *214*, 87.

(38)   Klomp, A. J. A.; Engbers, G. H. M.; Mol, J.; Terlingen, J. G. A.; Feijen, J. *Biomaterials* **1999,** *20*, 1203.

(39)   Leroux, J. C.; Gravel, P.; Balant, L.; Volet, B.; Anner, B. M.; Allemann, E.; Doelker, E.; Gurny, R. *J. Biomed. Mater. Res.* **1994,** *28*, 471.

(40)   Luck, M.; Pistel, K. F.; Li, Y. X.; Blunk, T.; Muller, R. H.; Kissel, T. *J. Control. Release* **1998,** *55*, 107.

(41)   Allemann, E.; Gravel, P.; Leroux, J. C.; Balant, L.; Gurny, R. *J. Biomed. Mater. Res.* **1997,** *37*, 229.

(42)   Bisgaier, C. L.; Siebenkas, M. V.; Williams, K. J. *J. Biol. Chem.* **1989,** *264*, 862.

(43)   Luck, M.; Schroder, W.; Paulke, B. R.; Blunk, T.; Muller, R. H. *Biomaterials* **1999,** *20*, 2063.

(44)   Lacasse, F. X.; Filion, M. C.; Phillips, N. C.; Escher, E.; McMullen, J. N.; Hildgen, P. *Pharm. Res.* **1998,** *15*, 312.

(45)   Vittaz, M.; Bazile, D.; Spenlehauer, G.; Verrecchia, T.; Veillard, M.; Puisieux, F.; Labarre, D. *Biomaterials* **1996,** *17*, 1575.

(46)   Chenoweth, D. E. *Artif. Organs* **1988,** *12*, 508.

(47)   Letourneur, D.; Champion, J.; Slaoui, F.; Jozefonvicz, J. *In Vitro Cell. Dev. Biol.-Anim.* **1993,** *29A*, 67.

(48)   Horbett, T. A. *Acs Symposium Series* **1995,** *602*, 1.

(49)   van Wachem, P. B.; Vreriks, C. M.; Beugeling, T.; Feijen, J.; Bantjes, A.; Detmers, J. P.; van Aken, W. G. *J. Biomed. Mater. Res.* **1987,** *21*, 701.

5

Polymersomes formed from biodegradable amphiphilic block-copolymers using chloroform/water mixtures

ABSTRACT: Amphiphilic block-copolymers based on poly(ethylene glycol) (PEG) and biodegradable polyesters or a polycarbonate have been synthesized by ring-opening polymerization of cyclic esters or a carbonate with zinc bis[bis(trimethylsilyl)amide]/methoxy PEG. High monomer conversion was achieved within 2 h. The polymerization of lactides and carbonate gives block-copolymers with controllable molecular weights and a well defined structure. Biodegradable polymersomes with a size ranging from ~50 nm to 80 μm were readily prepared by injecting a solution of the polymer in chloroform into an aqueous medium under stirring. The vesicular nature of the polymersomes was confirmed by confocal laser scanning microscopy.

INTRODUCTION

Polymersomes refer to self-assembled vesicles, which are similar to liposomes but based on amphiphilic block-copolymers instead of lipids. Polymersomes have fluid-filled cores with walls consisting of an amphiphilic bilayer membrane that separates the core from the outside medium. Compared to liposomes, polymersomes have many distinct properties. The membrane thickness can be controlled by the molecular weight of the hydrophobic block of the copolymer[1] and combined with the character of the hydrophilic block will determine polymersome properties such as elasticity, permeability and mechanical stability[2]. In general, the membranes of polymersomes are thicker, stronger and tougher than those of liposomes due to the higher molecular weight of the consisting polymer. The toughness of polymersomes provides resistance to local perturbations[3]. Due to the fact that polymersome membranes are thicker and tougher than those of conventional liposomes, polymersomes are inherently more stable. For instance, the areal strain of PEO-PBD based polymersomes was from 20 % to 40 %, in contrast with typically <5 % for liposomes[1].

Formation of polymersomes in aqueous media proceeds by self-assembly of the amphiphilic block-copolymers, which is driven by minimization of contact between the hydrophobic blocks and water. Polymersomes can be formed from a range of block-copolymers using organic solvents[4], organic solvent/water mixtures[5-9] or aqueous media[2,10-16]. For example, polymersomes of polyisoprene-b-poly(2-cinnamoylethyl methacrylate) (PIP-PCEMA) were obtained upon addition of hexane, a non-solvent for PCEMA, to a block-copolymer solution in THF[4]. Poly(2-methyloxazoline)-b-poly(dimethylsiloxane)-b-poly(2-methyloxazoline) yielded polymersomes upon dropping a polymer solution in ethanol in distilled water[9]. Polymersomes

of poly(ethylene oxide)-b-poly(ethyl ethylene) (PEO-PEE) and its crosslinkable analogue, poly(ethylene oxide)-b-poly(butadiene) (PEO-PBD), were prepared by well-known liposome preparation methods, e.g., by sonication of an aqueous copolymer dispersion or hydration of a polymer film[2]. Recently, peptosomes, polymersomes formed from a block-copolymer of a synthetic polymer and a polypeptide, e.g., poly(butadiene)-b-poly(L-glutamate), were obtained by directly mixing the copolymers in an aqueous solution[15,16]. These peptosomes showed a pH sensitive helix-coil transition. Besides polymersome formation that is driven by phase separation as described above, polymersome formation can also be induced by highly specific recognition, e.g., hydrogen bonding between the complementary random copolymers featuring diamidopyridine and thymine functionalities, respectively[17,18].

Polymersomes are interesting for many potential applications. Previous studies have shown that plasma proteins imposed no immediate effect on the stability of polymersomes of PEO-PEE and PEO-PBD and that the polymersomes did not adhere to macrophages. These properties make these polymersomes attractive for mimicking red blood cells[2,19]. Nardin et al.[9,20] prepared polymersomes of poly(2-methyl-oxazoline)-b-poly(dimethylsiloxane)-b-poly(2-methyl-oxazoline) to mimic cell membranes. The slow addition of a mixture of a channel protein (bacterial porin OmpF) and polymer solution in ethanol to an aqueous solution containing b-lactamase, yielded nano-reactors with encapsulated enzyme, of which the permeability was controlled by the channel proteins in the membrane. The enzyme was entrapped in the interior of the particles while the substrate and products were able to diffuse in and out of the nano-reactors.

For in vivo applications of polymersomes such as drug delivery systems, bioreactors and artificial cells, the ultimate membrane-forming materials should be biodegradable. Biodegradable block-copolymers containing a poly(ethylene glycol) (PEG) block and a polyester block such as polylactide (PDLLA), and poly(ε-caprolactone) (PCL) or a polycarbonate block such as poly(trimethylene carbonate) (PTMC), have been applied as drug delivery systems[21,22] like micelles, nano- or micro-particles and gels. These block-copolymers combine the most important properties required for biomedical applications, i.e., the biodegradability of polyesters or polycarbonates, and the protein resistance of PEG[23,24] and excretability of PEG with a molecular weight less than 50,000 g/mol[25].

In this study, we have prepared biodegradable polymersomes from PEG-polyesters and PEG-polycarbonate amphiphilic block-copolymers. These block-copolymers were synthesized by using non-toxic zinc bis[bis(trimethylsilyl)amide] as a catalyst. To study the influence of the copolymer structure on polymersome formation, a series of block-copolymers with different molecular weights, molecular weight ratio's of the two blocks, and hydrophobic block characteristics (glass transition temperature T_g and crystallinity) were synthesized. Biodegradable polymersomes were prepared by injecting a solution of the polymer in chloroform into an aqueous medium under vigorous stirring. Chloroform was removed subsequently by evaporation. The polymersome preparations were characterized microscopically and a mechanism for the polymersome formation is described.

EXPERIMENTAL

Materials

 d,l-Lactide (DLLA, Purac Biochem b.v., Gorinchem, the Netherlands) and trimethylene carbonate (TMC, Boehringer, Ingelheim, Germany) were purified by recrystallization from dry toluene. ε-Caprolactone (CL, Merck-Schuchardt, Darmstadt, Germany) and dichloromethane (Biosolve, Valkenswaard, the Netherlands) were dried over CaH_2 and distilled prior to use. Monomethoxy poly(ethylene glycol) with Mn's of 5800 and 1200 (denoted as PEG5800 and PEG1200, respectively) (Fluka Chemika, Buchs, Switzerland) were dried by dissolution in anhydrous toluene followed by azeotropic distillation under N_2. Fluoresceinamine isomer II, Nile Red, zinc bis[bis(trimethylsilyl)amide] (97%) (Aldrich, Milwaukee, USA), and phosphotungstic acid sodium salt (Sigma, St. Louis, USA) were used as received. De-ionized water (DI water) was obtained from a Milli-Q water purification system (Millipore, Molsheim, France). Phosphate buffered saline (PBS) (pH 7.4) was purchased from NPBI (Emmer Compascuum, The Netherlands).

Synthesis of PEG-b-polyesters and PEG-b-polycarbonate block-copolymers

All polymerization reactions were carried out at room temperature under a nitrogen atmosphere using dichloromethane as a solvent. In a typical experiment, to a solution (31.5 mL) of DLLA (8.922 g, 6.20×10^{-2} mol) and PEG 5800 (0.453 g, 1.86×10^{-4} mol) in dichloromethane, zinc bis[bis(trimethylsilyl)amide] (0.036 g, 0.93×10^{-4} mol) dissolved in 1.0 mL of dichloromethane was added under stirring. The reaction was allowed to proceed for 2 h and was then terminated by adding an excess of acetic acid. For the preparation of copolymers with random hydrophobic blocks, the procedure was the same except that a mixture of monomers (CL and TMC) with a certain ratio was polymerized. All copolymers were isolated by precipitation in a 20-fold volume of cold (4 ºC) diethyl ether/methanol (4:1 v/v), followed by filtration and drying under vacuum for 48 h. Monomer conversion and yield were typically 99 and 90%, respectively. The copolymers are denoted by PEG-PDLLA, PEG-PCL, PEG-PTMC or PEG-P(CL-co-TMC) followed by the molecular weights ($\times 10^{-3}$ g/mol) of the PEG and the hydrophobic blocks, respectively (Table 1).

Characterization of copolymers

Molecular weights and polydispersities of polymers were determined by NMR and GPC, respectively. ^{1}H (300 MHz) and ^{13}C NMR (75 MHz) spectra were recorded on a Varian Inova spectrometer (Varian, Palo Alto, USA) with chemical shifts relative to the non-deuterated solvent peak. GPC measurements were conducted with a Waters 6000A GPC apparatus (Waters, Milford, USA) equipped with a series of standard Waters Styragel HR columns (HR0.5, HR2, HR4) and a H502 viscometer detector (Viscotek Corp., Houston, USA) for absolute molecular weight determinations using universal calibration. Polystyrene standards with narrow molecular weight distribution (PSS, Mainz, Germany) were used for calibration. Polymers were dissolved in chloroform (1.0 %), and elution was performed at 25 °C at a flow rate of 1.5 mL/min using chloroform as eluent.

The thermal properties (glass transition temperature T_g and melting temperature T_m) of the polymers were determined with a DSC7 (Perkin-Elmer, Shelton, USA). Samples (5-10 mg) in aluminium pans were heated from –100°C to 100°C at 20 °C/min, and kept at 100°C for 2 min. Subsequently the samples were quenched to –100°C at 300°C/min, and kept at –100°C for 2 min before heating to 100 °C at 20 °C/min. Data of the second heating curve were used for determination of T_g and T_m.

Preparation of polymersomes

A solution of the polymer in chloroform (10 mg/mL, 0.1 mL) was added to 5 mL of DI water or PBS under vigorous stirring. Upon addition, stirring was continued for 1-2 h. To enable polymersome characterization by confocal laser scanning microscopy (CLSM), fluorescent probes were incorporated in the polymersomes during polymersome formation. Hydrophobic Nile red (excitation 550 nm,

emission 650 nm) was dissolved in the polymer solution (0.65 mg/mL) whereas hydrophilic fluoresceinamine (excitation 480 nm, emission 525 nm) was dissolved in the aqueous phase (1 mg/mL). To study the optimal conditions for the preparation of polymersomes, the concentration of polymer PEG-PDLLA5.8-48 solution was varied from 0.2 to 10 wt.%, the volume of the polymer solution from 0.01 to 0.2 mL and the volume of the aqueous phase from 5 to 100 mL. The mixture was stirred at a speed varying from 600 to 1300 rpm and stirring times of 5, 15, 30, 60, 120 or 180 min were selected.

To study the effect of chloroform removal on the stability of the polymersomes, chloroform was removed either by evaporation under vacuum using a rotary evaporator for a few minutes (until chloroform boiling subsided) or by evaporation at ambient conditions under stirring for three days. These methods are named fast and slow evaporation, respectively. Typically, after the preparation of polymersomes, 1/3 of the volume was taken for fast evaporation, 1/3 for slow evaporation, and the remaining 1/3 as control for comparison.

Characterization of polymersomes

CLSM images were recorded with a Confocal Scanning Laser Microscope (Insight Plus, Meridian Instruments Inc., Meridian, Oketos). A polymersome suspension (0.5 mL) was added to a homemade thin-glass-bottomed cuvette, which was placed on the lens with index matching oil. Suspensions of polymersomes with encapsulated Nile red were used directly, whereas suspensions of polymersomes with encapsulated fluoresceinamine were diluted with an equal volume of deionised water (DI water) before measurement.

For scanning electron microscopy (SEM), performed at 0.67 kV on a LEO Gemini 1550 FEG-SEM (LEO Electron Microscopy Ltd, Cambridge, UK), 5 μL of polymersome suspension was placed on a carbon substrate and dried in air before analysis.

For transmission electron microscopy (TEM), polymersome samples (5 μL) were placed on a carbon coated copper grid (400 mesh) and excess liquid was removed with a filter paper. After drying in air for 5 min the samples were stained by the addition of 5 μL of phosphotungstic acid sodium salt (2 wt.%) solution for 8 min. Then excess stain was removed with a filter paper from the edge of the copper grid and the sample was air-dried. TEM measurements were performed with a Philips CM30 Twin STEM (Philips, Eindhoven, the Netherlands) at an acceleration voltage of 200 kV.

RESULTS AND DISCUSSION

Block-copolymer synthesis

Block-copolymers were synthesized by ring-opening polymerization (ROP) of *d,l*-lactide (DLLA), ε-caprolactone (CL) or trimethylene carbonate (TMC) using zinc bis[bis(trimethylsilyl)amide] and monomethoxy PEG as an initiator (Scheme 1). Polymerizations were conducted at room temperature using dichloromethane as a solvent. Complete monomer conversion was obtained within 2 h. As revealed by ^{1}H NMR and GPC (Table 1), the polymerization of DLLA using $Zn[N(SiMe_3)_2]_2$/methoxy PEG yields block-copolymers with molecular weights that are close to the theoretical values and low polydispersities (M_w/M_n). The polymerization of CL and especially TMC gave polymers with high polydispersities. Similar results were obtained when analogous calcium based initiating systems were used. The relatively fast propagation as compared to the initiation in the ROP of CL and TMC has been proposed as a cause for high polydispersities [26].
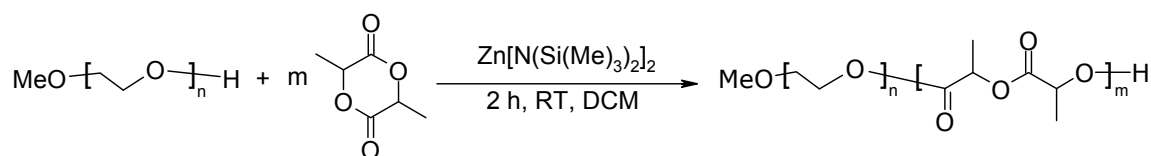
Scheme 1. *Synthesis of PEG-PDLLA using zinc bis[bis(trimethylsilyl)amide]/PEG as a catalyst system.*

The block structure of the copolymers was confirmed by NMR. In the ^{1}H NMR spectrum (300 MHz, CDCl$_3$) of methoxy PEG-PDLLA, besides signals assignable to PEG and PDLLA blocks, also signals that can be attributed to the α-protons of the ethylene glycol units connected to the PDLLA block (δ 4.25), the methine proton neighbouring the hydroxyl end group (δ 4.35), and the methoxy protons of PEG (δ 3.38) were clearly observed. Moreover, the ratio of the sum of the integrals of the peaks at δ 4.25 and δ 4.35 to that of δ 3.38 was close to 1. It is therefore evident that all methoxy PEG molecules have initiated the ROP of lactide to give a diblock-copolymer with a well-defined structure. Similarly, the block-copolymer structures of PEG-PCL and PEG-PTMC as well as PEG-P(CL-co-TMC) were also confirmed. The microstructure of PEG-P(CL-co-TMC) copolymers was studied by ^{13}C NMR. The carbonyl carbon region is particularly sensitive to the monomer sequence[27]. In ^{13}C NMR spectrum of the PEG-P(CL-co-TMC), in addition to signals arising from homo-sequences CL-CL (δ 173.0) and TMC-TMC (δ 154.5), peaks assignable to CL-TMC (δ 172.7) and TMC-CL (δ 154.2) sequences were also clearly detected. This result suggests that the P(CL-co-TMC) block is a random copolymer of CL and TMC. Moreover, thermal analysis showed that the hydrophobic block of PEG-P(CL-co-TMC) is amorphous with a T$_g$ lower than -50°C.

Table 1. Characteristics of diblock-copolymers

Block-copolymer [a]	Mn[b] NMR (× 10^{-3})	Mn[d] theor. (× 10^{-3})	PDI[c]	T$_g$	T$_m$
PEG-PDLLA1.2-4.8	6.6	6.1	1.1		
PEG-PDLLA1.2-12	14.8	13.2	1.1	37	
PEG-PDLLA1.2-24	23.5	23.8	1.2		
PEG-PDLLA3.0-24	22.8	24.0	1.4		
PEG-PDLLA5.8-14	20.4	22.4	1.1		
PEG-PDLLA5.8-24	28.2	30.2	1.1	37	
PEG-PDLLA5.8-48	50.5	53.0	1.5	35	
PEG-PCL1.2-12	11.0	12.1	1.1	-68	56
PEG-PCL5.8-24	29.8	29.7	1.9	-66	54
PEG-PTMC5.8-24	30.9	29.7.	9.0	-35	
PEG-P(CL-co-TMC)1.2-2.0	3.2	3.0		-58	36
PEG-P(CL-co-TMC)1.2-9	12.3	9.9		-59	45
PEG-P(CL-co-TMC)5.8-8.5	14.0	14.2		-54	52

[a] are denoted by PEG-polyester or polycarbonate followed by the Mn of the blocks (×10^{-3}); [b] determined by ^{1}H NMR using the integrals of the methylene peak of PEG and the main peaks of the polyester or polycarbonate block; [c] polydispersity index determined by GPC; [d] calculated from the initial ratio of monomer to PEG hydroxyl groups and the conversion.

It is clear that similar to the calcium bis[bis(trimethylsilyl)amide] catalyst system[28], zinc bis[bis(trimethylsilyl)amide] combined with methoxy PEG is highly active and initiates

controlled ring-opening polymerization of lactides and ε-caprolactone with high conversion under mild conditions, affording the synthesis of PEG-polyester block-copolymers with a predetermined molecular weight and defined structure (Table 1). The low toxicity of the zinc-based catalyst is desirable for the synthesis of polymers for medical applications.

Polymersome formation and characterization

An initial experiment showed that direct mixing of PEG-PDLLA with water did not yield polymersomes even after vigorous stirring for one week. This could be due to the relatively high molecular weight leading to increased physical entanglements between chains and slow relaxation dynamics[1], or possibly high T_g of the PDLLA block (35–37°C, if the block has similar T_g in an aqueous environment as in the dry state). PEG-PCL, PEG-PTMC and PEG-P(CL-co-TMC), which have a low Tg (–66, –35 and –50 °C, respectively), gave polymersomes (<3 μm) under the same conditions. However, most of the polymer did not form polymersomes. This is probably due to the high absolute and relative (with respect to PEG) molecular weight of the polyester or polycarbonate blocks.

In solutions of the block-copolymers in organic solvents, the polymer chains are much more mobile and after contact with water, phase separation is facilitated. Injection of a solution of a polymer in chloroform into a vigorously stirred aqueous medium resulted in an opaque dispersion within 5 min. Additional stirring for 1-2 h gave particles with a broad size distribution from 70 nm to 80 μm. Using this method, particles could be prepared from all polymers that are listed in Table 1. Unfortunately, also precipitates of the polymers were observed.

Verification of the vesicular structure. CLSM was applied to study the location of the fluorescent probes in the particles. Figure 1 shows images of giant polymersomes (20–80 μm) prepared from PEG-PDLLA1.2-12 with encapsulated hydrophilic fluoresceinamine (A) or hydrophobic Nile red (B, C). To reveal the polymersomes with encapsulated hydrophilic fluoresceinamine, the polymersome dispersion was diluted 1:1 with DI water just before CLSM measurements in order to decrease the fluorescence of the aqueous medium outside the polymersomes. Probably due to the low absolute fluorescence in combination with the low resolution of the microscope, this did not enhance the contrast between the inside and outside of the polymersomes. Nonetheless, dark rings were observed (Figure 1A), indicating the hydrophobic nature of the polymersome wall. CLSM of polymersomes prepared in the presence of Nile red (Figures 1B and 1C) showed that the hydrophobic dye was preferentially incorporated into the polymersome wall, as revealed by the high fluorescence of the polymersome wall and the relatively low fluorescence of the medium inside the polymersomes. Therefore, it is confirmed that particles formed via the chloroform/water system are indeed polymersomes. Moreover, scanning of a giant polymersome (20–50 μm) by changing the focal plane supported the vesicular and three-dimensional structure of the polymersomes.

It should be noted that besides unilamellar or multilamellar polymersomes, other structures, like "pregnant" polymersomes, large compound vesicles structures (partly fused aggregates of vesicles) (10-100 μm) as well as (branched) tubules (0.5-10 μm) were frequently observed in the polymersome preparations of all copolymers.
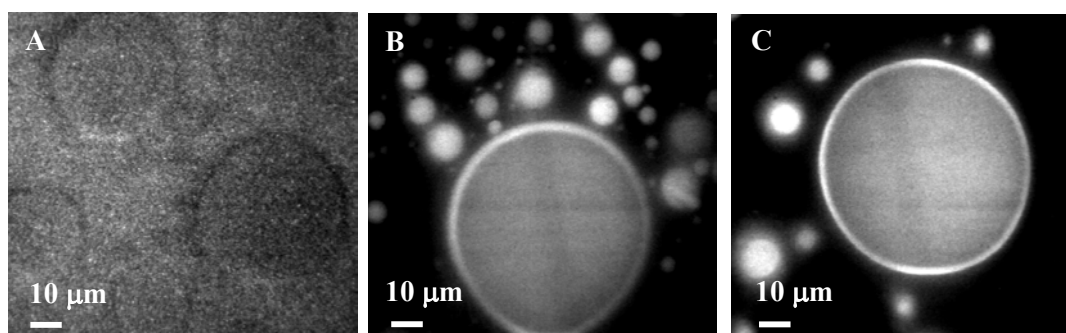
Figure 1. *CLSM images of polymersomes prepared by adding a solution of PEG-PDLLA1.2-12 in chloroform to an aqueous phase (A, B: DI water; C: PBS) in the presence of fluoresceinamine (A) or Nile red (B, C) as a fluorescent probe.*

Transmission electron microscopy (TEM) study. Negative staining TEM was applied to study the membrane thickness of the polymersome wall and to reveal the possible presence of other structures in the polymersome preparation that could not be resolved by CLSM. Phosphotungstic acid sodium salt, a staining agent for esters, was used to make PDLLA appear as the dark phase and PEG as the bright phase in TEM images. Figure 2 shows typical TEM images of polymersome preparations. Interestingly not only polymersomes, but also tubules and flat lamellae were formed in almost all cases. Long tubules (50–60 nm in diameter and up to 10 μm in length) with visible closed ends, which were reported for the PS-PEO/dioxane/water system,[29] were also observed for PEG-PDLLA5.8-14 and 5.8-24. The dark walls of the tubules consist of the hydrophobic block while the bright interiors correspond to a PEG-rich phase and empty space. Uni-lamellar polymersomes with a size ranging from 70 to 400 nm were also present. The observation of intermediate structures like "necklace" structured tubules as well as bilayer/lamellae with protruding rods may indicate that these structures are transition states from which vesicles are formed. Copolymers with longer hydrophobic blocks gave more vesicles than lamellae and tubules, and PEG-PTMC showed a wider variety of structures than PEG-PCL and PEG-PDLLA copolymers.
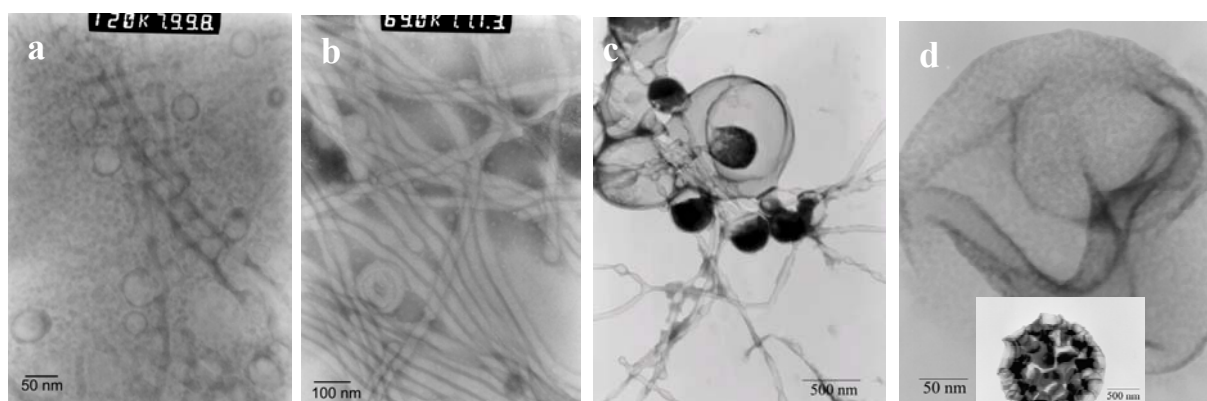

Figure 2. *TEM images of polymersome preparations obtained by adding a solution of PEG-PDLLA5.8-17 (a ,b), 5.8-24 (c), or 5.8-48 (d) in chloroform to an aqueous phase under stirring. The inset in d is an example of a large compound vesicle.*

The membranes of tubules or flat lamellae were somewhat thicker than that of the polymersomes using the same copolymer. The average thickness of bilayer structures (polymersomes, tubules or flat lamellae) was in the range of 10-35 nm. The thickness depended on the Mn and type of polymers used (Table 2). The range of the wall thickness of polymersomes reported in literature was similar[1,4,8,10,30]. For instance, the wall thickness of polymersomes of PEO-PBD increased more or less linearly with the square root of the molecular weight of the hydrophobic block. The membrane thickness increased from 8 nm to 22 nm when the molecular weight of hydrophobic block increased from 3.6×10^3 to 20×10^3 g/mol[1]. The membranes of the polymersomes from all copolymers were thinner than the fully extended hydrophobic blocks, suggesting a coiled or entangled hydrophobic block chain in the inner membrane structure.

Table 2. The membrane thickness of bilayer structures [a]

Diblock-copolymer	Thickness (nm)
PEG-PDLLA1.2-4.8	13.4 ±4.6
PEG-PDLLA1.2-12	12.1 ±2.1
PEG-PDLLA5.8-14	9.2±1.1
PEG-PDLLA5.8-24	21.6±5.4
PEG-PCL5.8-24	33.4±4.5
PEG-PTMC5.8-24	26.5±7

[a]measured from the thickness of vesicles, tubules and/or flat lamellae as revealed from TEM images.

Based on the observations as described earlier, a polymersome model is derived, in which the wall of the polymersomes consists of a layer of stacked,coiled polymer chains,held together by non-covalent forces with the PEG blocks protruding into the aqueous phases and the entangled hydrophobic block forming the core of the polymersome wall (Figure 3).
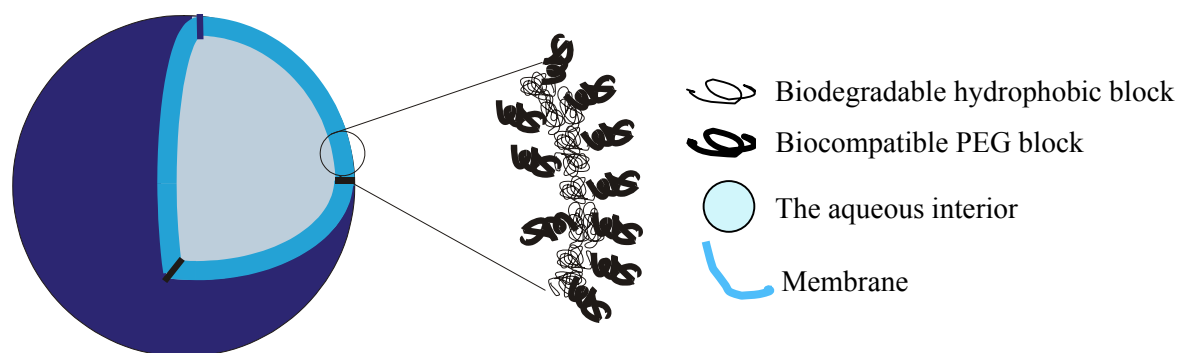

Figure 3. Schematic representation of a polymersome with a magnified wall structure.

Mechanism of polymersome formation. For the formation of polymersomes in the chloroform/water system a mechanism analogous to the formation of liposomes is suggested. When the organic phase is broken up by stirring into small droplets in an aqueous phase, the block-copolymer chains are present as randomly distributed polymer chains inside the chloroform droplets and ordered polymer chains at the chloroform/water interface. This is dictated by the low interfacial energy between PEG and water[31], as also expressed by the low

heat of solution of PEG in water (24 J/g for a PEG molecular weight of 6×10^3 g/mol at 30 $^{\circ}$C) as compared to the heat of solution in chloroform (52 J/g)[32]. Thus water is a better solvent for PEG but a non-solvent for polyesters and polycarbonate. Since water and chloroform are immiscible, the block-copolymer chains are forced to organize at the chloroform/water interface with the PEG blocks protruding into the aqueous phase and the hydrophobic block situated inside the droplet in a coil conformation.

As long as there is space at the chloroform/water interface, the block-copolymer will diffuse to the surface. At a certain interface occupation that provides the monolayer with certain mechanical properties, the monolayer may peel off under influence of the shear forces induced by mechanical stirring. In combination with other peeled monolayers or by reassembly they may form fragmented bilayers[33,34]. These newly formed fragmented bilayers have to bend and make a closed system in order to prevent the exposure of the hydrophobic part to the aqueous medium[35], which is energetically unfavourable. Possibly, some small pieces of fragmented bilayers will grow to a certain length before they assemble into vesicles. This process is quite similar to the formation of liposomes[33]. After the monolayers are peeled off, the "new" surface of the chloroform droplets will be covered again by copolymer chains that diffuse from the chloroform bulk and organize on the surface, thus continuing the formation of polymersomes.

A few points should be noted here. First of all, large polymersomes were formed in this system, which is mainly caused by the high interfacial tension between the chloroform droplets and the water phase and the total interfacial surface area is minimized by forming large spherical structures[36]. Secondly, the wide range of sizes of the formed polymersomes can be ascribed either to the broad size range of the original chloroform droplets, and/or to the breaking of bilayers as a result of vigorous stirring. Thirdly, the occurrence of polymer precipitate seems unavoidable for this method and is probably due to the fast evaporation of chloroform.

Influence of preparation parameters on polymersome formation. In order to qualitatively study the influence of preparation parameters on the polymersome formation, the effect of varying the polymer concentration of the chloroform phase, the relative volume of the chloroform phase as compared to the aqueous phase, the stirring time and speed and the nature of the hydrophobic block (M_n, T_g and crystallinity) on the number of polymersomes, their size, and the amount of precipitate was investigated by light microscopy.

An increase in the concentration of PEG-P(CL-co-TMC)5.8-8.5 from 0.2 to 10 wt.% under otherwise identical conditions led to an increase in the number and size of polymersomes. A high concentration of the copolymer gives a high viscosity of the copolymer solution. Thus at the same stirring speed bigger droplets will form, which leads to the formation of larger monolayer fragments and eventually to large polymersomes. An equal volume of copolymer solution with a higher polymer concentration can provide more polymer chains for coating of the chloroform/water interface, resulting in a larger amount of polymersomes.

Decreasing the volume ratio of organic phase to aqueous phase at a constant PEG-P(CL-co-TMC)5.8-8.5 concentration (10 wt.%) resulted in an increased number and decreased size of polymersomes. A smaller volume of the polymer solution at the same stirring speed leads to the formation of smaller droplets, which results in the formation of shorter monolayers and smaller bilayer fragments (even smaller if they are broken), thereby yielding smaller

polymersomes. At the same stirring speed, these monolayers or bilayer fragments tend to be broken more easily, giving more polymersomes.

Observations revealed that with the increase of stirring time (at 800 rpm) the number of polymersomes increased and after ca. 1 h a maximum was reached. Increasing the stirring speed from 600 to 1200 rpm drastically increased the number and decreased the size of polymersomes, which is ascribed to the formation of smaller chloroform droplet (see the previous paragraph) and/or the higher shear force exerted. When the solution was not stirred at all, only a few very small vesicles (< 1 μm) were spontaneously formed.

The nature of the hydrophobic block (rigidity or crystallinity) of the copolymers influenced the formed polymersomes as well. PEG-PDLLA formed relatively larger polymersomes as compared to the other polymers. This could be due to the rigidity of its amorphous hydrophobic block and thus the relatively high bending modulus[37]. Polymers having rubbery hydrophobic blocks e.g. PEG-P(CL-*co*-TMC) and those having hydrophobic blocks with possible crystallinity but low T_g, like PEG-PCL, gave smaller polymersomes, coexisting with a relatively large amount of fused structures.

Stability of the polymersomes after the removal of chloroform. The water immiscible organic solvent, chloroform, which may fluidize the membrane and thus jeopardize the stability of the polymersomes, was removed from the polymersome preparation after polymersome formation, either by fast or slow evaporation. This can freeze the polymersome structure as shown previously[38]. To study the influence of molecular weight, crystallinity and hydrophobicity on the stability of polymersomes after the removal of chloroform, polymersomes were prepared from PEG-PDLLA5.8-14, 5.8-24, 5.8-48, and 1.2-12, PEG-PCL1.2-12, 5.8-24 and PEG-PTMC5.8-24.

For PEG-PDLLA5.8-48 many polymersomes maintained intact for more than one month after either fast or slow evaporation of chloroform. This is in contrast with a life time of a few hours for polymersomes when chloroform is still present. Polymersomes of other polymers only became stable (more individual polymersomes and less precipitates after one month) when chloroform was evaporated slowly. Fast evaporation induced aggregation and fusion of polymersomes, possibly due to the lack of stirring during the rotary evaporation process. LM observations showed that after fast evaporation some polymersome surfaces were wrinkled or had collapsed (especially bigger vesicles > 10 μm were deformed). This is ascribed to membrane defects due to the slow chain rearrangement and/or to pressure differences between the membrane and its surroundings caused by the rapid chloroform efflux. The survival of polymersomes of PEG-PDLLA5.8-48 is most probably due to its relatively high molecular weight as well as the toughness of the resulting membrane.

Comparing the effect of chloroform evaporation on the morphology of polymersomes that were obtained from different copolymers, it was observed that polymersomes of copolymers with rubbery hydrophobic blocks, e.g., PEG-PTMC and PEG-P(CL-*co*-TMC) showed much more fusion than those from copolymers containing rigid hydrophobic blocks, e.g., PEG-PDLLA5.8-48 and 1.2-12, or those from copolymers with (possible) crystalline blocks, e.g., PEG-PCL1.2-12. The reason is that polymers with a high molecular weight, T_g or crystallinity have low chain mobility.

In the dry state, these survived polymersomes showed a spherical structure and a smooth surface. Some polymer precipitate and fused structures were also observed (Figure 4). In a few cases, polymersome surfaces from PEG-PDLLA5.8-48 appeared to be wrinkled or corrugated. The perseverance of the spherical shape of big polymersomes (> ca. 300 nm) under reduced pressure was ascribed to the high molecular weight and high T_g of PDLLA or the crystallinity of PCL. This is in contrast with control samples where chloroform was still present in the membrane, which showed much more precipitate and deformed big polymersomes. Therefore, it is concluded that evaporation of chloroform increases the stability of the polymersomes.
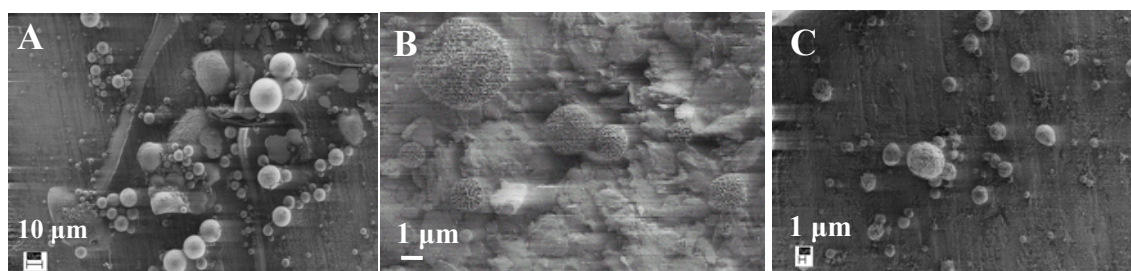

Figure 4. SEM micrographs of polymersomes after slow evaporation for 35 days. (A) PEG-PDLLA5.8-14, (B) PEG-PDLLA5.8-48 and (C) PEG-PCL1.2-12.

CONCLUSIONS

It was demonstrated that polymersomes can be formed from amphiphilic block-copolymers PEG-polyesters or PEG-polycarbonate upon injection of chloroform solutions of these polymers in aqueous media. The size distribution of polymersomes formed via this method was broad and ranged from 70 nm to 80 μm. The vesicular nature of the polymersomes was confirmed by CLSM and TEM. Removal of chloroform from the polymersomes enhanced their stability as evidenced by the survival of chloroform-free polymersomes for more than one month in aqueous media at 4°C whereas polymersomes still containing chloroform were only stable for a few hours. Copolymers with longer hydrophobic blocks, a high T_g or crystallinity afford large polymersomes with a relatively high yield.

However, due to the inherent problems related to the chloroform/water method like the broad size range and the presence of a large amount of precipitate, this method is not suitable for the preparation of well-defined polymersomes and therefore other methods should be developed.

REFERENCES

(1)   Bermudez, H.; Brannan, A. K.; Hammer, D. A.; Bates, F. S.; Discher, D. E. *Macromolecules* **2002,** *35*, 8203.

(2)   Lee, J. C. M.; Bermudez, H.; Discher, B. M.; Sheehan, M. A.; Won, Y. Y.; Bates, F. S.; Discher, D. E. *Biotechnol. Bioeng.* **2001,** *73*, 135.

(3)   Won, Y. Y.; Davis, H. T.; Bates, F. S. *Science* **1999,** *283*, 960.

(4)   Ding, J. F.; Liu, G. J. *Macromolecules* **1997,** *30*, 655.

(5)   Zhang, L. F.; Eisenberg, A. *Science* **1995,** *268*, 1728.

(6)   Shen, H. W.; Eisenberg, A. *Macromolecules* **2000,** *33*, 2561.

(7)   Yu, K.; Eisenberg, A. *Macromolecules* **1998,** *31*, 3509.

(8)   Holder, S. J.; Hiorns, R. C.; Sommerdijk, N. A. J. M.; Williams, S. J.; Jones, R. G.; Nolte, R. J. M. *Chem. Commun.* **1998**, 1445.

(9)   Nardin, C.; Hirt, T.; Leukel, J.; Meier, W. *Langmuir* **2000,** *16*, 1035.

(10) Cornelissen, J. J. L. M.; Fischer, M.; Sommerdijk, N. A. J. M.; Nolte, R. J. M. *Science* **1998,** *280*, 1427.

(11) Discher, B. M.; Won, Y. Y.; Ege, D. S.; Lee, J. C. M.; Bates, F. S.; Discher, D. E.; Hammer, D. A. *Science* **1999,** *284*, 1143.

(12) Li, Z. C.; Jin, W.; Liu, F. M. *React. Funct. Polym.* **1999,** *42*, 21.

(13) Schillen, K.; Bryskhe, K.; Mel'nikova, Y. S. *Macromolecules* **1999,** *32*, 6885.

(14) Dimova, R.; Seifert, U.; Pouligny, B.; Forster, S.; Dobereiner, H. G. *Eur. Phys. J. E* **2002,** *7*, 241.

(15) Kukula, H.; Schlaad, H.; Antonietti, M.; Forster, S. *J. Am. Chem. Soc.* **2002,** *124*, 1658.

(16) Checot, F.; Lecommandoux, S.; Gnanou, Y.; Klok, H. A. *Angew. Chem.-Int. Edit.* **2002,** *41*, 1339.

(17) Thibault, R. J.; Galow, T. H.; Turnberg, E. J.; Gray, M.; Hotchkiss, P. J.; Rotello, V. M. *J. Am. Chem. Soc.* **2002,** *124*, 15249.

(18) Drechsler, U.; Thibault, R. J.; Rotello, V. M. *Macromolecules* **2002,** *35*, 9621.

(19) Hammer, D. A.; Discher, D. E. *Ann. Rev. Mater. Res.* **2001,** *31*, 387.

(20) Nardin, C.; Widmer, J.; Winterhalter, M.; Meier, W. *Eur. Phys. J. E* **2001,** *4*, 403.

(21) Stolnik, S.; Dunn, S. E.; Garnett, M. C.; Davies, M. C.; Coombes, A. G. A.; Taylor, D. C.; Irving, M. P.; Purkiss, S. C.; Tadros, T. F.; Davis, S. S.; Illum, L. *Pharm. Res.* **1994,** *11*, 1800.

(22) Vittaz, M.; Bazile, D.; Spenlehauer, G.; Verrecchia, T.; Veillard, M.; Puisieux, F.; Labarre, D. *Biomaterials* **1996,** *17*, 1575.

(23) Jeon, S. I.; Andrade, J. D. *J. Colloid Interface Sci.* **1991,** *142*, 159.

(24) Jeon, S. I.; Lee, J. H.; Andrade, J. D.; Degennes, P. G. *J. Colloid Interface Sci.* **1991,** *142*, 149.

(25) Yamaoka, T.; Tabata, Y.; Ikada, Y. *J. Pharm. Sci.* **1994,** *83*, 601.

(26) Zhong, Z. Y. PhD thesis, University of Twente, Enschede : PrintPartners Ipskamp, **2002**.

(27) Albertsson, A. C.; Eklund, M. *J. Polym. Sci. Pol. Chem.* **1994,** *32*, 265.

(28) Zhong, Z. Y.; Dijkstra, P. J.; Birg, C.; Westerhausen, M.; Feijen, J. *Macromolecules* **2001,** *34*, 3863.

(29) Zhang, L. F.; Eisenberg, A. *Macromolecules* **1999,** *32*, 2239.

(30) Nardin, C.; Thoeni, S.; Widmer, J.; Winterhalter, M.; Meier, W. *Chem. Commun.* **2000**, 1433.

(31) Lee, J. H.; Kopeckova, P.; Zhang, J.; Kopecek, J.; Andrade, J. D. *Abstr. Pap. Am. Chem. Soc.* **1988,** *196*, 50.

(32) Orwoll, R. A. In *Polymer Handbook*; Brandrup, J., Immergut, E. H., Grulke, E. A., Eds.; John Wiley & Sons, Inc.: New York, **1999**, p VII 671.

(33) Lasic, D. D. *Liposomes: from physics to applications*; Elsevier: Amsterdam, **1993**.

(34) Lasic, D. D. *Biochem. J.* **1988,** *256*, 1.

(35) Fromherz, P.; Rüppel, D. *FEBS* **1985,** *179*, 155.

(36) Cameron, N. S.; Corbierre, M. K.; Eisenberg, A. *Can. J. Chem.-Rev. Can. Chim.* **1999,** *77*, 1311.

(37) Bergstrom, M.; Eriksson, J. C. *Langmuir* **1998,** *14*, 288.

(38) Zhang, L. F.; Eisenberg, A. *J. Am. Chem. Soc.* **1996,** *118*, 3168.

6

Polymersomes formed from biodegradable amphiphilic block-copolymers using a water miscible solvent/aqueous solution system

ABSTRACT: Biodegradable polymersomes were prepared from amphiphilic poly(ethylene glycol)-polyester and poly(ethylene glycol)-polycarbonate block-copolymers. Polymersomes with a size from ~170 nm to ~1200 nm and a low polydispersity index (<0.2) were readily obtained by injecting a solution of the polymer in a water miscible solvent in an aqueous phase that contained an organic solvent for the block-copolymers. TEM and confocal laser scanning microscopy analyses confirmed the vesicular structure of the particles. A systematic investigation showed that the nature of the solvent for the polymer, and of the aqueous phase, the polymer concentration and the volume ratio of the polymer solution and the aqueous phase are the factors that determine the size of the polymersomes. The composition of the copolymer, such as molecular weight of the two blocks and the nature of the hydrophobic block, only influences the polymersome yield and size distribution. Removal of the organic solvents from the polymersomes increases their stability. These biodegradable polymersomes have a great potential for biomedical applications e.g. as artificial cells and carriers for drug delivery.

INTRODUCTION

Polymersomes, i.e. polymer vesicles, have received great interest in recent years, and are promising systems for biomedical applications for instance as artificial cells, carriers for drug delivery and for mimicking cell membranes. For the in vivo application of polymersomes the membrane-forming materials should preferably be biodegradable. Biodegradable block-copolymers based on poly(ethylene glycol) (PEG) and polylactides (PDLLA) have been used to prepare carriers for controlled drug delivery[1,2] such as micelles, nano- or microparticles and gels. It has been shown that polymersomes can be formed from a range of block-copolymers using organic solvents,[3] organic solvent/water mixtures[4-8] or aqueous media[9-16].

Different from polymersomes of which the membrane consists of well organized polymer chains, capsules have membranes made of randomly distributed polymer chains. Two methods that are commonly used for the preparation of nano-capsules are interfacial deposition of polymers[17] and the emulsification-diffusion method[18-21].

In the interfacial deposition method[17], a lipophilic drug, oil, polymer and optionally phospholipids are dissolved in a water miscible semi-polar solvent such as acetone. This solution is then poured under stirring into an aqueous phase that may contain a surfactant. Nano-capsules are formed instantaneously by the fast diffusion of the water miscible solvent

into the water phase, which provokes interfacial turbulence that results in the spontaneous emulsification of the oily solution and the formation of a polymer film around the oily nano-droplets that contain the drug[17].

In the emulsification-diffusion method[18-21], a lipophilic drug, a polymer and an oil are dissolved in a partially water miscible solvent (e.g. ethyl acetate, benzyl alcohol or propylene carbonate), which is saturated with water. The aqueous phase containing a stabilizer is saturated with the same solvent. The addition of the organic solution into the aqueous phase under stirring results in spontaneous emulsification of the partially water miscible solution. The addition of extra water to the system causes the partially water miscible solvent to diffuse into the aqueous phase, leading to the formation of the nano-capsules with the lipophilic drug encapsulated in the oil core. Using this method, little or no precipitation occurs since the solutions are initially in thermodynamic equilibrium. A high yield is an additional advantage.

In the previous chapter, it was demonstrated that biodegradable polymersomes of PEG-polyesters and PEG-polycarbonate block-copolymers can be formed from two-phase systems e.g. chloroform/water using the self-organization of the copolymer chains at the interface of the two phases. However, the thus formed polymersome systems were not stable, which in many cases resulted in polymer precipitation. In addition, a broad polymersome size distribution is usually obtained. These disadvantages are related to the use of water immiscible chloroform as the copolymer solvent, and may therefore be overcome if a water-miscible solvent, that allows self-organization of the block-copolymer chains instead of precipitation, will be applied.

A method for polymersome preparation that combines the features of the above mentioned two methods for nano-capsule preparation is the addition of an amphiphilic block-copolymer in a water miscible solvent to an aqueous phase that is saturated with or contains a partially water-soluble solvent. The diffusion of the water miscible solvent in the aqueous phase will be fast enough to provide spontaneous agitation of organic solvent nonsolvent polymer system, or agitation/emulsification of the partially water soluble solvent, both resulting in self assembly of polymer chains.

It is the aim of the research described in this chapter to explore the above proposed method to prepare biodegradable polymersomes from PEG containing polyester or polycarbonate block-copolymers. Ethyl acetate and benzyl alcohol were used as partially water-soluble solvents. These solvents are widely used because of their recognized low toxicity and solubility properties. The influence of the preparation parameters on the polymersome preparations was systematically studied, and for both solvents a mechanism for the polymersome formation is proposed.

EXPERIMENTAL

Materials.

The PEG-polyester and PEG-polycarbonate block-copolymers that were used in this study are listed in Table 1. The copolymers except C-PEG-PDLLA3.4-30 were prepared using ring-opening polymerization of *d,l*-lactide, ε-caprolactone and trimethylene carbonate using zinc

bis[bis(trimethylsilyl)amide] and monomethoxy PEG as an initiator[22]. α-Carboxyl-ω-hydroxyl polyethylene glycol (HOOC-PEG-OH) with a molecular weight of 3400 was purchased from Shearwater Polymers (Huntsville, USA) and dried under vacuum for 2 days before polymerization. Fluoresceinamine isomer II and Nile Red were from Aldrich (Milwaukee, USA), and stannous octoate and phosphotunstic acid sodium salt were purchased from Sigma (St. Louis, USA). Other chemicals e.g. tetrahydrofuran (THF), acetone, 1,4-dioxane, ethyl acetate (EA) and benzyl alcohol (BA) were analytical grade and used as received. De-ionized water (DI water) was obtained from a Milli-Q water purification system (Millipore, Molsheim, France).

Table 1. Characteristics of PEG-polyester and PEG-polycarbonate diblock-copolymers[a]

Diblock-copolymers	Mn [b](NMR)	Mn theor [d]	Mw/Mn[c]
PEG-PDLLA1.2-4.8	6 600	6 100	1.11
PEG-PDLLA1.2-12	14 800	13 200	1.09
PEG-PDLLA5.8-17	20 400	22 400	1.12
PEG-PDLLA5.8-24	28 200	30 200	1.17
PEG-PDLLA5.8-48	50 500	53 000	1.47
PEG-PDLLA 3-24	22 820	24 000	1.40
C-PEG-PDLLA3.4-30	33 000	39 400	
PEG-PCL5.8-24	29 800	29 700	-
PEG-PTMC5.8-24	30 900	29 700	-

[a] Polymers are denoted by PEG-polyester or PEG-polycarbonate followed by the molecular weights (the Mn, $\times 10^{-3}$) of PEG and polyester or polycarbonate. [b] determined from ^{1}H-NMR analysis by calculating the ratio of the PEG methylene peak to the main peak of polyesters or polycarbonate. [c] determined from GPC measurements. [d] calculated from the initial ratio of monomer to PEG hydroxyl groups and the conversion.

Synthesis of diblock copolymer C -PEG-PDLLA3.4-30

To a reaction vessel equipped with magnetic stirring bar, HOOC-PEG-OH 3400 (0.173 g, 0.051 mmol), d,l-lactide (1.827 g, 12.7 mmol), stannous octoate (0.021 g, 0.051 mmol) and toluene (15 mL) were charged in that order. The vessel was closed with a stopper and immersed in an oil bath that was thermostated at 110 °C. The polymerization was allowed to proceed for 26 h at 110 °C under stirring and then quenched by cooling with cold water (15 °C). Excess HCl (37 %) was added to the reaction mixture to hydrolyze the tin-oxygen bond. A sample was taken to determine the monomer conversion by ^{1}H NMR. The copolymer was isolated by precipitation in a methanol/diethyl ether (15/85, v/v) mixture, filtration, washing several times with diethyl ether, and drying at 40 °C under vacuum. Monomer conversion was 98 %. ^{1}H NMR analysis showed that the molecular weight of the PDLLA block is 29,600 g/mol, so the copolymer was denoted as C-PEG-PDLLA3.4-30.

Polymersome Preparation.

In general, polymers were dissolved in a water miscible organic solvent and polymersomes were prepared by injecting the polymer solution using a syringe or a pipette into an aqueous phase without stirring. THF, 1,4-dioxane or acetone were employed as solvents and deionised water, a mixture of water and ethyl acetate or a mixture of water and benzyl alcohol (referred to as DI water, EA/water and BA/water, respectively) were used as aqueous media. Unless stated otherwise, the EA/water mixture was an aqueous solution containing 8.00 v.% of ethyl acetate and the BA/water mixture contained 4.25 v.% of benzyl alcohol.

In a typical experiment, a polymer solution in THF (0.1 mL, 10 mg/mL) was quickly injected into an aqueous phase (5.0 mL) using a pipette or syringe with the tip or needle immersed close to the bottom.

After approximately 10 min without agitation, the mixture was gently inverted twice. The dispersions prepared in BA/water were diluted with an equal volume of pure DI water. The dispersions were characterized either before or after dialysis (VISKING dialysis tubing, MWCO 12.000, SERVA, Heidelberg, Germany) against DI water for two days. An indication of the yield of the polymersomes was obtained from the count rate and size as determined with dynamic light scattering measurements (DLS).

To enable confocal laser scanning microscopy (CLSM) analysis, fluorescent probes were incorporated in the polymersomes during polymersome preparation. Hydrophobic Nile red (excitation 550 nm, emission 650 nm) was dissolved in the polymer solution (0.65 mg/mL), whereas hydrophilic fluoresceinamine (excitation 480 nm, emission 525 nm) was dissolved in the aqueous phase (1 mg/mL).

Polymersome Characterization.

Determination of the polymersome size was performed with a Malvern Zetasizer 4000 (Malvern Corp., Malvern, UK) at 25°C using a laser wavelength of 633 nm and a scattering angle of 90°. The CONTIN method was applied for data processing. The size, count rate and polydispersity index (PDI) were determined. To evaluate the polymersome stability (with respect to size), the size, count rate and PDI of the polymersome dispersion was determined as a function of time. Count rate is in kilo count per second (KCtps), and is an indication of the concentration of the particles. A high concentration of particles causes a too high count rate (> 600 KCtps), which leads to multiple scattering resulting in smaller size values than the actual size. In this case the dispersion was diluted with DI water to a desired concentration and the size and PDI were recalculated. PDI is a measure for the homogeneity of the particle size. The smaller the PDI, the smaller the size distribution of the particles. The effective refractive index (RI) and viscosity (η) of the medium used in the DLS measurements were calculated from the values of the individual components (i) in the mixture according to the following equations:

$$RI = \sum_i \phi_i RI_i, \text{ and } \log \eta = \sum_i \phi_i \log \eta_i,$$

where ϕ_i is the volume fraction of the component i in the mixture.

CLSM analyses were performed with a Confocal Laser Scanning Microscope (Zeiss LSM 510, Carl Zeiss International, Germany). A drop of polymersome suspension was placed between two clean cover glasses. Nile red encapsulated polymersomes were used directly; whereas fluoresceinamine encapsulated polymersomes were diluted with an equal volume of deionized water before measurement. A water immersion microscope objective with a magnification of 63× was used for all measurements. A step of 100 nm in depth (z) was applied for z-scanning measurements. For the excitation of Nile red, a laser light (He/Ne) of wavelength 543 nm was used and emitted light was recorded after passing through a long pass filter for wavelengths equal to and larger than 650 nm. Excitation of the hydrophilic dye was realized with laser light (Argon) of wavelength 488 nm and emitted light was recorded after passing through a long pass filter for wavelengths equal and larger than 505 nm.

For scanning electron microscopy (SEM), performed at 0.67 kV on a LEO Gemini 1550 FEG-SEM (LEO Electron Microscopy Ltd, Cambridge, UK), 20 μL of polymersome suspension was placed on a polished aluminum substrate and dried in air before measurement.

For transmission electron microscopy (TEM), a polymersome sample (5 μL) was placed on a carbon coated copper grid (400 mesh) and excess liquid was removed with a filter paper. After drying in air for 5 min the samples were stained by the addition of 5 μL of phosphotunstic acid (2 wt.%) solution for 8 min. Then excess stain was removed from the edge of the copper grid with a filter paper and the sample was air-dried. TEM measurements were performed on a Philips CM30 Twin STEM (Philips, Eindhoven, the Netherlands) at an acceleration voltage of 200 kV.

RESULTS AND DISCUSSION

Polymersome formation from EA/water and BA/water systems will be discussed in the following section. The polymersome formation, the influence of preparation parameters on the polymersome size and PDI and on the count rate of the polymersome dispersions will be addressed and a mechanism for the polymersome formation for the respective system will be proposed.

EA/water system

Polymersome formation. The injection of THF into EA/water does not induce phase separation. In contrast, the addition of copolymer solutions in THF to EA/water without stirring results in almost instantaneous formation of an opaque top layer and a clear bottom layer. After ca. 20 min without agitation a homogenous, less opaque dispersion is obtained. Gently inverting the container twice facilitates homogenisation of the dispersion. The particles in the milky dispersions have a size of 170 to 350 nm and a PDI that ranges from 0.05 to 0.80. The actual value depends on the preparation conditions.

TEM analysis (Figure 1) of the dispersions reveals a vesicular structure for the particles. The stained walls of the particles can be clearly distinguished from the nonstained center, indicating a polymer free interior. Notably, no deformed or collapsed polymersomes were observed.
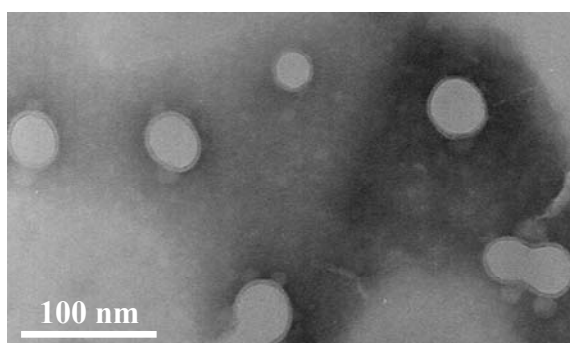

Figure 1. TEM micrograph of polymersomes prepared by injecting a polymer solution of PEG-PDLLA1.2-12 in acetone into DI water. The dark ring and the light interior correspond to the polymer wall and a polymer free interior, respectively.
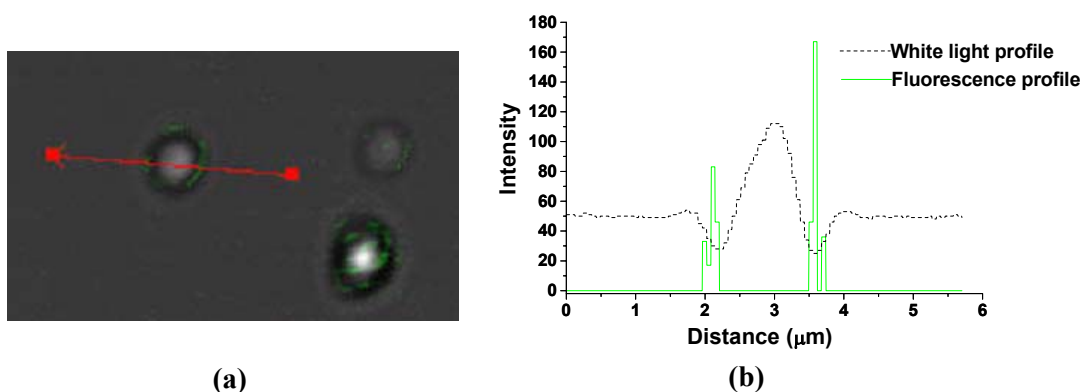

(a)　　　　　　　　　　　　(b)

Figure 2. CSLM image of Nile red incorporated polymersomes in DI water that were prepared by injecting a PEG-PDLLA5.8-48 solution in THF (0.05 mL, 10 mg/mL) in EA/water containing Nile red (0.65 mg/mL) (a); line scans of a polymersome as indicated in (a) by an arrow (b).

Figure 2 shows a result of the CLSM analysis of a few relatively large polymersomes that were prepared in the presence of hydrophobic Nile red as a fluorescent probe. Assuming that the hydrophobic dye only stains the hydrophobic blocks (HB) of the copolymer, the two peaks in the fluorescence profile (Figure 2b) indicate that the spherical structures have a hydrophobic wall that encloses a hydrophilic interior. Thus CLSM analysis confirms the vesicular structure of the polymersomes. Similarly, liposomes and non-degradable polymersomes have been prepared by using a system that consists of a water miscible organic solvent and an aqueous phase[6-8].

The zeta potentials of the polymersomes of C-PEG-PDLLA3.4-30 in MES buffer (0.05 M, pH 5.4) or in PBS (pH 7.4) are -39.5 ± 0.4 mV and -37.2 ± 0.5 mV, respectively. These values are ~20-25 mV lower than those of PEG-PDLLA3-24 polymersomes in the same media, suggesting that the terminal COOH groups of the PEG block of the copolymer are present at the surface of the polymersomes. These results also indicate that the PEG blocks of all the copolymers orient at the surface of polymersomes. This confirms the proposed structure of the polymersome model, in which the wall of the polymersomes consists of a layer of stacked, coiled polymer chains that are held together by non-covalent forces with the PEG blocks protruding into the aqueous phases and the entangled hydrophobic blocks forming the core of the polymersome wall (see Figure 3 of chapter 5). Most interestingly, the availability of COOH groups on the polymersome surface allows polymersome surface modification for instance for targeting purposes.

It is noteworthy that polymersomes can be prepared from all the copolymers listed in Table 1, and that depending on the preparation conditions, free polymer chains or micelles (for instance when the volume ratio of THF to water is high), or a large amount of precipitate are present in some of the polymersome preparations. The effect of parameters that may influence the formation and the quality of polymersomes, such as the nature of the solvent and of the aqueous phase, the molecular weights of the two blocks and the nature of the hydrophobic block, the polymer concentration and the volume ratio of THF to the aqueous phase, were systematically studied.

Table 2. Characteristic parameters of solvents and polymers that were used in this study

	acetone	THF	dioxane	EA	BA	PDLLA	PCL	PTMC	PEG
δ^c	20.3[a]	18.6[a]	16.2[a]	18.6[a]	24.8[a]	19.8[b]	20.0[b]	20.3[b]	17.9[b]
sol in w[d]	∞	∞	∞	8.5%	4.0%[g]				
sol of w[e]	∞	∞	∞	3.3%	8.0 %				
density[f]	0.790	0.889	1.034	0.902	1.045				

[a] obtained from ref[23]; [b] calculated according to the group contribution method[24]; [c] δ solubility parameter of solvents and polymers; [d] solubility in water (wt%), [e] solubility of water (wt%), [f] density in g/mL, and [g] at 25 °C, the rest all at 20 °C.

Organic solvent. Different organic solvents for the copolymers were evaluated with respect to their effect on polymersome size, yield and PDI. From the water miscible solvents that were used to prepare the copolymer solutions (THF, acetone, 1,4-dioxane), THF gave the best results: the polymersome dispersions had a homogeneous, bluish, milky appearance, and a high

count rate and a low PDI. This is most probably due to the fact that the solubility parameter of THF is close to that of all blocks yielding optimal dissolution of the copolymers[25]. Therefore, THF was chosen as the solvent to study the influence of the other preparation conditions on the polymersomes.

PEG block. Although polymersomes with similar average size are obtained (Figure 3a), block-copolymers with a high Mn PEG block yield better polymersomes (i.e. more homogeneous and stable dispersions) as compared to those with a low Mn PEG block. For instance, during preparation of polymersomes of PEG-PDLLA 1.2-12 and PEG-PDLLA 1.2-4.8 instantaneous precipitation occurs (left side of the dashed line in figure 3a). This is probably caused by the short PEG chains that cannot provide enough steric repulsion to prevent aggregation of the organized layer structures, or that can not afford the formation of organized structures at all.

(a)

(b)

(c)

(d)
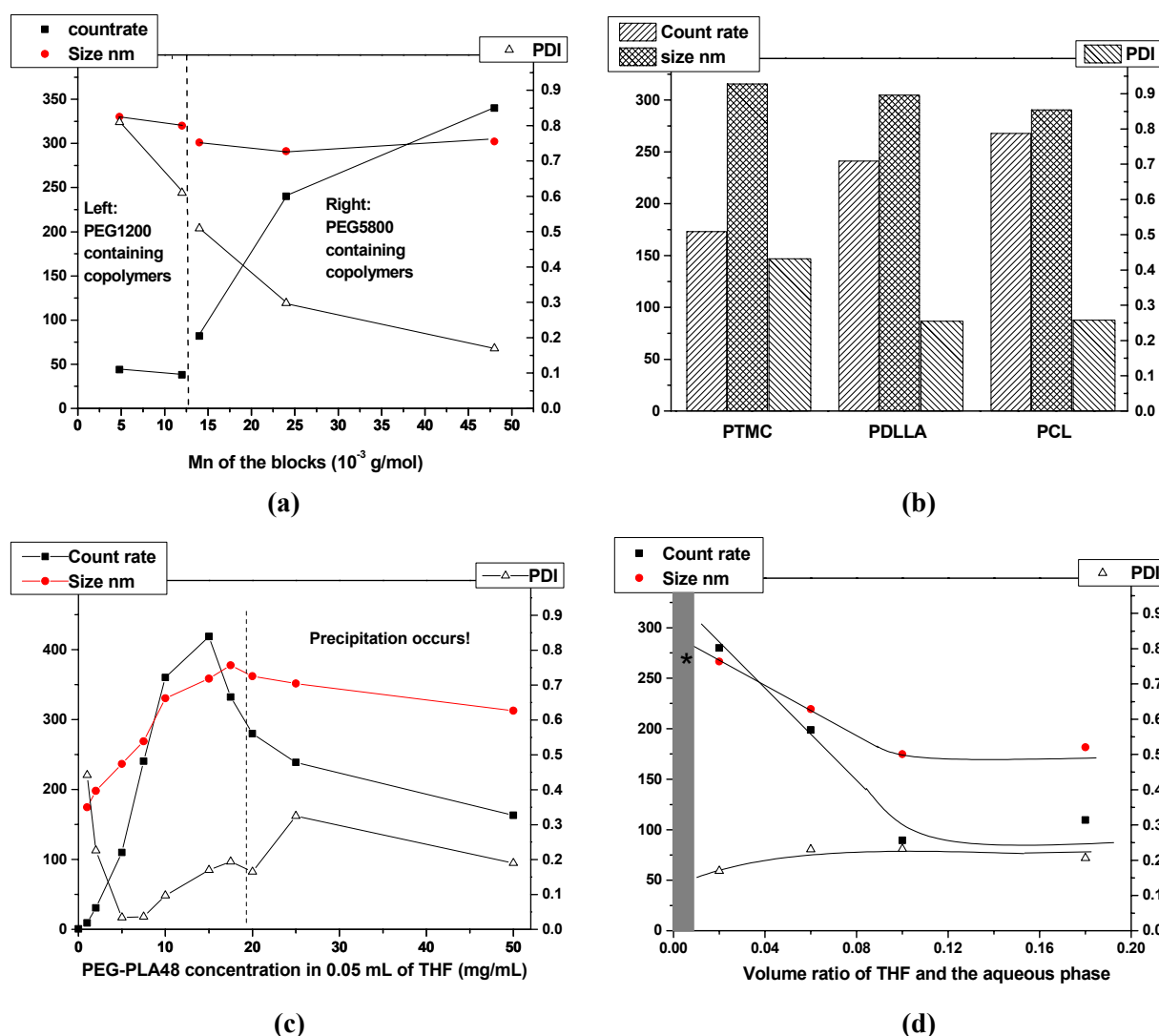
Figure 3. *The dependence of the polymersome size (nm), PDI and the count rate of the dispersion on the following parameters: (a) Mn of the PDLLA block, copolymers with PEG5800 and PEG1200 were presented; (b) the nature of the hydrophobic block (HB) of the copolymers (Mn of the HB was ca. 24000 g/mol); (c) the polymer concentration in THF used for injection; and (d) the volume ratio of THF to the aqueous phase. Unless stated otherwise, the polymersomes were prepared by injecting PEG-PDLLA5.8-48 polymer solutions (0.1 mL, 10 mg/mL) in THF to EA/water (5 mL, 8.00 v.%).*

Hydrophobic block. The influence of the HB, including the type and the molecular weight (Mn), and Mn ratio of the two blocks, on the polymersome dispersion was investigated and the results are shown in figure 3a. For PEG-PDLLA with PEG5800 as the hydrophilic block, an increase of the Mn of the PDLLA block from 14000 to 48000 results in a large increase in count rate from 75 to 300, whereas the PDI decreases from 0.50 to 0.15, and the average polymersome size remains the same (270 nm). This implies that the Mn of the HB does not influence the size of the polymersomes, but affects the polymersome yield and PDI: the higher the Mn of the HB, the higher the polymersome yield and the lower the PDI of the polymersome preparation.

Figure 3b shows the effect of the type of the HB of the copolymers on the polymersome characteristics. Using the same PEG5800 as hydrophilic block and HB with comparable Mn's (ca. 24,000 g/mol), three different copolymers PEG-PTMC5.8-24, PEG-PDLLA5.8-24 and PEG-PCL5.8-24, in that order, yield polymersome preparations with an increased count rate, a decreased PDI and more or less the same average size of the polymersomes. From PEG-PTMC5.8-24 to PEG-PDLLA5.8-24 to PEG-PCL5.8-24, an increase in the hydrophobicity of the HB of the copolymer can be derived via the static water contact angle of spin-cast films of the homo-polymer of the hydrophobic blocks, being ~72.5°, 73.2°, 80.5°, respectively[26]. From this it is concluded that the HB of the copolymers (the Mn and the nature) does not influence the average size of the polymersomes, but affects the yield and the quality of the polymersome dispersion: the more hydrophobic the HB, the higher the polymersome yield and the smaller the PDI.

Based on the results and discussions described above, PEG5800 is preferred over PEG1200, and a higher hydrophobicity and/or a high Mn of the HB is desired for generating polymersomes with high yield and a homogeneous size distribution. Most possibly a HB with a high Mn or high hydrophobicity and/or a PEG block with a high Mn facilitates the self-assembly of the copolymer chains.

Polymer concentration. The polymersome size increases more or less linearly from 170 to 370 nm with the increase of the polymer concentration from 1 to 15 mg/mL. Above 15 mg/mL the effect of polymer concentration levels off (Figure 3c). The count rate of the dispersion first increases with increasing polymer concentration and reached a maximum at 15 mg/mL above which it declines, possibly due to the occurrence of polymer precipitation. An optimal polymer concentration of 10-15 mg/mL is derived.

Organic phase versus aqueous phase. Figure 3d demonstrates the dependence of the polymersome size and PDI and the count rate of the dispersions on the volume ratio of THF to the aqueous phase. For a total volume of the dispersion of 5 mL and a final polymer concentration of 0.2 mg/mL, no good dispersion could be obtained for THF/water (v/v) <0.01 (shown as the bar in Figure 3d). This is possibly because such a small amount of THF dissolves and strips from the copolymer chains too fast, so that the copolymer chains have not sufficient time to readjust to a stable form. It should be noted that for a final polymer concentration of 0.2 mg/mL, a THF/water (v/v)<0.01 means a polymer concentration >20 mg/mL, which results in a large amount of precipitate (Figure 3c). When the THF/water ratio (v/v) increases from 0.01 to 0.1 while the amount of copolymer stays the same, the polymersome size and count rate should stay constant or one should increase while the other

decreases. However, it was observed that an increase of the ratio leads to a decrease in both polymersome size and count rate while the PDI remains the same. This can be explained by the increased amount of free polymer chains or micelles in the mixture due to the decreased interfacial tension with more THF molecules dissolved in water. After the THF/water (v/v) is higher than 0.1, this effect reduces and the polymersome size and count rate remain constant.
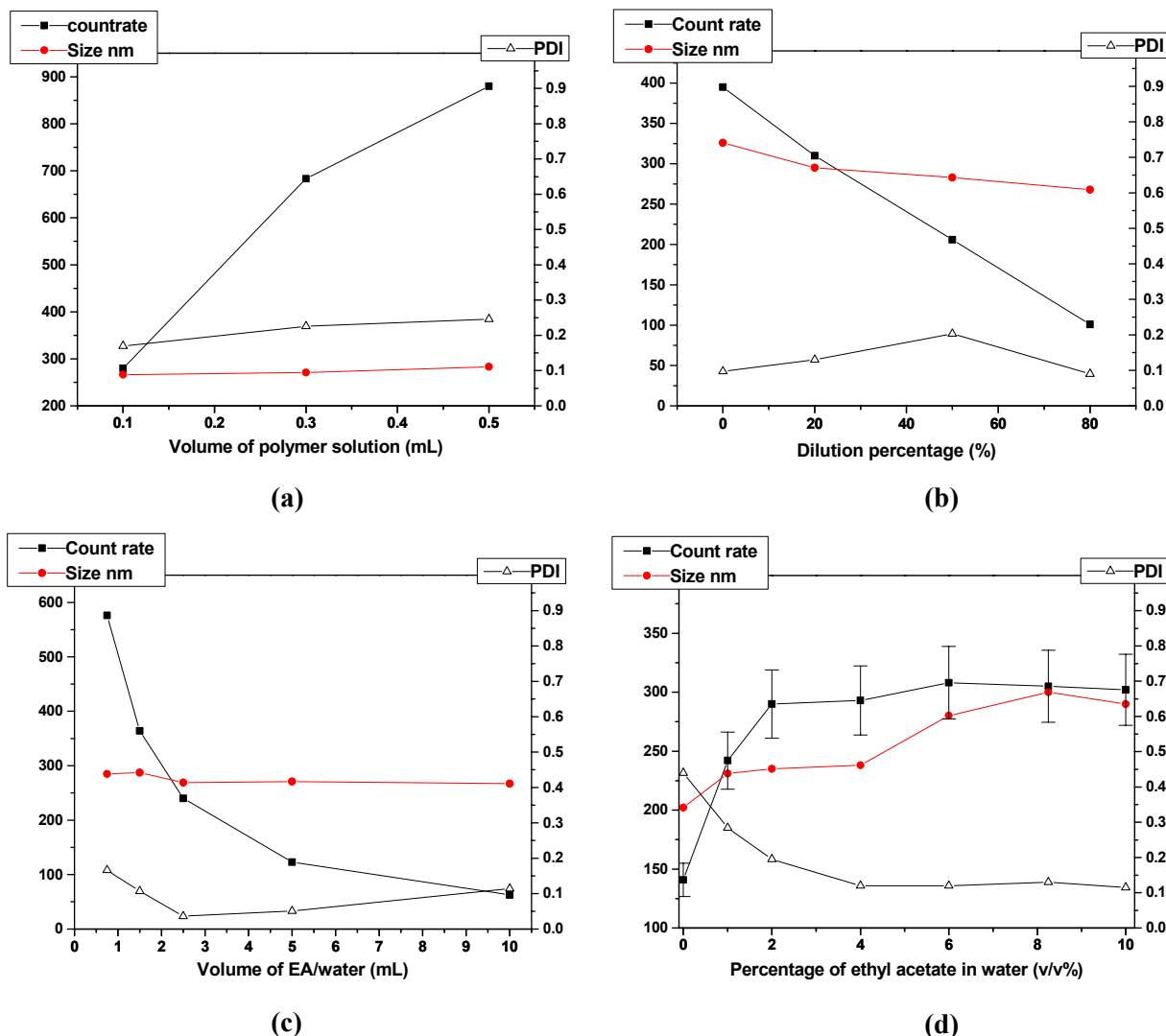

(a)

(b)

(c)

(d)

Figure 4. The dependence of the polymersome size (nm), PDI and the count rate of the dispersion on: (a) the volume of injected polymer solution in THF; (b) the dilution percentage with DI water after polymersome preparation; (c) the volume of the aqueous phase; and (d) the percentage of ethyl acetate in the aqueous phase. Unless stated otherwise, the polymersomes were prepared by injecting PEG-PDLLA5.8-48 polymer solutions in THF (0.1 mL, 10 mg/mL) to EA/water (5 mL).

The injection of more polymer solution (with the same concentration) to EA/water increases the count rate of the polymersome dispersion without affecting the size (270 nm) and PDI (Figure 4a). This indicates that after the initial formation of the polymersomes no growth occurs. This can also be seen when the polymersome preparation was diluted with DI water (Figure 4b). No significant change in polymersome size and PDI, but a decreased count rate was observed for increasing dilution. Increasing the volume of the aqueous phase has no influence on the size of the polymersomes and the PDI, however it results in a decreased count

rate (Figure 4c). Hence, it can be concluded that the characteristics of the polymersome dispersion are largely dependent on the volume ratio of THF/aqueous phase but not on the absolute volume of the aqueous phase.

The percentage of ethyl acetate in the aqueous phase. The study of the influence of the percentage of ethyl acetate in the aqueous phase on the polymersome characteristics shows that the polymersomes formed by addition of polymer in THF to pure DI water have a smaller size, a lower count rate and a higher PDI than those formed in EA/water (Figure 4d). The increase of the EA content of the aqueous phase from 0 to 2 v.% results in an increase of the count rate from 140 to 290. At an EA content above 2 v.%, the count rate remains constant. With the increase of the EA content of the aqueous phase from 0 to 8 v.%, the size of the polymersomes increases gradually from 200 nm to 280 nm. For an EA content that increases from 0 to 4 v.% the PDI drops from 0.50 to 0.13 and remains constant at an EA content > 4 v.%. From this it can be concluded that the composition of the aqueous phase has a large effect on the characteristics of the polymersomes.

The mechanism of polymersome formation from the EA/water system. Based on the results presented above, a mechanism for polymersome formation that applies for the EA/water system is proposed. Upon the injection of a solution of a copolymer in THF to the aqueous phase, THF dissolves rapidly in the aqueous phase, which causes a localized lowering of the interfacial tension[27]. This leads to interfacial turbulence and spontaneous agitation of the interface of the non-equilibrated liquid phases[17]. Due to the dissolution of THF, copolymer molecules get stripped from their solvent molecules. Since water is a good solvent for the PEG block but a bad solvent for the HB, these polymer chains have a tendency to assemble in layers with the PEG block facing the aqueous phase and the HB on the inside, directed towards each other. These layers close upon themselves to avoid the unfavourable exposure of HB edges to the aqueous phase. Figure 5 schematically shows the process of polymersome formation using the EA/water system.
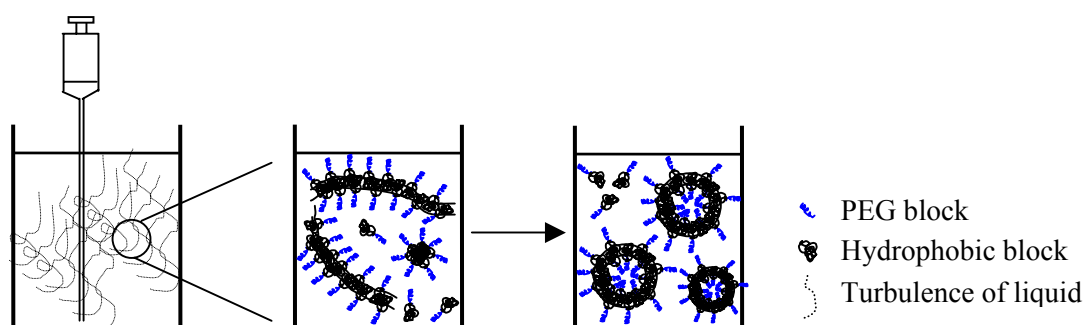

Figure 5. Schematic presentation of the process of polymersome formation using the THF/EA/water system.

Nonetheless, copolymers with low Mn PEG like PEG1200 induce a lot of coalescence and agglomeration, possibly due to the fact that low Mn PEG cannot provide enough steric repulsion for the newly formed polymersomes, or that the formation of organized layers is prevented. The occurrence of the interfacial turbulence/spontaneous agitation excludes the need for external agitation. Extra stirring only results in precipitation, probably because the copolymer chains cannot adjust themselves fast enough to adopt a new stable form such as a vesicular structure.

The role of ethyl acetate in the aqueous phase is that it slows down the dissolution of THF molecules in the aqueous phase, and/or that EA entrapped in the hydrophobic part of the membrane during the polymersome formation softens the HB, thus giving the copolymer molecules enough time to self assemble into more homogeneous, larger polymersomes.

BA/water system

The addition of a water miscible solvent such as THF, acetone or dioxane to benzyl alcohol saturated water leads to turbulent mixing and an instantaneous formation of a cloudy dispersion of BA micro-droplets in the aqueous phase, which quickly (within 5-10 min) separates into two liquid layers with large BA drops at the bottom. In contrast, injection of a THF, acetone or dioxane solution of a copolymer containing the PEG5800 block into the BA/water phase, results in a much more stable emulsion. It is anticipated that the block-copolymer molecules self organize on the surface of the BA droplets, thus stabilizing the emulsion (for at least a few hours). Copolymers containing PEG1200 blocks are not able to stabilize the emulsion, due to the fact that the short PEG chains cannot provide enough steric repulsion to prevent the BA droplets from merging.

After dialysis of the emulsion against DI water or dilution of the emulsion with an equal volume of DI water, the cloudy dispersion turns homogenous milky with a bluish color. The size of the particles is in the range of 330 to 1200 nm and the PDI depends on the preparation conditions.
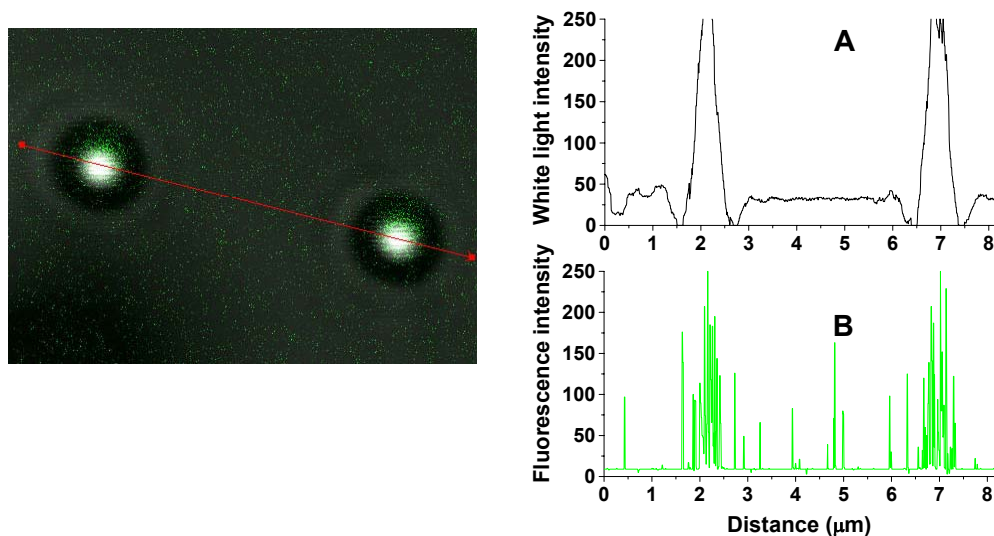

***Figure 6.** CLSM image and intensity profiles of polymersomes prepared from a THF/BA/water system. Intensity profiles of white light (A) and fluorescence (B) following the line as indicated in the left image are shown. Polymersomes were obtained by injecting PEG-PDLLA5.8-48 in THF (10 mg/mL, 0.04mL) into 5 mL of BA/water containing fluoresceinamine (~0.1 mg/mL). After 10 min emulsification, the sample was dialyzed against DI water for two days.*

CLSM measurements of the particles suggest a vesicular structure. In Figure 6, the left figure shows a typical polymersome image of PEG-PDLLA5.8-48 prepared in the presence of fluoresceinamine. The right two figures display intensity line scans of white light (A) and fluorescent light (B) following the line as indicated in the upper image. High fluorescence observed within the particles suggests the encapsulation of fluoresceinamine inside the

polymersomes. Scanning CLSM (Figure 7) reveals a spherical structure. Similar CLSM images are obtained for particles formed by dilution of the emulsion with an equal volume of fluoresceinamine solution in DI water. TEM images of polymersomes (Figure 8) are quite similar to those of nanocapsules of PCL[21], with the interior of the polymersomes appearing brighter than the surrounding matrix which is negatively stained.
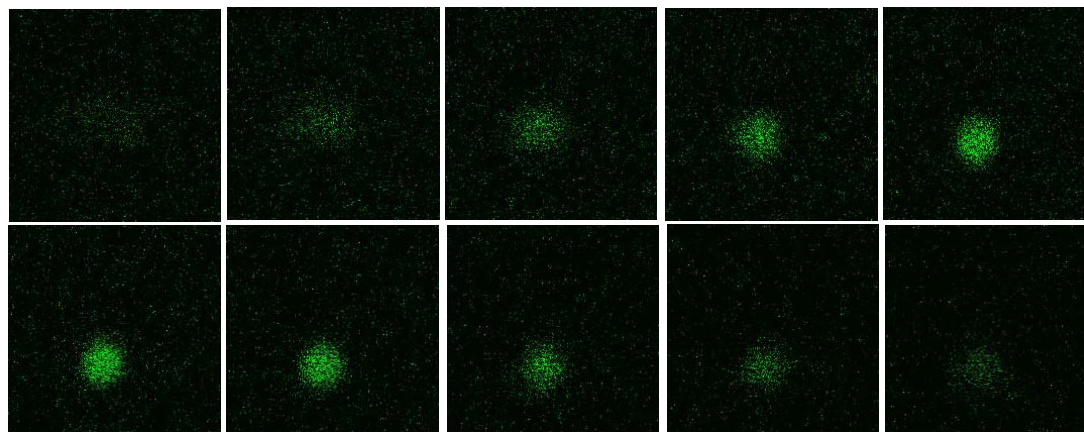

Figure 7. Z-scanning CLSM images of a polymersome of PEG-PDLLA5.8-48 prepared by injecting a solution in THF (10 mg/mL, 0.04mL) into 5 mL of BA/water containing fluoresceinamine (~0.1 mg/mL). After 10 min, the sample was dialyzed against water for 2 days. The images are at 200 nm per step. The length of the frame represents 5 μm.
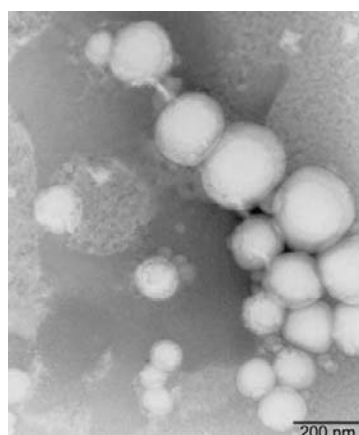

Figure 8. TEM image of polymersomes (negative stained with 2 wt.% phosphotunstic acid) of PEG-PDLLA 5.8-48 prepared by injecting a solution in THF (10 mg/mL, 0.04mL) into 5 mL of BA/water. After 10 min, the sample was dialyzed against DI water for two days.

Table 3. Characteristics of polymersomes of diblock-copolymers after dialysis [a]

Copolymers	System	Size (nm)	PDI	Count rate	Precipitation
PEG-PDLLA5.8-48	THF/BA.water	680 ±30	0.13±0.04	112±4	---
PEG-PDLLA5.8-24	THF/BA.water	600 ±10	0.55±0.20	103±2	+
PEG-PCL5.8-24	THF/BA.water	450 ±10	0.16±0.08	82±2	--
PEG-PDLLA5.8-48	Acetone/BA.water	560 ±30	0.78±0.21	112±5	++
PEG-PDLLA5.8-48	Dioxane/BA.water	330 ±5	0.11±0.05	433±13	+
PEG-PDLLA5.8-48	THF/EA.water	260 ±10	0.05±0.02	462±8	-----

[a] polymersomes were prepared by injecting polymer solutions (0.1 mL, 10 mg/mL) into an aqueous phase (5 mL). After 10 min, polymersome dispersions were dialyzed against DI water for two days.

Table 3 shows the effect of some preparation conditions on the characteristics of polymersomes of different polymers that were prepared from the BA/water system at otherwise identical conditions. Similar trends were observed as for the EA/water system with THF being the best solvent giving the least polymer precipitation and larger polymersomes. Copolymers with a high Mn of the HB produce larger polymersomes with a smaller PDI and copolymers with a more hydrophobic HB form smaller polymersomes with smaller PDI.

The mechanism of polymersome formation in the BA/water system. The formation of the polymersomes from the BA/water system is somewhat similar to the formation of the nanocapsules as described in literature[17-21]. The injection of a solution of a polymer in THF in BA/water results in the instantaneous dissolution of the THF in the aqueous phase, leading to interfacial turbulence and spontaneous emulsification[17,27] of BA, observed as violent spreading/turbulent phase separation of BA droplets. Due to the different solubilities of the two blocks in the different phases, the block-copolymer molecules self organize on the BA droplet surface. Most of the block-copolymer chains organize, presumably, in a monolayer morphology with the PEG chains protruding into the aqueous phase and the hydrophobic block as coiled chains at the interface, as also suggested by the solubility parameters of BA and polymers in Table 2. However, part of the copolymers maybe still dissolved in the BA droplets. At this stage, the interfacial turbulence induces shear forces that may strip the polymer chain monolayer off the droplet surface forming bilayers. Closure of these bilayers can result in polymersomes. However, the majority of the polymersomes is expected to be formed upon the addition of DI water to the emulsion/dispersion or dialysis of the emulsion/dispersion against DI water. The concentration gradient of BA across the block-copolymer monolayers on the BA droplets causes BA molecules to diffuse into the aqueous phase and water will diffuse into the interior as well. Gradually the liquid phase of the droplets becomes a worse solvent for the hydrophobic block, and at a certain point the copolymer molecules have to adopt another morphology such as a bilayer. These bilayer fragments can couple with each other and/or close to form polymersomes. Figure 9 schematically shows the process of polymersome formation from BA/water system.
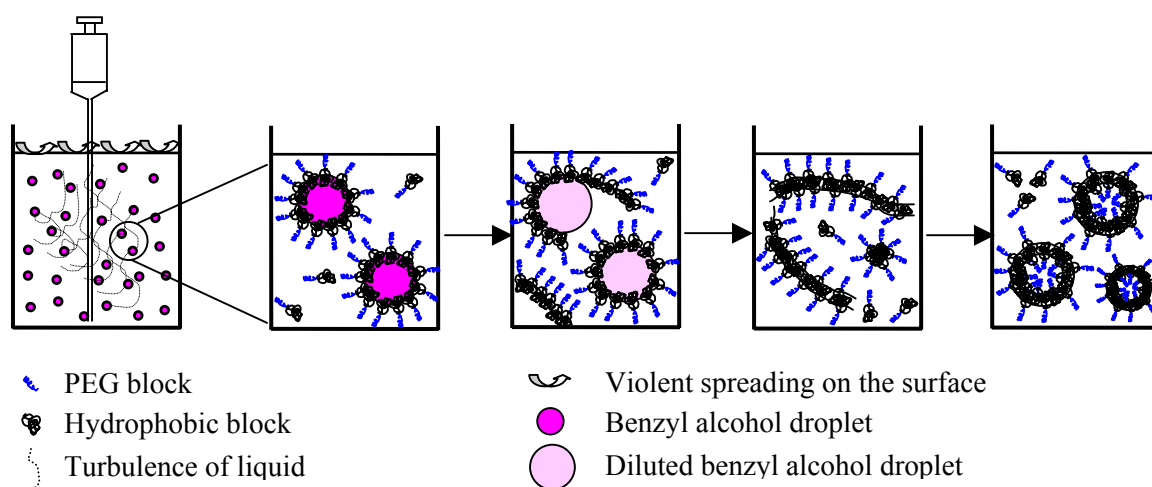

⤸ PEG block	∽	Violent spreading on the surface
🦑 Hydrophobic block	🔴	Benzyl alcohol droplet
⋮ Turbulence of liquid	🟣	Diluted benzyl alcohol droplet

Figure 9. *Schematic presentation of the process of polymersome formation using the THF/BA/water system.*

The main difference between the EA/water and the BA/water systems is that in the EA/water system polymersomes form directly from the copolymer chains, while in the BA/water system, the copolymer chains first form monolayers on the BA droplet surfaces which then form the bilayer-like structures. This causes that the size of the polymersomes obtained from the latter system is larger in average.

Stability of the polymersomes

The removal of organic solvents from the polymersome preparations by dialysis against DI water does not change their spherical morphology (Figure 10). The stability of the un-dialyzed and dialyzed polymersomes was evaluated by determination of the polymersome size by DLS as a function of time. After dialysis the average size and the PDI of the polymersomes become smaller. This smaller size (10-15 %) can be due to the more compact polymer membranes in the absence of organic solvent. In contrast with the un-dialyzed polymersomes, the solvent-free polymersomes are stable at 4 °C (in terms of vesicle integrity) for at least 4 months as indicated by visual observation and DLS analysis (Figure 11).
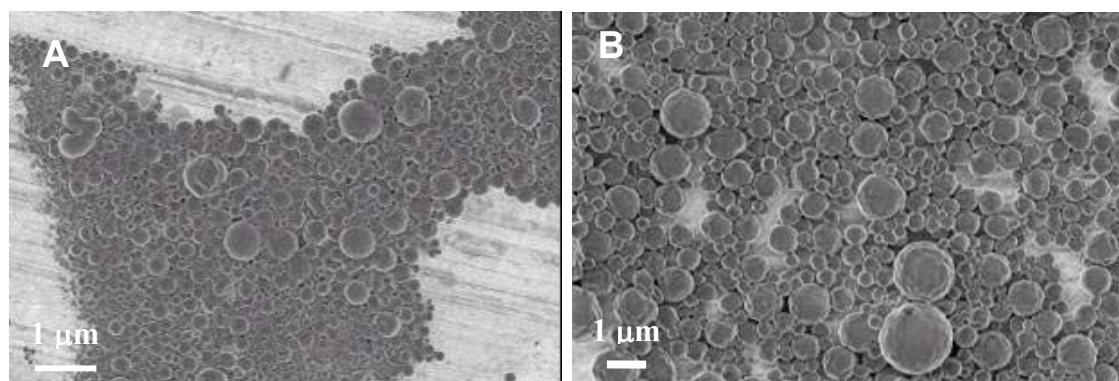

Figure 10. *SEM micrograps of polymersomes of PEG-PDLLA5.8-48/THF/EA/water (A) and PEG-PDLLA5.8-48/THF/BA/water. The sample was dialyzed against water for 2 days.*

It is worth noting that although the hydrophobic component in the membrane is biodegradable, the rate of degradation is so low that the integrity of the polymersomes is maintained during the 4 months study. It has been reported that, for example, complete mass loss of pure PDLLA takes place in between 12 and 16 months depending on the molecular weight and the device dimension[28]. For different applications of the polymersomes, the degradation rate can be tuned by replacing the hydrophobic block with poly(*d,l*-lacide-co-glycolide) (PLGA), which can have a much shorter degradation time, e.g., from 6 months to 1 month when the GA content of PLGA increases from 15 % to 50 %[28].
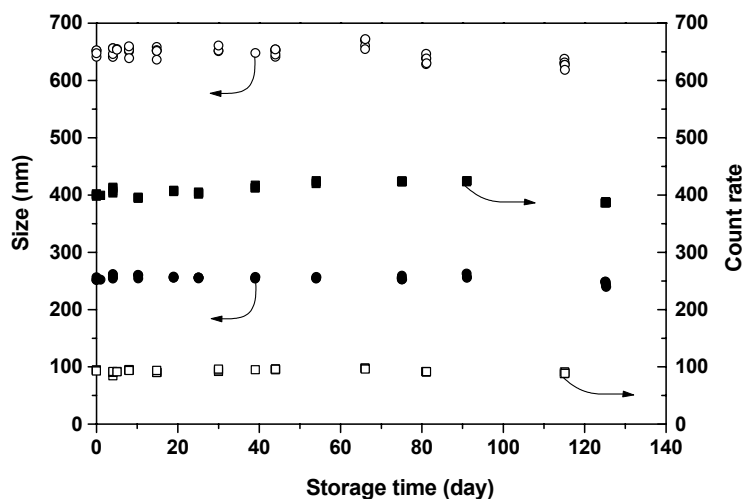
Figure 11. *Count rate (■, □) and polymersome size (●, ○) of dialyzed polymersome dispersions of PEG-PDLLA5.8-48 from EA/water (■, ●) and BA/water (□, ○) as a function of storage time in DI water. Immediately after preparation, polymersomes were subjected to dialysis for two days, and stored at 4℃.*

CONCLUSIONS

This chapter demonstrates the preparation of biodegradable polymersomes of PEG-polyester and PEG-polycarbonate block-copolymers from water miscible solvents in aqueous media. Polymersomes with average sizes ranging from 170 to 350 nm can be readily prepared from the EA/water system, and with an average size from 330 to 1200 nm from the BA/water system. The vesicular structure is confirmed by TEM and CLSM measurements.

For the EA/water system, the organic polymer solvent (type, relative volume) and the composition of the aqueous phase as well as the polymer concentration are the parameters that can be used to tune the properties of the polymersomes such as the average size and PDI. The nature and length of the hydrophobic block and the length of the PEG block of the copolymer do not influence the average size of the polymersomes, but mainly affect the yield and PDI of the polymersome dispersions. For a high yield and low PDI, a high Mn of the HB with a high hydrophobicity is preferred, and a Mn of PEG higher than a certain value (between 1200 and 5800) is required.

Removal of the organic solvents from the polymersomes prepared from both systems enhances their stability and at 4℃ in DI water the polymersomes show shape integrity for at least 4 months. These biodegradable polymersomes have a potential for biomedical applications e.g. as ultimate carriers in drug delivery. Furthermore, since these polymersomes can be prepared with the size as small biological cells (0.2-0.5 μm), they are very promising as a basis for artificial cells.

REFERENCES

(1)   Stolnik, S.; Dunn, S. E.; Garnett, M. C.; Davies, M. C.; Coombes, A. G. A.; Taylor, D. C.; Irving, M. P.; Purkiss, S. C.; Tadros, T. F.; Davis, S. S.; Illum, L. *Pharm. Res.* **1994,** *11*, 1800.

(2)   Vittaz, M.; Bazile, D.; Spenlehauer, G.; Verrecchia, T.; Veillard, M.; Puisieux, F.; Labarre, D. *Biomaterials* **1996,** *17*, 1575.

(3)   Ding, J. F.; Liu, G. J. *Macromolecules* **1997,** *30*, 655.

(4)   Zhang, L. F.; Eisenberg, A. *Science* **1995,** *268*, 1728.

(5)   Shen, H. W.; Eisenberg, A. *Macromolecules* **2000,** *33*, 2561.

(6)   Yu, K.; Eisenberg, A. *Macromolecules* **1998,** *31*, 3509.

(7)   Holder, S. J.; Hiorns, R. C.; Sommerdijk, N. A. J. M.; Williams, S. J.; Jones, R. G.; Nolte, R. J. M. *Chem. Commun.* **1998**, 1445.

(8)   Nardin, C.; Hirt, T.; Leukel, J.; Meier, W. *Langmuir* **2000,** *16*, 1035.

(9)   Cornelissen, J. J. L. M.; Fischer, M.; Sommerdijk, N. A. J. M.; Nolte, R. J. M. *Science* **1998,** *280*, 1427.

(10)   Discher, B. M.; Won, Y. Y.; Ege, D. S.; Lee, J. C. M.; Bates, F. S.; Discher, D. E.; Hammer, D. A. *Science* **1999,** *284*, 1143.

(11)   Lee, J. C. M.; Bermudez, H.; Discher, B. M.; Sheehan, M. A.; Won, Y. Y.; Bates, F. S.; Discher, D. E. *Biotechnol. Bioeng.* **2001,** *73*, 135.

(12)   Li, Z. C.; Jin, W.; Liu, F. M. *React. Funct. Polym.* **1999,** *42*, 21.

(13)   Schillen, K.; Bryskhe, K.; Mel'nikova, Y. S. *Macromolecules* **1999,** *32*, 6885.

(14)   Dimova, R.; Seifert, U.; Pouligny, B.; Forster, S.; Dobereiner, H. G. *Eur. Phys. J. E* **2002,** *7*, 241.

(15)   Kukula, H.; Schlaad, H.; Antonietti, M.; Forster, S. *J. Am. Chem. Soc.* **2002,** *124*, 1658.

(16)   Checot, F.; Lecommandoux, S.; Gnanou, Y.; Klok, H. A. *Angew. Chem.-Int. Edit.* **2002,** *41*, 1339.

(17)   Fessi, H.; Puisieux, F.; Devissaguet, J. P.; Ammoury, N.; Benita, S. *Int. J. Pharm.* **1989,** *55*, R1.

(18)   Leroux, J. C.; Allemann, E.; Doelker, E.; Gurny, R. *Eur. J. Pharm. Biopharm.* **1995,** *41*, 14.

(19)   QuintanarGuerrero, D.; Allemann, E.; Doelker, E.; Fessi, H. *Colloid Polym. Sci.* **1997,** *275*, 640.

(20)   Quintanar-Guerrero, D.; Allemann, E.; Fessi, H.; Doelker, E. *Int. J. Pharm.* **1999,** *188*, 155.

(21)   Guinebretiere, S.; Briancon, S.; Fessi, H.; Teodorescu, V. S.; Blanchin, M. G. *Mater. Sci. Eng. C-Biomimetic Supramol. Syst.* **2002,** *21*, 137.

(22)   Chapter 5 of this thesis .

(23)   Grulke, E. A. In *Polymer Handbook*; Brandrup, J., Immergut, E. H., Grulke, E. A., Eds.; John Wiley & Sons, Inc.: New York, **1999**, p VII 675.

(24)   Small, P. A. *J. Appl. Chem.* **1953,** *3*, 71.

(25)   Cameron, N. S.; Corbierre, M. K.; Eisenberg, A. *Can. J. Chem.-Rev. Can. Chim.* **1999,** *77*, 1311.

(26)   Pego, A. P. G. M. PhD thesis, University of Twente, Enschede, **2002**.

(27)   Davies, J. T.; Rideal, E. K. *Interfacial phenomena*, 2nd ed.; Academic Press Inc.: New York, **1963**.

(28)   Middleton, J. C.; Tipton, A. J. *Biomaterials* **2000,** *21*, 2335.

7

Biodegradable polymersomes as a basis for artificial cells: encapsulation, release and targeting

ABSTRACT: The encapsulation of biofunctional compounds, release properties and targetability prepared from polymersomes of amphiphilic block-copolymers based on poly(ethylene glycol) (PEG) and biodegradable polyesters or polycarbonate are described. Carboxyfluorescein (CF), as a model for hydrophilic biofunctional compounds, could be readily incorporated in the polymersomes by adding the compound to the aqueous phase during polymersome preparation. The release of encapsulated material from the polymersomes can be adjusted by changing the copolymer composition, especially the molecular weight and type of hydrophobic block of the copolymer. The presence of plasma proteins other than albumin suppressed the release of CF. CF release in PBS both at room temperature and at 60 °C followed first order kinetics, confirming that the CF containing polymersome system is a membrane controlled reservoir system. These biodegradable polymersomes have the potential to be targeted to specific sites in the body as shown by the specific interaction of anti-human serum immobilized polymersomes with a human serum coated sensor surface.

INTRODUCTION

Artificial cells refer to water-insoluble man-made particles that can perform a specific biological function in the body without being recognized by the defense system. Polymersomes are of particular interest as a basis for artificial cells because of the large compartment for encapsulation of biofunctional compounds, tunable membrane properties, and stability. The development of biodegradable polymersomes makes them even more attractive[1,2].

For an artificial cell, biofunctionality means that the biofunctional compound that is included in the cell can locally alter physiological events or a physical parameter, such as preventing the growth of tumor cells by delivering anticancer drugs, treating enzyme defects in inborn problems of metabolism by delivering encapsulated enzymes, transporting O_2/CO_2 or locally changing the electron density allowing visualization of certain cells or organs by imaging techniques. An artificial cell body can be provided with biofunctionality by encapsulation or immobilization of biofunctional compounds such as drugs, enzymes, peptides, antibodies, DNA, or by the incorporation of living cells. Encapsulation of biofunctional compounds[3-10] in the artificial cell body can be performed during its formation. Immobilization of biofunctional compounds onto the artificial cell surface[11,12] can be done via covalent binding[13] or adsorption. Compared to immobilization, encapsulation has the advantage that large amounts of biofunctional compounds can be entrapped.

For the potential application of site-specific release of compounds, it is important that the release from the artificial cell can be controlled. A wide range of drug delivery systems has been developed over the years, including membrane-controlled reservoir systems, diffusion-controlled monolithic systems, biodegradable systems, systems of which the release is controlled by osmosis, swelling, erosion or external control (e.g. temperature, magnetic, ultrasonic or electrical stimulation), and (bio)chemically controlled systems. The release of the incorporated biofunctional compound from the artificial cells can be controlled by modifying the properties of the membrane of the cells.

Homing devices on the cell body surface can guide the cell to the specific site where it performs its function. By applying proteins including antibodies, antibody fragments and lipoproteins, lectins, hormones, mono-, oligo- and polysaccharides as targeting moieties, microcapsules, microparticles, liposomes, and micelles could be successfully used for targeted drug delivery[14-18]. Providing a particle surface with monoclonal antibodies is one of the most effective ways to target antigen expressing cells[15,19] and depending on the dimensions, specific uptake of particles by target cells has been observed[20]. This approach has been applied to improve the therapeutic efficacy of anticancer drugs[15,21] and to design advanced diagnostic systems[22]. Of particular interest is the attachment of antibodies through the distal end of PEG chains[15,23]. By using PEG as a spacer the binding of the antibody located on the artificial cell to the target cell is not sterically hindered, and non-specific binding is reduced[24]. Recombinant protein A and G can be used in order to provide site specific immobilization of an antibody due to the specific interaction with the Fc portion of the antibody without affecting the antigen-antibody interaction.

In previous chapters, we have demonstrated that biodegradable polymersomes can be formed from amphiphilic PEG-polyester and PEG-polycarbonate diblock copolymers in either chloroform/water systems (chapter 5) or water miscible solvent/aqueous phase systems (chapter 6). To complete these polymersomes as artificial cells, they should also be provided with a biofunctional compound and a homing device.

In the study described in this chapter, carboxyfluorescein (CF) which is self quenching[25-27] was applied as a model hydrophilic substance for encapsulation and release studies using polymersomes that were prepared from water miscible solvent/aqueous phase systems. Anti-human IgG (a-HIgG) or anti-human serum albumin (a-HSA) was covalently immobilized via carboxyl groups present at the polymersome surface using the carbodiimide method. a-HIgG and a-HSA were also coupled to the polymersome surface via protein G, which was first covalently immobilized onto the carboxyl group containing polymersome surface. The targetability of these polymersomes was evaluated by following the interaction of these polymersomes with their corresponding immobilized antigens, i.e., human IgG and HSA by imaging surface plasmon resonance (iSPR).

EXPERIMENTAL

Materials

5(6)-Carboxyfluorescein (CF, 97%) was purchased from Molecular Probes (Eugene, Oregeon, USA). Sodium deoxycholate (DOC) was purchased from Aldrich. Freshly frozen, citrated, human plasma was

obtained from the Blood Transfusion Service Twente-Achterhoek (Enschede, The Netherlands). 1-Dimethylaminopropyl-ethylcarbodiimide hydrochloride (EDC), N-hydroxy-succinimide (NHS), 2-(N-morpholino)ethanesulfonic acid (MES), human albumin, 2-amino-2-(hydroxymethyl)-1,3-propanediol and tris(hydroxymethyl)aminomethane hydrochloride were obtained from SIGMA Chemical Inc. (St. Louis, MO, USA).

Human albumin antibody (a-HSA) in PBS (pH 7.2, 0.5 mg/mL), developed in goat, was bought from Bethyl Laboratories, Inc. (Montgomery, TX, USA). Goat anti-human IgG (γ chain specific) (a-HIgG), protein G (recombinant), Human IgG (HIgG, ≥95%), Human serum albumin (HSA, 99%), Bovine serum albumin (BSA) were bought from Sigma. Rabbit antibody (polyclonal Rabbit anti(human PSA), affinity-purified) in phosphate buffer (1.18 mg/ml, pH 7.4) was purchased from Cortex Biochem (San Leandro, CA). Mouse IgG (29 mg/ml in PBS) was bought from Future Diagnostics (Wijchen, The Netherlands).

The PEG-polyester copolymers used in this study were prepared using the ring-opening polymerization of *d,l*-lactide using zinc bis[bis(trimethylsilyl)amide] and monomethoxy PEG as an initiator[2,28]. α-Carboxyl poly(ethylene glycol)-b-poly(*d,l*-lactide) copolymer with PEG molecular weight 3400 and PDLLA molecular weight of 29600 was denoted as C-PEG-PDLLA3.4-30 and the synthesis was described in chapter 6. Deionized water (DI water) was obtained from a Milli-Q water purification system (Millipore, Molsheim, France). All other chemicals were from Merck (Darmstadt, Germany) and used as received. MES buffer (0.05M, pH 5.4, containing 0.02 wt.% NaN_3), and phosphate buffer (PB, 0.01M, pH 7.4, containing 0.02 wt.% NaN_3) were used in the immobilization or targeting experiments.

Preparation of CF encapsulated polymersomes (CF-PS)

CF encapsulated polymersomes (CF-PS) were prepared by injecting a solution of a block-polymer (see Table 1) in THF (0.05 mL, 10 mg/mL) into an aqueous solution with the tip of the pipette or syringe immersed close to the bottom of the bottle. The aqueous solution consisted of 1.225 mL of 165 mM CF in TRIS (20 mM, pH 7.4) and 1.225 mL of an aqueous solution of ethyl acetate (8 v.%) in a glass bottle. The osmolarity of the final solution was approximately 290 mOsm. After 15-30 min, the bottle was inverted twice to obtain a homogenous opaque dispersion. Subsequently, the CF-PS was separated from non-entrapped CF by gel filtration using a PD-10 column (Amersham Pharmacia Biotech, Roosendaal, The Netherlands) at room temperature applying 10 mM of TRIS (pH 7.4) as eluent.

Preparation of carboxyl group containing polymersomes (C-PS)

Carboxyl group containing polymersomes (C-PS) were made by injecting 0.5 mL of a solution of C-PEG-PDLLA3.4-30 in THF (10 mg/mL) into 5.0 mL of MES buffer (0.05M, pH 5.4, with 0.02 wt.% NaN_3) with the tip of the pipette or syringe immersed close to the bottom of the bottle. After 15 min without agitation, the bottle was gently inverted a few times and a homogenous bluish polymersome dispersion was obtained. The dispersion was then subjected to overnight dialysis against MES buffer using VISKING® dialysis tubing (MWCO 12000-14000, φ 16 mm) (SERVA Electrophoresis GmbH, Heidelberg, Germany).

Immobilization of antibodies directly onto C-PS (Ab-PS)

Solid NHS (5.75 mg) and EDC (38.3 mg) were subsequently added to 2.0 mL of a C-polymersome dispersion in a reaction tube. Inversion of the tube ensured complete dissolution of NHS and EDC. The reaction was allowed to proceed for 10 min before ultracentrifugation (60,000×g, 18 min, Centrikon T-2180, Kontron Instruments, Watford, UK) at 10 °C. The supernatant was removed using a pipette. a-HIgG or a-HSA solution (0.8 mL, 0.1 mg/mL) in MES buffer was added to the tube. The polymersomes were re-dispersed by gently shaking or aspirating/dispensing. The coupling reaction was allowed to proceed for 2.5 h at room temperature under mild shaking.

Free antibody was separated from the Ab-PS by gel filtration of the dispersion over a Sepharose® 4B (Pharmacia Fine chemicals AB, Uppsala, Sweden) column (volume 12 mL), which had been equilibrated with 25 mL of PB buffer before use. The polymersome dispersion (0.8 mL) was loaded on the column which was then eluted with 20 mL of PB buffer. Fractions (n = 20, V = 1.0 mL) were collected, and the count rate (DLS, see chapter 6) and protein content (micro BCA protein assay, see chapter 4) of each fraction were determined. The fractions that only contained Ab-PS were pooled. The polymersomes are denoted as a-HIgG-PS and a-HSA-PS, respectively.

Immobilization of antibodies via protein G onto C-PS (Ab-G-PS)

Protein G immobilized polymersomes (G-PS) were prepared and purified in the same way as mentioned for Ab-PS only the antibody solution was replaced by a protein G solution (0.1 mg/mL) in MES. The purified G-polymersomes in PB buffer were stored at 4 °C for 16 h, and then centrifuged (60,000×g, 18 min) at 10 °C to remove the supernatant. The pellet was re-suspended in a-HIgG or a-HSA solution (0.1 mg/mL, 1.0 mL) in PB buffer and the polymersomes were incubated for 2 h under mild shaking. The obtained Ab-G-PS, denoted respectively as a-HIgG-G-PS and a-HAS-G-PS, were purified from free antibody by gel filtration as described for the preparation of the Ab-PS.

Characterization of polymersomes

The size and zeta potential of C-PS, Ab-PS and Ab-G-PS in PB buffer were measured at 25°C using a Malvern Zetasizer 4000 and 2000 (Malvern Corp., Malvern, UK), respectively. Determination of the polymersome size was performed at a wavelength of 633 nm and a scattering angle of 90°. The CONTIN method was applied for data processing. The size, count rate and polydispersity index (PDI) were determined.

The zeta potential of polymersomes in PB buffer was measured using Laser Doppler Velocimetry (LDV), in which the velocity of particles moving in a fluid that is exposed to an electric field is measured. By applying the Smoluchowski equation[29] the ξ-potential can be determined. Measurements were carried out at 25°C using a 1000 Hz modulator frequency, and a cell drive voltage of 120V. Results are the mean of data obtained with three samples, which were each measured 4 times.

CF release from CF-PS

The fluorescence emission of CF is quenched to a marked extent[25-27] when the molecules are confined at high concentration. Thus, a marked increase in fluorescence intensity results when CF is released from the CF-PS to the surrounding aqueous medium.

The release of CF from polymersomes in different media at different temperatures was monitored as a function of time using a Perkin-Elmer LS-3 fluorescence spectrometer (Perkin-Elmer Co., Wellesley, MA, USA). Gel filtrated CF-polymersome dispersions (0.2 mL) were mixed with different media (1.1 mL) at room temperature (PBS, 4 wt.% human albumin in PBS, 15 v.% and 85 v.% human plasma in PBS) or at 60 °C (PBS) under stirring. The time between the gel filtration of the polymersomes and the start of the release experiment was 20-30 min. This time was not included in the release time.

At periodic intervals, 0.1 mL of the mixture was withdrawn and diluted with 1.0 mL of tris buffer (10 mM, pH 7.5), and then the fluorescence (F) was measured. The total fluorescence of CF encapsulated (F_T) was determined by adding DOC (0.1 mL, 3 wt.%) to 0.05 mL of a freshly gel filtrated dispersion, boiling briefly (ca. 2 min) and diluting with 0.95 mL of tris buffer before the fluorescence was measured. The total amount of encapsulated CF can be calculated from F_T, a calibration curve of CF fluorescence as a function of CF concentration, and the dilution factor. Since the quenching of the fluorescence inside the polymersomes initially was more than 95 %[27], the contribution of the CF inside the polymersomes to the total fluorescence was neglected. Even at 90% release, the fluorescence from the CF in the polymersomes is only 3-5% of the total fluorescence. The CF release (%) over time is presented by $100 \times F/F_T$.

Immobilization of the C-PS on an aminated sensor surface

The reaction of C-PS with an aminated surface was studied by SPR. An aminated SPR sensor disk (P-NH$_2$, IBIS Technologies, Hengelo, The Netherlands) was equilibrated in MES buffer (150 μL, 0.05 M, pH 5.4) in the cuvette sensor compartment of an IBIS II SPR instrument (IBIS Technologies, Hengelo, The Netherlands). After the removal of MES buffer, C-polymersome dispersion (150 μL) in MES buffer was added to both channels and the interaction of the polymersomes with the sensor surface was studied for 20 min under continuous mixing. Meanwhile, C-PS (150 μL in MES) were activated for 5 min by the addition of NHS and EDC subsequently with a final molar EDC to NHS ratio of 4 and [EDC] of 0.4 M. After 20-min interaction, the C-polymersome dispersions were drained from both channels followed by four times rinsing with MES buffer. Thereafter C-polymersome suspension (150 μL) in MES buffer was added to the reference channel, and the activated C-PS (150 μL) were added to the reaction channel. The aminated surface was incubated with polymersomes for 1 h under continuous mixing. After the reaction, both channels were rinsed with MES buffer for five times. During the whole experiment the SPR angle in milli-degree (m°) was monitored.

Preparation of antigen-spotted surfaces

Human serum albumin (HSA), bovine serum albumin (BSA), rabbit IgG (RIgG), mouse IgG (MIgG), and human IgG (HIgG) in MES buffer (50 mM, pH 5.4) were spotted on a pre-activated SPR sensor (iSPR-P-AE-sp, IBIS Technologies, Hengelo, The Netherlands) in an array of 6×4 protein spots (1 nL) using a TopSpot™ contactless spotter (HSG IMIT, Villingen-Schwenningen, Germany). From left to right, the columns corresponded to HSA (0.5 mg/mL), BSA (0.5 mg/mL), RIgG (0.5 mg/mL), MIgG (0.5 mg/mL), HIgG (0.5 mg/mL) and HIgG (0.2 mg/mL).

Directly after spotting, the sensor was transferred to a humidity chamber and incubated at 4 ºC overnight. Subsequently, un-reacted active esters were quenched with ethanol amine (0.1 M, pH 8.5) for 10 min at room temperature and the sensor surface was rinsed with PBS and stored in PBS at 4 ºC until use.

Interaction of Ab-PS or Ab-G-PS with protein immobilized surface

Targetability of the polymersomes was investigated by studying the interaction of the Ab-PS and Ab-G-PS with the protein spotted sensor surfaces by imaging SPR (IBIS iSPR, IBIS Technologies, Hengelo, The Netherlands). In a typical experiment, the sensor surface was rinsed with PB buffer and incubated with 150 μL of PB buffer for 10 min before regeneration with 100 μL of HCl (4 mM) followed by PB (150 μL) rinsing 5 times. 100 μL of PB buffer was then removed from the cuvette and 100 μL of polymersome dispersion was added and incubated for 1 h. Subsequently, the polymersomes were removed and the surface was 5 times rinsed with PB (150 μL) before regeneration with 4 mM HCl followed by 5 times rinsing with PB (150 μL). Thereafter, the sensor surface was reused to study the interaction with other polymersome dispersion following the same procedure. During the whole procedure the SPR shift was followed as a function of time.

RESULTS AND DISCUSSION

Encapsulation of CF

The fluorescence emission of CF is quenched to a marked extent[25-27] when the molecules are confined at high concentration, for example inside polymersomes. Thus, a marked increase in fluorescence intensity is observed when CF is released by the polymersomes in the surrounding aqueous medium. The total fluorescence is determined after disruption of the

polymersomes with the detergent DOC[25]. CF has an excitation maximum at ~491 nm at pH 7.4 and an emission maximum at ~520 nm, which is independent of the presence of DOC.

The injection of a solution of block copolymers in THF (see Table 1) into an aqueous phase, which contained CF and ethyl acetate, yielded polymersomes with incorporated CF. Untrapped CF was removed by gel filtration over a PD-10 column. Gel filtration of the polymersomes did not cause loss of particles as evidenced by the DLS measurements.

The polymersomes were disrupted by adding DOC in combination with brief boiling and the encapsulated CF was liberated. Table 1 lists the count rate of the polymersome dispersions, the average size of the polymersomes and the total amounts of CF that were incorporated in the polymersomes. For all copolymers a similar polymersome size was obtained. With an increase of molecular weight of the hydrophobic block (HB) of the copolymer, CF encapsulation increased due to the formation of more polymersomes. No effect of the type of HB (PDLLA or PCL) on the amount of encapsulated CF was observed. The percentage of CF encapsulation, however, is generally very low.

Table 1. Characteristics of polymersomes of different copolymers made in the presence of CF [a]

Copolymers	Count rate [b]	Size (nm)	Encapsulated CF per preparation (nmol) [c]
PEG-PDLLA5.8-15	157± 4.3	255± 2.1	4.85± 0.7
PEG-PDLLA5.8-24	236 ± 1.4	258± 4.3	5.33± 0.3
PEG-PDLLA5.8-48	457 ± 20.0	250± 3.5	9.00 ± 1.0
PEG-PDLLA5.8-48 [d]	1921± 10.0	248± 2.0	30.14± 1.3
PEG-PCL5.8-24	251± 1.0	261± 6.1	4.96± 0.5

[a] Data presented are the average value of duplicate experiments followed by the variation, except the third entry of this table, of which the data is the mean value followed by the standard deviation. [b] count rate of the original CF-PS dispersions based on the DLS measurement of its dilutions. [c] calculation based on the fluorescence measured after DOC treatment. [d] for the preparation of these polymersomes, 0.25 mL instead of 0.05 mL of PEG-PDLLA5.8-48 solution was used.

Release of CF

The release of CF from the polymersomes into different media at different temperatures was studied by measuring at different time intervals the fluorescence of the media in which the polymersomes were incubated. The presence of plasma proteins suppresses the fluorescence[27] and the extent of the suppression depends on the protein concentration. This dependency was studied and all data were corrected for this fluorescence suppression. Even at 90% release, the fluorescence from the CF inside the polymersomes is still quenched 40 % and only accounts for 3-5% of the total fluorescence, as calculated based on the quenching factor at different CF concentrations[27]. Also the initial CF concentration used is very high giving more than 95 % quenching, therefore, the fluorescence contribution of the CF inside the polymersomes is neglected.

The release of CF from all polymersomes that were studied had the same trend and typical release profiles of CF from polymersomes at room temperature in different media are shown in Figure 1. All the profiles show an initial rapid release followed by a gradual decrease of the release rate, which practically decreased to zero after 5-6 days. CF release profiles of the first 4 h are "magnified" and shown in Figure 1 B. At the first time point measured (2 min) the

release was already 30%. It should be noted however, that the time between the gel filtration of the polymersomes and the start of the release experiment (20-30 min) was not taken into account.
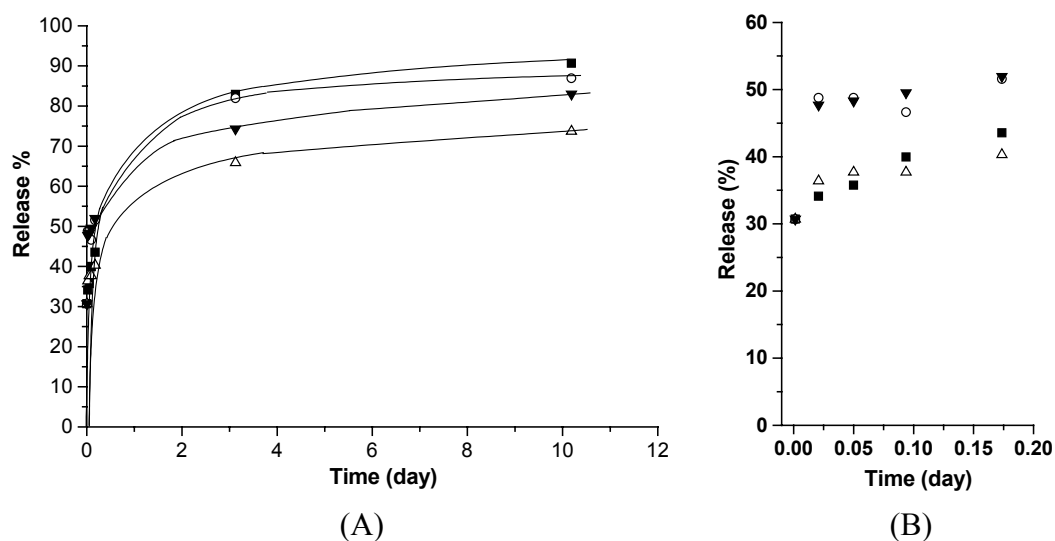

(A)   **(B)**

Figure 1. *CF release profiles of polymersome of PEG-PDLLA5.8-48 in different media at room temperature (A): ■ PBS, ○ human serum albumin in PBS (4 wt.%), ▼ human plasma in PBS (85 v.%) and △ human plasma in PBS (15 v.%). N=3, standard deviation is <12 %. (B) is the magnified part of the release of the first 4 h. The lag time (20-30 min) between the gel filtration of the polymersomes and the start of the release experiment was not taken into account.*

The CF containing polymersome system can be considered as a membrane-controlled reservoir device system. If the device contains an unsaturated solution, the release rate, dM_t/dt, which is proportional to the mass of the encapsulated agent, and declines exponentially with time[30], can be described by

$$\frac{dM_t}{dt} = k(M_0 - M_t) = kM_0 \exp(-kt)$$

where M_0 and M_t is the mass of agent in the device at time $t = 0$ and the mass released at time t, respectively, and k is a constant.

To validate this, the data for the release in PBS at 20 °C was re-plotted as $\ln(F_T/(F_T-F))$ as a function of the release time. This resulted in a linear relation (r = 0.996, see Figure 2 dashed line). This confirms that the CF containing polymersome system is a membrane-controlled reservoir system, with CF in an unsaturated solution inside the polymersomes. As CF is released its concentration decreases, resulting in a release rate that declines exponentially, giving a first-order release profile[30].

The release of CF in PBS at 20 °C lasted about two weeks. The release of CF in a physiological albumin solution (4 wt.% in PBS) was almost identical to the release of CF in PBS. This indicates that albumin adsorption and/or albumin insertion in the polymersome membrane does not take place or does not affect CF release. However, CF release into plasma dilutions (15 and 85 v.% in PBS) was slower than in PBS and surprisingly the release in 85 v.% plasma was faster than in 15 v.% plasma. This can be ascribed to the complex process of

protein adsorption from plasma dilutions onto the polymersomes. Some proteins other than albumin may penetrate the PEG layer and stick to the hydrophobic part resulting in a thicker membrane, thus slowing down the release of CF. The reason that 15 v.% plasma has a larger influence on the CF release than 85 v.% plasma, is probably due to the adhesion and insertion of certain proteins that is inhibited at high plasma concentration. For example, Fn adsorption onto poly(ethylene teraphthalate) and Teflon films reached a maximum value at a serum concentration of ~0.1 %[31], and was significantly decreased or completely blocked by other proteins when the serum concentration was higher than 1 %. A faster CF release in PBS than in plasma dilutions was also observed for multi-lamellar liposomes[32], where the rate of CF release was 3-8 fold less in the presence of up to 25 v.% human serum as compared to the release in PBS. The reason was due to the association of serum proteins with the outermost lipid bilayer, which led to stabilization of the liposomes (less bilayer defects), resulting in restricted permeability of the lipid membrane[32].

This also indicates that the pegylated surface of the polymersomes does not fully prevent non-specific protein adsorption. Besides influencing the release properties of the polymersomes, non-specific protein adsorption may also lead to clearance of the particles from the body by the mononuclear phagocytic system. It is anticipated that it is not easy to tune the PEG surface concentration of the polymersomes by varying the polymersome formation conditions. Therefore, the use of a PEG block with a higher molecular weight may be a better alternative to further suppress non-specific protein interactions with the polymersomes.
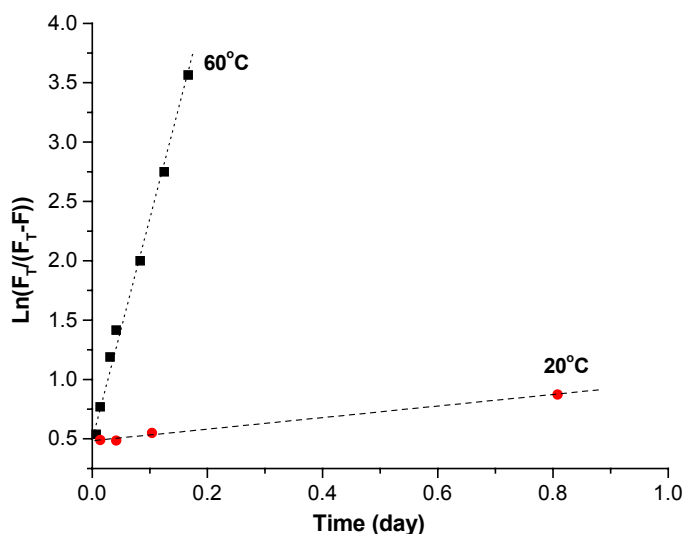

Figure 2. *The kinetics of CF release from polymersomes of PEG-PDLLA5.8-48 in PBS at 20 °C (●, the dashed line is the linear fit for Y=0.482+0.486X, R=0.997) and 60 °C (■, the dotted line is the linear fit for Y=0.492+18.470X, R=0.996).*

When the temperature was increased from 20 to 60 °C, the release of CF in PBS was enhanced drastically (Figure 3). At 20 °C polymersomes of PEG-PDLLA5.8-48 completely released the encapsulated CF within ca. 12 days, whereas at 60 °C release was complete within 4 h. The kinetics of CF release in PBS at 60 °C also showed a linear relationship (r= 0.997) between

$\ln(F_T/(F_T-F))$ and the release time (Figure 2, dotted line), suggesting a first order release profile of CF. In addition, the CF containing polymersomes retained their integrity also at 60 °C.

Although the CF release profile was the same for polymersomes of all block-copolymers that are listed in table 1, the composition of the block-copolymer had an influence on the release rate of CF. The lower the Mn of the whole copolymer (with similar HF/HB ratio), the higher the release rate (data not shown). This is probably due to the relatively thinner membrane of the polymersomes of copolymers with a low Mn of HB (see chapter 5). The CF release rate decreased in the order: PEG-PCL5.8-24>PEG-PDLLA5.8-24>PEG-PDLLA5.8-48. This sequence can be expected considering the softness and/or thickness of polymersome membranes, i.e., PCL has a low glass transition temperature as compared to PDLLA and polymersomes of PEG-PDLLA5.8-24 may have thinner membranes than those of PEG-PDLLA5.8-48.
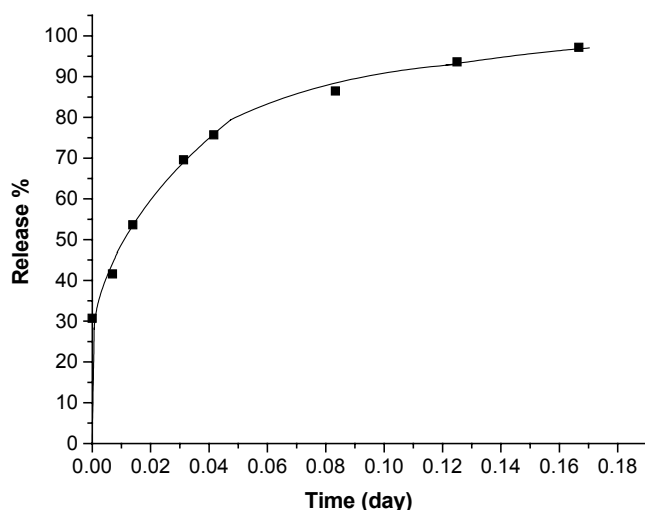

Figure 3. The release profile of CF from polymersomes of PEG-PDLLA5.8-48 in PBS at 60 °C.

In conclusion, hydrophilic substances can be readily encapsulated inside these biodegradable polymersomes. At room temperature (20 °C) and 60 °C the CF release of the polymersomes followed first order kinetics, suggesting that the CF containing polymersome system can be considered as a membrane-controlled reservoir system. The release can be adjusted by the copolymer composition (Mn and/or type of HB).

Targetability of the polymersomes

A targeting moiety present on the polymersome surface can render it site specific and thus reduce unwanted side effects. In this section, the accessibility of the carboxyl groups of the polymersomes for the immobilization of antibodies as targeting moieties is evaluated. Furthermore, preparation and purification of Ab-PS and Ab-G-PS, as well as their interaction with immobilized antigens will be addressed.

Availability of carboxyl groups of C-PS. To prepare polymersomes with covalently immobilized antibodies, polymersomes with -COOH groups on the surface were prepared from copolymer C-PEG-PDLLA3.4-30. The availability of the -COOH groups of the C-PS was

evaluated by zeta potential and SPR measurements. The zeta potential of C-PEG-PDLLA3.4-30 polymersomes in MES buffer and in PBS were −39.5±0.4 mV and −37.2±0.5 mV, respectively, which are ~20-25 mV less than those of PEG-PDLLA3-24 polymersomes, suggesting that -COOH end groups of the PEG block of the copolymer are present at the surface of the polymersomes.
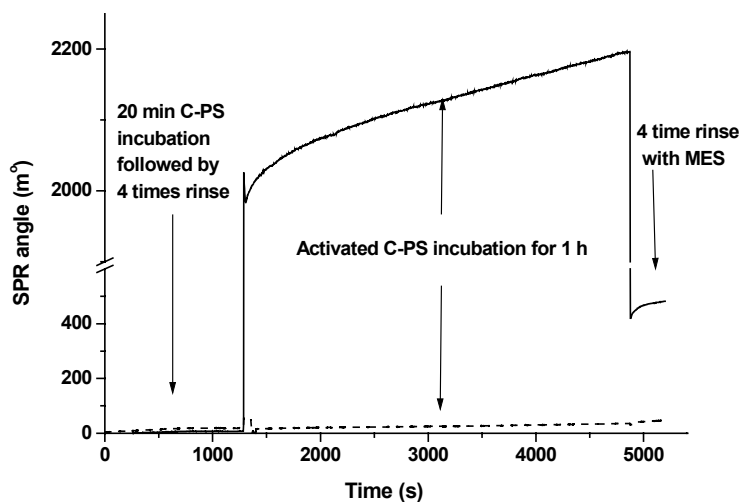

Figure 4. SPR profile of the interaction between C-PS and an aminated sensor surface. The solid line is the SPR angle of the reaction channel where the interaction of EDC/NHS activated C-PS with the surface takes place, and the dashed line represents the SPR angle of the reference channel where the aminated surface was incubated with non-activated C-PS.

This was further confirmed by an SPR measurement of which the results are shown in Figure 4. Incubation of the aminated surface with C-PS in MES for 20 min did not induce any adhesion of polymersomes to the surface. Incubation of the surface with EDC/NHS activated C-PS generated a large shift of the SPR angle of which most was due to the refractive index change by the dispersion of EDC/NHS activated polymersome. Washing 5 times with MES buffer eliminated the bulk effect, and an SPR shift of ca. 475 m° was left which can be attributed to the covalent immobilization of the C-PS to the aminated sensor surface. In the reference channel, where exactly the same procedure was performed except that non-EDC/NHS activated polymersomes were applied, no significant SPR shift was detected. The covalent attachment of C-PS to the sensor surface in MES buffer was also confirmed by tapping mode AFM measurements (results not shown).

These results confirm the proposed structure of the polymersome model, in which the wall of the polymersomes consists of a layer of stacked coiled polymer chains held together by non-covalent forces with the PEG blocks protruding into the aqueous phases and the entangled hydrophobic block forming the core of the polymersome wall, as was also displayed in Figure 3 of chapter 5. Most interestingly, the availability of the -COOH groups on the polymersome surface allows polymersome surface modification for instance for targeting purposes.

Interaction of Ab-PS, Ab-G-PS and G-PS with protein patterned surface.

After purification of the Ab-PS, G-PS and Ab-G-PS dispersions by gel filtration, the obtained polymersomes were free of free antibodies/protein G as shown by determination of the protein

concentration in the collected fractions. Table 2 shows the characteristics of these purified polymersomes. Immobilization of protein G (42 kDa) did not cause much increase in the polymersome size, but an increase in zeta potential (9 mV) was observed, indicating the substitution of the -COOH groups on the polymersome surface. a-HSA-PS had a larger size (~20 nm) and a higher zeta potential (~14 mV) than the starting C-PS. With a similar increase in zeta potential (8 mV), Ab-G-PS were larger (100 nm) and had a much higher polydispersity (PDI) than the C-PS. The large increase in size of polymersomes can be ascribed to the immobilization of antibodies on the surface and to partial polymersome aggregation. Upon the immobilization of the antibodies to the G-PS surface, which involved an additional ultracentrifugation step, it was difficult to redisperse the polymersomes.

Table 2. Size and zeta potential of different polymersomes in PB buffer

	C-PS	a-HSA-PS	G-PS	a-HSA-G-PS	a-HIgG-G-PS
Zeta potential (mV)	-26.1± 1.5	-12.0± 0.4	-17.0± 0.2	-17.7± 0.1	-17.9± 0.1
Size (nm)	288± 2.2	310± 1.2	286± 0.4	382± 3.9	392± 5.0
PDI	0.12± 0.02	0.16± 0.05	0.13± 0.03	0.45± 0.08	0.31± 0.05

The targetability of the polymersomes was investigated by following the interaction of purified Ab-PS and Ab-G-PS with surface immobilized antigens in time by iSPR. SPR shifts due to the interaction of protein surfaces with polymersomes are shown in Figure 5.

All the spots showed some non-specific interaction when the surface was incubated with C-PS, probably due to electrostatic interactions. The interaction of a-HSA-PS with HSA spots only gave a slightly higher SPR angle shift than for other protein spots. This is probably due to the low amount of a-HSA that was immobilized onto the polymersomes and/or to the random immobilization of the a-HSA on the polymersome surface.

Recombinant protein G can be used to provide site specific immobilization of an antibody due to its specific interaction with the Fc portion of the antibody without affecting the antigen-antibody interaction. Therefore, coupling of an antibody via protein G can improve the orientation of the antibody on the polymersome surface and thus enhance the binding efficiency. The results show that antibody immobilization via protein G is indeed more efficient than direct immobilization of antibody, whereas the G-PS only gave a small SPR shift, especially the a-HSA-G-PS showed specific interaction with immobilized HSA. The interaction of these polymersomes with BSA may be non-specific or due to some cross-reactivity of the antibody. The pattern of the interaction between a-HSA-G-PS and surface immobilized IgG's was the same as for the G-PS, showing that a-HSA-G-PS had no affinity for the immobilized IgG's.

The same trend as was observed for a-HSA-G-PS was observed for the interaction of free a-HSA with the immobilized protein spots. However, the SPR angle shifts caused by the free a-HSA were much larger. This is probably due to a smaller diffusion constant of the polymersome immobilized a-HSA. For the interaction of free a-HSA with immobilized HAS, an SPR angle shift of 265 m° was obtained which corresponds to ~0.22 μg/cm^2, indicating that less than a monolayer of a-HSA was present on the surface.

The a-HIgG-G-PS showed a strong interaction with the immobilized HIgG spots. However, also the interaction with the albumin spots and RIgG and MIgG spots was rather large. This is probably due to the fact that the a-HIgG that was used for the immobilization was not cross-adsorbed.
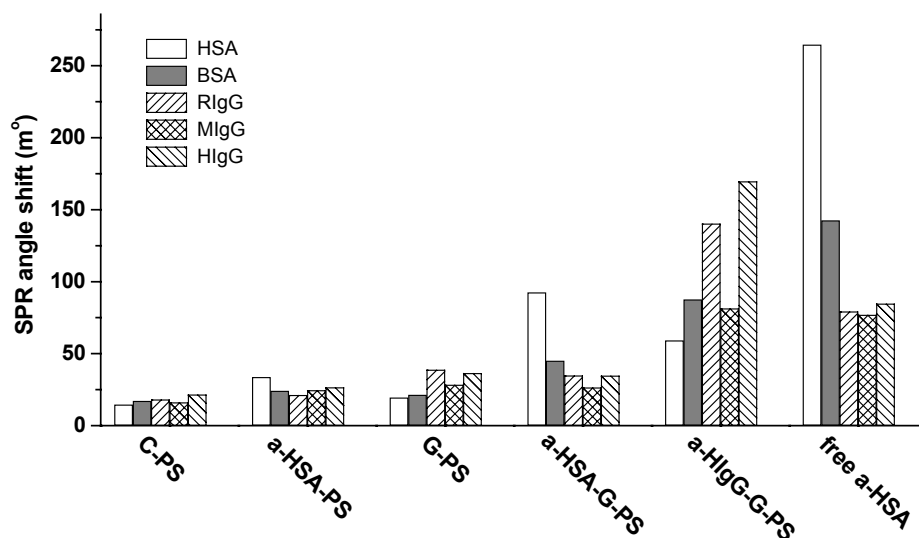

Figure 5. *SPR angle shift as a result of the interaction of different polymersome preparations (C-PS, a-HSA-PS, G-PS, a-HSA-G-PS, a-HIgG-G-PS) and free a-HSA with different immobilized protein spots (HSA, BSA, rabbit IgG, mouse IgG and Human IgG).*

Although these targeting experiments are preliminary, it can be concluded that the targeting of polymersomes by immobilization of antibodies is possible and that site-specific immobilization through protein G is favoured over direct immobilization of the antibodies.

CONCLUSIONS

As shown by the encapsulation of carboxyfluorescein (CF), hydrophilic biofunctional materials can be readily incorporated in polymersomes of amphiphilic biodegradable block copolymers simply by adding biofunctional materials to the aqueous phase during the polymersome preparation. The CF release in PBS at room temperature was complete within ca. 2 wks and the presence of plasma proteins other than albumin decreased the release rate. The release of encapsulated material from the polymersomes can be tailored by changing the copolymer composition, especially the Mn and type of hydrophobic block of the copolymer. CF release in PBS both at room temperature and at 60 °C followed first order kinetics, confirming that the CF containing polymersome system is a membrane controlled reservoir release system. These biodegradable polymersomes have potential for targeting to specific sites in vivo as shown by the specific interaction between a-HAS-G-PS and immobilized HSA in imaging SPR experiments.

ACKNOWLEDGEMENTS

REFERENCES

(1)   Chapter 6 of this thesis .

(2)   Chapter 5 of this thesis .

(3)   Quellec, P.; Gref, R.; Dellacherie, E.; Sommer, F.; Tran, M. D.; Alonso, M. J. *J. Biomed. Mater. Res.* **1999,** *47*, 388.

(4)   Lasic, D. D. *Angew. Chem. Int. Edit. Engl.* **1994,** *33*, 1685.

(5)   Annesini, M. C. *Chem. Biochem. Eng. Q.* **1998,** *12*, 1.

(6)   Woodle, M. C. *Adv. Drug Deliv. Rev.* **1998,** *32*, 139.

(7)   Lasic, D. D. Liposomes: from physics to applications. Amsterdam: Elsevier, **1993**.

(8)   Gregoriadis, G. Liposome technology. Boca Raton: CRC Press, Inc., **1984**.

(9)   Quintanar-Guerrero, D.; Allemann, E.; Doelker, E.; Fessi, H. *Pharm. Res.* **1998,** *15*, 1056.

(10)   Quintanar-Guerrero, D.; Allemann, E.; Fessi, H.; Doelker, E. *Drug Dev. Ind. Pharm.* **1998,** *24*, 1113.

(11)   Kasuya, Y.; Fujimoto, K.; Miyamoto, M.; Juji, T.; Otaka, A.; Funakoshi, S.; Fujii, N.; Kawaguchi, H. *J. Biomater. Sci.-Polym. Ed.* **1993,** *4*, 369.

(12)   Vingerhoeds, M. H.; Haisma, H. J.; Belliot, S. O.; Smit, R. H. P.; Crommelin, D. J. A.; Storm, G. *Pharm. Res.* **1996,** *13*, 604.

(13)   Inaki, Y. In *Functional monomers and polymers: procedures, synthesis, applications*; Takemoto, K., Inaki, Y., Ottenbrite, R. M., Eds.; Marcel Dekker: NewYork, **1987**, p 461.

(14)   Davis, S. S.; Illum, L.; Stolnik, S. *Curr. Opin. Colloid Interface Sci.* **1996,** *1*, 660.

(15)   Allen, T. M.; Brandeis, E.; Hansen, C. B.; Kao, G. Y.; Zalipsky, S. *Biochim. Biophys. Acta-Biomembr.* **1995,** *1240*, 285.

(16)   Gessner, A.; Olbrich, C.; Schroder, W.; Kayser, O.; Muller, R. H. *Int. J. Pharm.* **2001,** *214*, 87.

(17)   Bendas, G.; Krause, A.; Bakowsky, U.; Vogel, J.; Rothe, U. *Int. J. Pharm.* **1999,** *181*, 79.

(18)   Mosqueira, V. C. F.; Legrand, P.; Gref, R.; Heurtault, B.; Appel, M.; Barratt, G. *J. Drug Target.* **1999,** *7*, 65.

(19)   Hansen, C. B.; Kao, G. Y.; Moase, E. H.; Zalipsky, S.; Allen, T. M. *Biochim. Biophys. Acta-Biomembr.* **1995,** *1239*, 133.

(20)   Zalipsky, S.; Hansen, C. B.; deMenezes, D. E. L.; Allen, T. M. *J. Control. Release* **1996,** *39*, 153.

(21)   de Menezes, D. E. L.; Pilarski, L. M.; Allen, T. M. *Cancer Res.* **1998,** *58*, 3320.

(22)   Basinska, T.; Slomkowski, S. *J. Biomater. Sci.-Polym. Ed.* **1991,** *3*, 115.

(23)   Maruyama, K.; Takizawa, T.; Takahashi, N.; Tagawa, T.; Nagaike, K.; Iwatsuru, M. *Adv. Drug Deliv. Rev.* **1997,** *24*, 235.

(24)   Emanuel, N.; Kedar, E.; Bolotin, E. M.; Smorodinsky, N. I.; Barenholz, Y. *Pharm. Res.* **1996,** *13*, 352.

(25)   Lelkes, P. I. In *Liposome technology*; Ed.Gregoriadis, G., Eds.; CRC Press: Boca Raton, **1984**; Vol. III, p 225.

(26)   Senior, J.; Gregoriadis, G. In *Liposome technology*; Ed.Gregoriadis, G., Eds.; CRC Press: Boca Raton, **1984**; Vol. III, p 263.

(27)   Weinstein, J. N.; Ralston, E.; Leserman, L. D.; Klausner, R. D.; Dragsten, P.; Henkart, P.; Blumenthal, R. In *Liposome technology*; Ed.Gregoriadis, G., Eds.; CRC Press: Boca Raton, **1984**; Vol. III, p 183.

(28)   Meng, F. H.; Hiemstra, C.; Engbers, G. H. M.; Feijen, J. *Macromolecules* **2003,** *36*, 3004.

(29)   Hunter, R. J. *Zeta potential in colloid science: principles and applications*, 3rd ed.; Academic Press: London, **1988**.

(30)   Baker, R. *Controlled release of biologically active agents*; John Wiley &Sons: New York, **1987**.

(31) van Wachem, P. B.; Vreriks, C. M.; Beugeling, T.; Feijen, J.; Bantjes, A.; Detmers, J. P.; van Aken, W. G. *J. Biomed. Mater. Res.* **1987,** *21*, 701.

(32) Lelkes, P. I.; Friedmann, P. *Biochim. Biophys. Acta* **1984,** *775*, 395.

Summary

Based on the structure of biological cells and the existence of physico-chemical principles such as self-assembly, it can be perceived that artificial cells can be prepared. These artificial cells are water-insoluble particles that can perform specific functions in the body without being recognized by the defense system. Besides being applied as a model for natural cells, artificial cells can also be used for pharmaceutical applications and in biotechnology, for instance, gene therapy, targeted drug delivery systems, diagnostics, or as blood cell substitutes.

The components of an artificial cell may vary according to the intended application. Principally, artificial cells are based on a cell body, which contains a biofunctional compound (e.g. drugs, proteins, DNA) and possesses a bioinert surface to prevent recognition of the artificial cells by the defense system. This bioinert surface can be provided with a homing device that renders the artificial cell biospecific. For in vivo applications, the whole cell should be preferably biodegradable with a tunable degradation time depending on the desired duration of the biofunction.

Artificial cells developed by Chang contain isolated contents of red blood cells within semi-permeable capsules and have been evaluated as artificial red blood cells. Liposome formulations and nano-particle formulations have received much attention in targeted drug delivery systems. However, the major problems related to the application of artificial cells are the lack of material biocompatibility, specificity, tunable stability or, once they have performed their function, biodegradability.

To cope with these problems, biodegradable, biocompatible polymersomes were proposed to be used as a basis for artificial cells. Polymersomes, i.e., polymer vesicles, are similar to liposomes but based on amphiphilic block-copolymers instead of lipids. The combination of a large compartment for efficient encapsulation, tunable membrane properties, stability and the large diversity of copolymers that can be applied render polymersomes very suitable as an artificial cell body.

Chapter 1 gives a general introduction on the subject and the structure of this thesis. Chapter 2 is a review of artificial cells, with an emphasis on artificial cell bodies (material and structure), biofunctionality, bioinert cell surfaces and homing devices that can provide the artificial cell with site specificity. Although 'artificial cells' is a relatively new topic, chapter 2 also contains a comprehensive historical overview of artificial cells.

Surface pegylation, i.e., the immobilization or grafting of polyethylene glycol onto a surface, is a frequently used method to render a surface bioinert. The effect of surface pegylation largely depends on the surface density of the immobilized PEG chains. Chapter 3 describes the application of the pegylation strategy to carboxyl group containing polystyrene particles (PS-COOH) that serve as a model for an artificial cell body. The PS-COOH particles are pegylated via carbodiimide chemistry and a range of particles with different PEG surface concentrations

are prepared. The optimal conditions for obtaining high surface concentrations of immobilized PEG are established. Under optimized grafting conditions, a dense "brush-like" PEG layer is formed. A PEG surface concentration of approximately 60 $p$mol/cm^2, corresponding with an average distance between grafted PEG chains of ~17 Å, can be realized. In order to get insight in the effect of surface pegylation on protein adsorption, protein adsorption experiments were conducted. It was shown that surface pegylation could reduce the adsorption of proteins from an 85 v.% human plasma dilution in PBS to 90 % as compared to the protein adsorption on PS-COOH.

A more detailed study of the effect of immobilized PEG (molecular weight, surface concentration and end group) on protein adsorption and on complement activation is described in Chapter 4. Furthermore, in this chapter the interaction of the pegylated particles with cultured human umbilical vein endothelial cells (HUVEC) is also described. Protein adsorption from 85 v.% human plasma onto PS-PEG with a PEG surface concentration higher than 40 pmol/cm^2 was reduced up to 90-95 % as compared to PS-COOH, resulting in a final protein surface concentration of ~20 ng/cm^2. Two dimensional gel electrophoresis analyses revealed that about 30 % of the total amount of adsorbed proteins onto PS-PEG was due to the adsorption of dysopsonins. For PS-COOH, this was less than 15 %. In addition, when the PEG surface concentration was less than ~55 pmol/cm^2, the generation of terminal complement compound (TCC) by PS-PEG was insignificant, and PS-PEG with a PEG surface concentration >~35 pmol/cm^2 showed minimal interaction with cultured HUVEC.

Aiming for artificial cells that have a long circulation time and are not removed by the MPS, a preferred PEG modification in terms of surface concentration, end group and molecular weight of PEG was deduced from the results of the in vitro evaluation of the pegylated particles. An artificial cell surface should preferably contain a PEG coating with PEG molecular weight $\geq$ 3400 g/mol, surface concentration ca. 45-55 pmol/cm^2 (for PEG 3400-5000), and methoxy end groups or methoxy groups mixed with amine groups for further functionalization.

Based on the pre-study of the pegylated model surface, biodegradable biocompatible polymersomes were prepared that can serve as a basis for artificial cells. The formation of these polymersomes is the subject of Chapter 5 and 6. The polymersomes are based on amphiphilic PEG-polyester or PEG-polycarbonate block-copolymers. By combining biodegradable, hydrophobic blocks with biocompatible hydrophilic blocks with a molecular weight that is such that the hydrophilic blocks can be excreted by the body, fully bio-degradable polymersomes with an inert surface can be obtained.

In chapter 5 the formation of polymersomes in chloroform/water systems is described. Unfortunately, this system only yielded polymersomes with a broad size distribution in combination with polymer precipitate. Chapter 6 deals with the formation of polymersomes in mixtures of a water miscible solvent and an aqueous solution. With this system, the problems encountered with the chloroform/water system could be overcome, and polymersomes (170-1200 nm) with a narrow size distribution and free of precipitates were obtained. For both systems, the influence of the preparation parameters on the polymersome yield, size and size distribution was studied systematically, and mechanisms for polymersome formation are proposed.

To complete these polymersomes as artificial cells, biofunctionality and a homing device were incorporated into the polymersomes. Chapter 7 describes the encapsulation and release of a model biofunctional compound, the fluorescent probe carboxyfluorescein (CF). CF could be readily incorporated in the polymersomes by adding the compound to the aqueous phase during polymersome preparation. The release of the encapsulated compound from the polymersomes depended on the copolymer composition, especially the molecular weight and type of hydrophobic block of the copolymer. CF release in PBS both at room temperature and at 60 °C followed first order kinetics, confirming that the CF containing polymersome system is a membrane controlled reservoir system. The presence of plasma proteins other than albumin suppressed the release of CF.

Antibodies (anti-human albumin and anti-human IgG) were coupled on the polymersome surface directly or through protein G, and the targeting properties of these polymersomes to a protein coated surface were evaluated by imaging surface plasmon resonance analysis. Specific interaction of anti-human serum albumin immobilized polymersomes with an immobilized human serum albumin was observed, from which it was concluded that the targeting of polymersomes by immobilization of antibodies is possible and that site-specific immobilization through protein G is favoured over direct immobilization of the antibodies.

The biodegradable, biocompatible polymersomes thus prepared have a defined structure, a narrow size distribution, a large volume for encapsulation, and tuneable release properties. Furthermore, they have the potential to be targeted to specific sites in the body.

Samenvatting

Kunstmatige cellen zijn water onoplosbare deeltjes, die specifieke functies in het lichaam kunnen uitvoeren, zonder daarbij herkend te worden door het immuunsysteem. Behalve als model voor natuurlijke cellen kunnen kunstmatige cellen ook gebruikt worden voor toepassingen zoals gentherapie, doelgerichte medicijnafgifte, diagnostiek en als vervangers voor natuurlijke bloedcellen. De vervaardiging van kunstmatige cellen kan worden gebaseerd op de structuur van biologische cellen door gebruik te maken van fysisch-chemische principes zoals zelf-assemblage.

De opbouw van de kunstmatige cel kan worden aangepast aan de gewenste toepassing. In principe zijn kunstmatige cellen gebaseerd op een cellichaam dat een biofunctionele component bevat en een biologisch inert oppervlak heeft om te voorkomen dat deze cellen herkend worden door het afweersysteem. Dit inerte oppervlak kan worden voorzien van een herkennings-systeem dat ervoor zorgt dat de cel zijn specifieke bestemming bereikt. Om de cel in het lichaam te kunnen toepassen dient deze bio-afbreekbaar te zijn waarbij de degradatietijd moet worden afgestemd op de gewenste tijdsduur van de biologische functie.

Kunstmatige cellen zoals ontwikkeld door Chang bevatten geïsoleerde actieve componenten van rode bloedcellen in een gedeeltelijk doorlaatbare capsule en worden momenteel geëvalueerd als kunstmatige rode bloedcellen. Veel onderzoek naar kunstmatige cellen is gebaseerd op het onderzoek naar doelgerichte medicijn-afgifte-systemen, waarin de bereiding van liposomen en nanodeeltjes veel aandacht heeft gekregen. De belangrijkste problemen die zijn gerelateerd aan de toepassing van kunstmatige cellen zijn het gebrek aan biocompatibiliteit, specificiteit, af te stemmen stabiliteit en gecontroleerde, biologische afbreekbaarheid.

Om deze problemen op te lossen worden bio-afbreekbare en biocompatibele polymerosomen voorgesteld als basis voor kunstmatige cellen. Polymerosomen zijn te vergelijken met liposomen maar gebaseerd op amfifiele blok-copolymeren in plaats van lipiden. De combinatie van relatief grote compartimenten voor een efficiënte encapsulering, af te stemmen membraan eigenschappen, stabiliteit en grote diversiteit van de te gebruiken copolymeren maken deze polymerosomen zeer geschikt als kunstmatig cellichaam.

In hoofdstuk 1 wordt een algemene inleiding op het onderwerp en de opbouw van dit proefschrift gegeven. Hoofdstuk 2 geeft een overzicht van kunstmatige cellen met de nadruk op kunstmatige cellichamen (materiaal en structuur), biofunctionaliteit, biologisch inerte cel-oppervlakken en herkennings-systemen, die de kunstmatige cel naar het doel kunnen brengen. 'Kunstmatige cellen' worden nog niet zo lang bestudeerd. Hoofdstuk 2 geeft een overzicht van de bestaande literatuur.

De immobilisatie of het enten van polyethyleen glycol (PEG) op een oppervlak, ook wel genoemd "pegylering", is een veel gebruikte manier om een oppervlak biologisch inert te

maken. Het effect van oppervlaktepegylering hangt sterk af van de oppervlaktedichtheid en lengte van de geïmmobiliseerde PEG ketens. Hoofdstuk 3 beschrijft de pegylering van polystyreen deeltjes met carbonzuurgroepen op het oppervlak (PS-COOH) welke dienen als een model voor een kunstmatig cellichaam. The PS-COOH deeltjes zijn gepegyleerd met behulp van carbodiimide chemie, waarbij een serie deeltjes met verschillende PEG oppervlakteconcentraties is bereid. De optimale condities voor het verkrijgen van een hoge concentratie geïmmobiliseerd PEG zijn vastgesteld. Onder optimale immobilisatiecondities wordt een borstelachtige PEG-laag gevormd. Een PEG oppervlakteconcentratie van ongeveer 60 pmol/cm^2 die overeenkomt met een gemiddelde afstand van ~ 17Å tussen de geïmmobiliseerde-PEG ketens, kan worden gerealiseerd. Om meer inzicht te krijgen in het effect van oppervlaktepegylering op eiwit-adsorptie werden eiwitadsorptie-experimenten uitgevoerd. Hierbij bleek dat in vergelijking met de eiwit-adsorptie aan PS-COOH, de eiwit-adsorptie na pegylering van PS-COOH tot 90 % kan worden gereduceerd vanuit een 85 v.% menselijke plasma verdunning in PBS.

Een meer gedetailleerde studie naar het effect van geïmmobiliseerd PEG (molgewicht, oppervlakteconcentratie en eindgroepen) op eiwit-adsorptie en op complement-activering is beschreven in hoofdstuk 4. Tevens is in dit hoofdstuk de interactie van gepegyleerde deeltjes met gekweekte endotheelcellen afkomstig van de menselijke navelstreng (HUVEC) beschreven. In vergelijking met PS-COOH, was de eiwit-adsorptie vanuit een 85 v.% menselijk plasma aan PS-PEG met een PEG oppervlakteconcentratie hoger dan 40 pmol/cm^2 90-95 % minder, resulterend in een uiteindelijke eiwit oppervlakteconcentratie van ~20 ng/cm^2. Tweedimensionele gel-elektroforese analyse liet zien dat ongeveer 30 % van de totale hoeveelheid geadsorbeerd eiwit aan PS-PEG was toe te schrijven aan de adsorptie van eiwitten met een dysopsonisch karakter. Voor PS-COOH was dit minder dan 15 %. Voor deeltjes met een PEG concentratie < ~55 pmol/cm^2 was de generatie van het terminale complement complex (TCC) niet significant. PS-PEG met een PEG oppervlakteconcentratie > ~35 pmol/cm^2 vertoonde een minimale interactie met de gekweekte HUVEC.

Uit de resultaten van de *in vitro* evaluatie van de gepegyleerde deeltjes werd voor kunstmatige cellen met een lange circulatietijd een optimaal gepegyleerd oppervlak afgeleid m.b.t. de oppervlakteconcentratie, eindgroepen en moleculair gewicht van het geïmmobiliseerde PEG. Een dergelijk kunstmatig celoppervlak zou bij voorkeur een PEG laag moeten bevatten met een PEG molgewicht ≥ 3400, een oppervlakteconcentratie van circa 45-55 pmol/cm^2 (voor PEG 3400-5000) en methoxy-eindgroepen of methoxy-groepen in combinatie met aminegroepen. Deze aminegroepen kunnen worden toegepast voor verdere oppervlakte-modificatie.

Naar aanleiding van deze voorstudie naar gepegyleerde modeloppervlakken, werden biodegradeerbare, biocompatibele polymerosomen gemaakt die kunnen dienen als basis voor kunstmatige cellen. De vorming van deze polymerosomen is het onderwerp van hoofdstuk 5 en 6. De polymerosomen zijn gebaseerd op amfifiele PEG-polyester of PEG-polycarbonaat blok-copolymeren. Volledig biodegradeerbare polymerosomen met een inert oppervlak kunnen worden gemaakt door biodegradeerbare, hydrofobe blokken te combineren met biocompatibele hydrofiele blokken die door het lichaam kunnen worden uitgescheiden.

In hoofdstuk 5 wordt de vorming van polymerosomen in chloroform/water beschreven. Helaas werden op deze wijze polymerosomen met een brede deeltjesgrootte-verdeling gevormd, terwijl er relatief veel geprecipiteerd polymeer werd aangetroffen. Hoofdstuk 6 behandelt de vorming van polymerosomen vanuit een mengsel van een met water mengbaar oplosmiddel en een waterige oplossing. Het gebruik van dit systeem resulteerde in polymerosomen met een smalle deeltjesgrootte-verdeling en er werd geen precipitaat waargenomen. Voor beide systemen is de invloed van de proces-variabelen op de polymerosoom-opbrengst, -grootte en deeltjesgrootte-verdeling systematisch bestudeerd. Tevens wordt er een mechanisme voor de vorming van de polymerosomen voorgesteld.

Om de polymerosomen te completeren tot kunstmatige cellen werd een biofunctionaliteit en herkennings-systeem toegevoegd. Hoofdstuk 7 beschrijft de encapsulering en afgifte van carboxyfluoresceine (CF), een fluorescerende stof die als model werd toegepast. CF kan gemakkelijk door de polymerosomen worden ge-encapsuleerd door de stof op te nemen in de waterige fase die wordt toegepast bij de bereiding van de polymerosomen. De afgiftesnelheid van het ge-encapsuleerde CF bleek af te hangen van de samenstelling van het copolymeer met name het molgewicht en het type hydrofobe blok van het copolymeer. De afgifte van CF in PBS bij kamertemperatuur en bij 60°C volgde een eerste orde kinetiek, hetgeen bevestigt dat het CF houdende polymerosoomsysteem kan worden beschouwd als een membraan gecontroleerd reservoir systeem. De aanwezigheid van plasma eiwitten anders dan albumine onderdrukten de afgifte van CF.

Om de kunstmatige cellen te voorzien van een herkennings-systeem, zijn de antilichamen, anti-humaan serum albumine en anti-humaan IgG, direct of via Protein G aan het polymerosoomoppervlak gekoppeld. De doelgerichtheid van deze polymerosomen werd bestudeerd met "imaging surface plasmon resonance" spectroscopie. Hierbij werd een specifieke interactie van de polymerosomen die waren voorzien van geïmmobiliseerd anti-humaan serum albumine met geïmmobiliseerd humaan albumine waargenomen. Hieruit werd geconcludeerd dat het mogelijk is om polymerosomen naar een specifieke plaats in het lichaam te leiden door immobilisatie van een antilichaam op het polymerosoomoppervlak. Voor deze immobilisatie wordt vooralsnog de plaats-specifieke immobilisatie van het antilichaam via Protein G geprefereerd boven de directe immobilisatie van het antilichaam.

Het onderzoek werd afgesloten met de eindconclusie dat de ontwikkelde biodegradeerbare, biocompatibele polymerosomen een gedefinieerde structuur, een smalle deeltjesgrootte-verdeling, een relatief groot volume voor encapsulering en controleerbare afgifte eigenschappen bezitten. Bovendien hebben de polymerosomen de potentie om naar een specifieke plaats in het lichaam te worden gestuurd, hetgeen deze polymerosomen zeer geschikt maakt als basis voor kunstmatige cellen.

Gratitude

Each piece of works involves the contribution of numerous individuals from different aspects. This one is no exception. My thesis could not be accomplished without many warm-hearted help and support, and my life would not be so wonderful without so many good friends and colleagues. I could never thank them enough.

I cannot emphasize enough how important to have supportive and engaging mentors. Professor Jan Feijen, thank you for giving me the opportunity to work in the group and creating such nice environment in the group. Your spirit and insight always inspire me. I must convey my gratitude to Dr. Gerard Engbers for his valuable guidance on the project, stimulating discussion, and critical correction of the thesis.

My gratitude has to be extended to Karin, Gerda and Geneviève for all the help whenever I ask, to Zlata and John for their assistance in the lab. I appreciate very much for all the help from Kees van der Werf (AFM), Alma Dudia (CLSM), Mark Smithers (SEM, TEM), Albert van de Berg (XPS) and Netty de Groot (CT, library).

I wish to thank all the members from PBM, RBT, STEP and MTP, especially Priscilla, Laura, Miechel, Menno, Annemeike, Christine, Zheng, Boon-Hua, Ype, Joost, Marianne, Francesca, Louis, Pratip, Kinsuk, Shan, and Chuan-liang. We had so much fun together! Jokes and occasionally serious talks by the coffee table, fine parties and activities like annual triathlon, study tour, wadlopen, sailing etc. will always remind me with joy. My dear roommates Alma,

Mark, Luuk, Priscilla, Qing-pu, Laura, Christine, thank you so much for not only sharing the space, but also information, stories, experience and feelings. I really enjoyed staying in this famous "chicken house"!

There are many people who gave me great help and whom I had fun with during my stay here, you made my life so easy and pleasant. Xue-mei & Tao, Kathrin & Miechel, Menno, Annemieke, Priscilla, and Laura, I appreciate very much your friendship and the wonderful time we spent together. I must extend my sincere gratitude to Piet for giving me so much advice and helping check the concept, and to Janny for the interesting conversations and kind help, especially the lovely gift to my baby!

My special thanks goes to my Paranimfen Kathrin and Priscilla. Thank you for being there to share the most difficult and unforgettable time with me! I really want to have a few times more "official dinner" together!

I own great debt to my family, in-laws and relatives for so much support during the past years. Though my parents may not have taught me how to pursue a PhD degree, their eternal support, love and confidence in their daughter have contributed significantly in making me the individual I am today.

No word could express my appreciation and affection to *Yuangu*, the love of my life, my best friend and "soul mate". I do not want to mention the daily care you are giving to me, especially during the period of my writing and my pregnancy. You fill up every corner of my life every day and inspire me. My unborn baby boy, you are the most generous gift I have ever received! Without realizing it, you are giving me much more than I can ask. You make me full of life and spirit, and look at the life with a brand new perspective. I am the luckiest person in the whole world!

Fenghua

Curriculum Vitae

Fenghua MENG was born on 7 April 1973 in Jilin, P. R. China. In 1991, she passed the national exams and entered the College of Chemical Engineering, Dalian University of Technology (Dalian, P. R. China) to study Polymer Science & Engineering. Four yearslater, she obtained her Bachelor's degree with a dissertation entitled "synthesis of heat-resistant PEK and PEEK for membrane". In the same year, she joined the research group of Prof. Baotong HUANG to pursue Msc. degree in the Changchun Institute of Applied Chemistry, Chinese Academy of Sciences (Changchun, P. R. China). With a thesis entitled "preparation & characterization of polymer-supported zirconocene catalysts and their olefin polymerization", she graduated in 1998. Thereafter, she worked as a temporary researcher in the same group for half a year to continue studying the co-polymerization of ethylene and 1-olefins with polymer-supported zirconocene catalysts and characterization of the thermoplastic behavior of the resulting copolymers. In August 1999, she joined the polymer chemistry and biomaterials group in University of Twente (Enschede, The Netherlands) to pursue her PhD degree under the supervision of Prof. Dr. Jan Feijen and Dr. Gerard H. M. Engbers. Her research subjects cover supra-structures of amphiphilic block copolymers, biocompatibility of biomaterials, biodegradable polymers and surface modification technologies.